

Hallvard Berner Hammer

Accuracy of CPTUs in deltaic sediments and the effect of cone penetrometer type

Trondheim, September 2019

PROJECT THESIS: TBA4510

Supervisor: Professor Jean-Sébastien L'Heureux

Department of Civil and Environmental Engineering

Norwegian University of Science and Technology (NTNU)



Norwegian University of
Science and Technology

Preface

This study is a project thesis as part of the Master of Science in Civil and Environmental Engineering at the Norwegian University of Technology and Science (NTNU). It is part of the course TBA4510 led by the Department of Civil and Environmental Engineering and comprise 7,5 ECTS. The report was written during the mid-half of 2019.

The basis of the study has throughout the working period been assessments of the CPTU measurements done at the river delta of Øysand. However, the original intent was to consider the *Inverse filtering procedure* presented by R.W. Boulanger and J.T. DeJong on the CPT'18 conference in Delft. The inverse filtering procedure attempts to correct CPT profiles to a "true" value by correcting for interfaces and transition zones between layers caused by the mechanical nature of the cone penetration test. The focus was intended towards discovery and correction of values at thin, weak interbedded layers at the Øysand site. This topic was studied in detail and the procedure was reproduced through coding. However, the author raised questions about the quality of the data and the validity of comparing results of different equipment after some time working with the Øysand CPTUs. The focus of the study then turned towards evaluating the accuracy of the measurements in deltaic sediments, also considering the effects of using different equipment. The potential of such an evaluation was tempting with the vast amount of CPTU data densely spaced at the site. It is also believed that these results are of greater interest for both the characterization of the site and as a reference for the quality of CPTU data in river deltas as an argument for more frequent and extensive use of CPTUs in site investigations.

In total, a significant greater amount of time was been spent on the project than the credits reflect. Key reasons to for this are firstly due to the prolonged early phase where another objective was pursued in detail, and secondly due to a comprehensive nature of the final objective. Furthermore, literature search has been time-consuming with little results. The intent was to find procedures of trend removals through depth adjustment, though no paper was found on this matter.

Amongst other time consuming tasks which eventually were not included are work covering characterization of the soils at Øysand, including multiple different techniques of correlating soil type soil behavior to CPTUs. Great efforts were also put into the development of a statistical algorithm to automatically adjust for trends between CPTUs. This procedure was not completed nor included in the study due to the somewhat limited usefulness for the project, thus manual comparisons were done instead. The procedures mentioned above, as well as those presented in the study are all developed using MATLAB coding.

The supervisor of the study has been Prof. Jean-Sébastien L'Heureux, whom also holds the position as a principal engineer at NGI and is the project manager of NGTS (Norwegian Geo-Test Sites). The Øysand site is included in the NGTS research project, a project led by NGI with NTNU is a partner.

Trondheim, 15/09/2019



Hallvard Berner Hammer

Summary

Deltaic sediments are known to have a complex structure of very mixed soils and non-horizontal layering consisting of materials varying from clays to gravels. Sampling of these materials are often very challenging, making the in situ measurement techniques and the piezocone test (CPTU) in particular very attractive. A great stratigraphic detail is found from CPTU results, and the measured values are normally used for classification of the soils and sometimes parameter determination. The CPTU is very popular due to its cost-effectiveness and expected repeatability. However, the accuracy of the CPTU parameters is poorly documented for deltaic soils, as well as the impact of cone type. It is crucial to understand the degree one can rely on the results when the data is used for geotechnical design procedures.

This study is focusing on using results from densely spaced CPTUs at a river delta to quantify the accuracy of the CPTU parameters. The site is at Øysand, Norway, which is a part of the Norwegian Geo-Test Sites research project. This site includes 30 CPTUs performed in a space of less than 10m by 10m, containing a series of 12 consecutive measurements distanced by only half a meter in between.

Significant trends of for instance layer inclinations are caused by the sedimentation process of a river delta. The depth in which a certain sediment is encountered for the CPTUs varies in the horizontal directions. This causes direct comparisons between measurements to show poor matching at first glance. The trends must be removed in order to correctly compare the results and evaluate the accuracy. Depths of reoccurring characteristics of neighboring measurements are connected by lines using the closely spaced CPTUs. The measurement of cone resistance is used to compare the characteristics. These connections are called isolines, as the line between tests is assumed to describe the position where the same features are found. A procedure of depth adjustment based on these isolines is presented, where a measurement of the relative vertical distance between the matching characteristics is given. This procedure then allows for trend removal and comparison between results.

The evaluation of accuracy shows that the cone resistance has the best accuracy of the three parameters, values are within 5% error. The sleeve friction and pore pressure measurements show the same order of accuracy, with errors at about 10%. However, the sleeve friction shows a larger variation between cone penetrometers than the pore pressure measurement. The best accuracy of the measurements was achieved from cone penetrometers using compression type cone design and larger diameter of the cone.

The bedding in the river delta of Øysand complies with the classical bedding division of three parts, the topset, foreset and bottomset beds, which was found from the CPTU tests. While the topset and bottomset normally have an almost horizontal layering, the foreset bed is expected to have an inclination reflecting the angle of repose of the materials it consists of. The results show that the evaluated part of Øysand consists of a horizontal topset bed and a bottomset of a slight inclination. The foreset bed has an inclination of 0,55, i.e. a 29° angle and has a thickness of about 10m. Where the foreset inclination is as steep as it is here it is necessary to perform CPTUs very densely to discover all materials, with no larger distance than $10m/0,55 = 18m$.

Table of contents

Preface	I
Summary	II
List of figures	V
1. Introduction.....	1
1.1. Background	1
1.2. Objective	2
1.3. Limitations.....	2
1.4. Structure of the report.....	3
2. Theory	4
2.1. Properties of the CPTU.....	4
2.2. Stratigraphy and sedimentation process of a river delta.....	6
2.3. Characterization of a river delta using CPTUs.....	8
2.4. Accuracy of CPTU parameters.....	9
2.5. Corrections of CPTU measurements.....	10
3. The Øysand research site.....	11
3.1. About the site.....	11
3.2. Performed CPTUs at Øysand	13
3.2.1. Overview	13
3.2.2. Example of a CPTU measurement at Øysand	15
3.2.3. Cone types.....	16
4. Processing of CPTU data	19
4.1. Sections	19
4.2. Determination of stratigraphic isolines along a section	24
4.2.1. Stratigraphic isolines.....	24
4.2.2. Using the cone resistance data to determine isolines	25
4.2.3. Stratigraphic reference isolines	25
4.3. Depth adjustment	27
4.3.1. Concept	27
4.3.2. Relative vertical distance, z_{rel}	28
4.3.3. Depth normalization	32
4.3.4. Interpolated adjusted values	33
4.4. Accuracy of depth adjusted CPTU measurements.....	34

5. Results	37
5.1. Determined SRLs	37
5.2. Depth adjusted data.....	38
5.3. Trends along sections.....	40
5.3.1. <i>Isolines for sections</i>	40
5.3.2. <i>SRL inclination for sections</i>	40
5.3.3. <i>The direction of progradation at Øysand</i>	43
5.4. Determined precision for cone types on depth adjusted CPTU measurements	44
5.5. Determined accuracy of the CPTU parameters in deltaic sediments	49
6. Discussion	51
6.1. Comparison between isolines and GPR data	51
6.2. Comparison between borehole and CPTU measurements – detecting thin layers.....	53
6.3. Effect of cone penetrometer type	58
6.4. The accuracy of CPTU parameters in deltaic sediments	62
6.5. Stratigraphic isolines and depth adjustments	65
6.6. Practical use of CPTUs in a river delta.....	66
7. Conclusion	67
8. Recommendations	68
9. Further work	69
References	70
Appendix	73

List of figures

Figure 2.1 – Cone penetrometer (Lunne et al., 1997)	4
Figure 2.2 – General structure of a delta (Haslett, 2009, p. 118)	7
Figure 2.3 – Geomorphology of a river delta, (a) plan view, (b) cross-section (Haslett, 2009, p. 119) ..	7
Figure 2.4 – Definition of accuracy of CPTU measurements (Peuchen & Terwindt, 2014)	9
Figure 3.1 – Location of the Øysand research site.....	11
Figure 3.2 – Data found from a bore hole at Øysand (Quinteros et al., in press).....	12
Figure 3.3 – Map of Øysand with the CPTU locations with a box that covers the cluster.....	13
Figure 3.4 – CPTUs in the cluster, with the cone type in parenthesis	15
Figure 3.5 – A characteristic CPTU profile at Øysand, CPTU 21	16
Figure 4.1 – Map with section lines	20
Figure 4.2 – Direction of section 1 through 10	20
Figure 4.3 – Illustration section plot	21
Figure 4.4 – CPTU data of Section 1.....	22
Figure 4.5 – Section plot of Section 1	23
Figure 4.6 – Color map of Section 1	23
Figure 4.7 – Illustration of stratigraphic isolines.....	24
Figure 4.8 – Illustration section plot with chosen SRLs	26
Figure 4.9 – Illustration section set with and without depth adjustment relative to t1	27
Figure 4.10 – Combination of Figure 4.8 and Figure 4.9, section plot to the left and z_{rel} to the right .	29
Figure 4.11 – Original depth vs adjusted depth (left) and z_{rel} plot (right).....	29
Figure 4.12 – Illustration section plot (left), original depth vs adjusted depth (right)	31
Figure 4.13 – Illustration section set with and without depth adjustment relative to t4	31
Figure 4.14 – Total and effective stresses used at Øysand.....	32
Figure 4.15 – Explanation of the depth adjustment	33
Figure 5.1 – Section plot of section 1 with SRLs	37
Figure 5.2 – Depth adjusted data for section 1	38
Figure 5.3 – Adjusted colormap plot of section 1	39
Figure 5.4 – Stratigraphic isolines along the sections 1, 2 and 5	41
Figure 5.5 – Slope inclination for section 1-4 (top), 5-7 (middle) and 8-10 (bottom)	42
Figure 5.6 – Foreset bed slope inclination of sections by direction	43
Figure 5.7 – Plots of standard deviation for the cone types in section 1	44
Figure 5.8 – Depth adjusted data for cone type 3 (top), 4 (middle) and 5 (bottom)	45
Figure 5.9 – Depth adjusted data for cone type 11 (top) and 12 (bottom)	46
Figure 5.10 – Depth adjusted data for cone type 1	47
Figure 5.11 – Depth adjusted data for cone type 6	48
Figure 5.12 – Depth adjusted data for cone type 7	48
Figure 5.13 – Average error	49
Figure 5.14 – Average of average errors.....	49
Figure 5.15 – Comparison of representative profiles for cone types 3, 4, 5, 11 and 12	50
Figure 6.1 – Map of GPR1	51
Figure 6.2 – Data from GPR1.....	51
Figure 6.3 – Data from GPR1 with expected isolines in red	52
Figure 6.4 – Image of stratigraphy from borehole 09 (Quinteros et al., in press).....	53
Figure 6.5 – SRLs along section 8 including borehole 09	54
Figure 6.6 – Depth adjusted measurements on top of borehole data	55
Figure 6.7 – Enhanced presentation of marked depth in Figure 6.6	56
Figure 6.8 – Details of the colormap plot of section 1 presented in Figure 4.6	57
Figure 6.9 – Detection of thin clay layer for section 1 (top), 3 (middle) and 9 (bottom)	57
Figure 6.10 – Average of all profiles in section 1 vs average of representative profiles	62
Figure 6.11 – Representative profiles with accuracy requirements	64

1. Introduction

1.1. Background

River deltas are sites for large and often complex structures and infrastructure all around the world, often due to its attractive location. Sediments encountered in the river delta are known to have large variations in layering and soil properties due to the sedimentation process. The variations in layer thickness resulting from coastal progradation may cause serious problems such as uneven settlements, as for example seen at the famous Leaning Tower of Pisa (Sarti et al., 2012). Weak and loose soils should be discovered and treated with care in the geotechnical design. To accurately assess these issues comprehensive site investigations must be carried out. These investigations should include a combination of in-situ tests and laboratory investigations. However, loose sands are for instance very challenging to sample, and where samples can be taken it is normally with significantly disturbances which may impair the results.

The cone penetration test (CPT) is an in situ test which is very favorable in sands. It measures the tip resistance and friction resistance of the soil as it advances. An enhanced version of the CPT that is used the most today is called CPTU, which also includes a measurement of the pore pressure. CPTUs measures these three parameters continuously with depth which makes it great for discovering stratigraphic details. Furthermore, the CPTU is cost-effective and very popular in geotechnical site investigation. CPTUs are normally used for characterization of the soil based on its measured behavior from the parameters. Soil parameters for design may also in some cases be estimated from developed empirical correlations. However, it is of great importance to know the quality of the data from a CPTU tests to know the degree to which one can rely on the results, as well as how the results can be used in the design. The quality of the data depends on multiple factors, including the accuracy of the CPTU equipment. The accuracy is a measurement of the repeatability of the test results as well as if the true value is measured. The impact of using different cone penetrometer types is should be well understood. An example of an issue is for large infrastructure projects where multiple different rigs with cone types from different manufactures are used.

Modern CPTUs are known to have a good repeatability, meaning that one can expect the same results from multiple tests run in the same conditions. This is known to be the case homogenous materials of particularly fine grained materials like clays and silts (J. J. Powell & Lunne, 2005), while the accuracy of CPTUs in sand is poorly documented. Furthermore, the accuracy in inhomogeneous materials or very mixed such as deltaic sediments is ambiguous and less known. If the understanding of the data quality is lacking, the its use for design is unjustifiable. In the opposite case, with known quality and systemization of the CPTU data, the utility and potential of the data will increase substantially. Of the greater challenges in determining the accuracy of CPTUs in deltaic sediments is to define the true in situ value. This value can be found, and the measurement can be compared based on understanding of the geotechnical, geological as well as the mechanical aspects of the problem.

1.2. Objective

The purpose of this study is to better understand the potential and utility of CPTUs in site investigations performed at river deltas. Furthermore, it is desired to understand the importance of consideration to sedimentation process and proximity between tests in order to correctly discover all soil materials in the investigated area. This should be done by determining the accuracy of the measurements. A large amount of CPTUs of good quality is required to achieve this. The results of the tests may then only be compared if the measurements are expected to reflect the same true value. At the river delta research site of Øysand, Norway, tens of CPTUs have been performed together with multiple other state-of-the-art site investigation tests. The evaluation presented in this study is based on the data from this site.

The main objective of this study is to quantify the accuracy of the three CPTU parameters from densely spaced tests conducted at a river delta site, thus defining the most accurate parameter in deltaic sediments.

The main objective shall be reached through the following, secondary objectives:

- Use CPTU measurements to discover trends in the horizontal directions caused by sedimentation process of the river delta.
- Develop a procedure to remove said trends from the CPTU measurements.

1.3. Limitations

Though the CPTU mainly is a geotechnical tool for characterization and in some cases determination of parameters of the sediments, this study does not intend to perform these interpretations. With the objectives described above, the focus is instead in a systemization of measurements through geological considerations and properties of the equipment. The geotechnical aspect is then included in the understanding of the response and the consequence of the determined accuracy of measurements for geotechnical use. Exact repeating patterns in the measurements is of greater interest in this study rather than an overall evaluation of the materials. This is due to other articles already in development on parameter selection for the Øysand site. These articles will be presented in this study.

Mechanical aspects of the cone penetrometer will be covered on a general level, though the mechanics behind the measurements will not be studied. These are for instance the effect of grain size on the progressive failure zones and the influence of transitional effects when a layer boundary is encountered.

In the determination of accuracy, advanced geostatistical methods will not be used, such as Kriging methods, but rather measurements of error and standard deviation. The evaluation of accuracy can only be done based on the information available, which excludes errors such as operating error and equipment wear.

1.4. Structure of the report

To reach the objectives of the report in a coherent way, the report is built up towards the final evaluation of the depth adjusted profiles and the subsequent estimation of the accuracy. To begin with, theory about CPTUs and river deltas is presented in chapter 2. First, the properties of the CPTU is presented, followed by a brief description of a river sedimentation process model. A brief literature study then presents how CPTUs have been used to characterize river deltas. Then articles about the accuracy of CPTU is presented and how measurements should be corrected.

Following is the presentation of the site evaluated in this study, the Øysand site in chapter 3. The previous studies on the characterization of the site is presented together with the data which will be used in this study.

Chapter 4 presents the developed procedures for this study to eventually allow an evaluation of accuracy. This includes systemization of the data, discovery of trends and the following removal of trends. The report includes multiple procedures and some terminology defined by the author where no such procedures were found from literature. This includes the depth adjustment procedure, which is presented in detail. Lastly, a method for assessment of accuracy of CPTU measurements is presented.

The results are presented in chapter 5. The most important figures are presented continuously in the report, while additional figures of results are found in the appendix.

In chapter 6, the results are discussed. Here, results of the CPTUs are compared to other site investigations at Øysand, including GPR measurements and a borehole sample. The performance of the cone penetrometers used at Øysand is discussed here. The utility of the parameters is also discussed.

Conclusions from the study is presented in chapter 7, followed by recommendation regarding the use of CPTUs in river delta and effect of cone penetrometers in chapter 8. Lastly, potential topics for further work on the discussed matter is given in chapter 9.

2. Theory

2.1. Properties of the CPTU

When geotechnical site investigations are performed it is with the intention to determine particularly the stratigraphy, the mechanical properties of the soil and the groundwater conditions (Lunne et al., 1997). This is normally achieved through a combination of field testing and laboratory testing. Through the latter, advanced tests can be performed from which all kinds of parameters can be interpreted. However, there are often great uncertainties of the reliability of the data due to for instance sample disturbances and the testing can be costly and time consuming. Furthermore, in some conditions taking good quality samples may not even be possible, such as in loose sands and coarse materials. In situ tests like the CPTU, on the other hand, does not encounter these problems. The CPTU is known to be cost-effective, repeatable, reliable and quick – all attractive features for site investigations.

Cone penetration tests have been used since its introduction in the 1930s for purposes of stratification and to describe the mechanical behavior of the subsurface strata. The CPT has been under continuous development improving aspects of its reliability, durability and effectiveness. Since the first inclusion of CPTs with pore pressure measurements in the 1970s, the feature has gradually gained popularity and is today standard in Norway. This kind of CPT is called CPTU or piezocone test.

The suitability of the piezocone is dependent on the ground type. It is regarded as appropriate to use in sand, silt, clay and peat, however, due to the mechanical limitations it is often not suited for gravels. It is therefore a normal procedure to do tests that give a rough description of the soils to begin with, such as total soundings. Preboring is normally done where very coarse soils are discovered to avoid damage to the equipment.

The CPTU test records parameters of cone resistance (q_c), side friction (f_s) and pore pressure (u) with depth for the advancing tip. These parameters are the stresses derived from the mechanical response their respective components on the cone penetrometer, presented in Figure 2.1. Filters, saturated in fluids, allow for pore pressures to be measurements inside the cone. The most popular pore pressure filter location is u_2 .

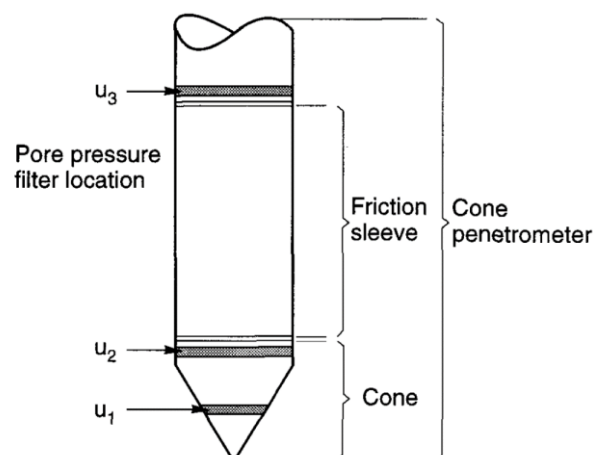


Figure 2.1 – Cone penetrometer (Lunne et al., 1997)

Two different standardized cone diameters are available, giving either a cone area of 10cm^2 or 15cm^2 . Measurements of the cone resistance and sleeve friction are either done with two separate measurements, or with one cone resistance measurement and another cone resistance plus friction sleeve measurement. The first of these is referred to as *compression type*, while the second is referred to as *subtraction type*. For pore pressure measurements, the selection of filter type and saturation liquid is of interest.

The three recorded parameters with depth are not enough to perfectly characterize the soil. However, through understanding of what physical properties the parameters reflect, and extensive calibrations and testing over a long time, the values of the parameters can be used to fairly accurately predict the soil it encounters. I.e., by applying knowledge to what combination of q_c , f_s and u_2 is expected in what type of soil, interpretations can be made. Popular interpretations are those of Robertson (Robertson, 1990), which was updated in 2016 (Robertson, 2016) and a rather new classification method using the pore pressure (Schneider et al., 2008). These methods use the parameters to discover what soil behavior type (SBT) the tested soil fits into. As the name of the SBT implies, the soil is classified by how it behaves rather than by the grain size distribution found in the laboratory. None the less, the SBT normally corresponds well with the laboratory description, for soils finer than gravel, that is. The soil types which are described through these interpretations are either clays, transitional (often silts) and sands, as well as whether it is in a dense or loose state. A very rough description of expected values for silts and sands, based on the classifications mentioned above and (Lunne et al., 1997) are shown in Table 1.

As mentioned, the CPTU is a great tool to characterize stratigraphy, this is due to the continuous measurements with a high measurement frequency with depth, normally about every 20mm , thereby detecting small variations. The cone reacts to the soil at some distance around the advancing tip, thereby creating a transitional effect. Transitional effects may have a significant impact on characterization in interbedded soils, such as deltaic soils. These effects will not be considered in this study; however, the accuracy of the parameters is. The accuracy of the parameters is of great importance to characterization.

Table 1 – Rough classification of expected CPTU values in silts and sands

Soil type	q_c	f_s	u_2
Loose silts	Medium	Low to medium	Low
Dense silts	Medium to high	Medium	High
Loose sands	Medium	Low	Low/negative
Dense sands	High		

2.2. Stratigraphy and sedimentation process of a river delta

The stratigraphy of the soil, or the variation of the soil characteristics with depth, is normally in geotechnical terms discretized into a certain number of layers. Within each layer the geotechnical properties assumed to be constant. Instead of defining discrete division into layers (or stratums), this study will rather focus on the entire stratigraphy. The stratigraphy is used as a term of the vertical continuous and gradually changing properties of the soil.

When investigating a complicated stratigraphic structure like the river delta, it is important to consider how it was formed through fluvial processes and progradation to better understand and interpret measured results. The classical theory for sedimentation structure of river deltas was first proposed by Gilbert (1885). In short, it states that the morphology and sedimentary structure of the delta may generally be simplified to three parts. These are, in the order of creation are bottomset bed, foreset bed and topset bed, illustrated in Figure 2.2 (Haslett, 2009). Alternative names of these parts are delta plain, delta front and prodelta, respectively, describing the part by its location when it was formed (Figure 2.3).

Sediments are deposited due to the river flow meeting still water, causing particles to sink. The properties of the three parts are simplified as follows:

1. **Bottomset beds** are made up of the finer materials that the river transports the farthest, laying down on top of the seabed. Thus, this part is likely to be either flat or at a slight inclination depending on the slope of the seabed.
2. **Foreset beds** contains larger particles of variable sizes which are distributed in the delta front. These sediments are transported along the bed of the river and are deposited by rolling along the foreset bed. The foreset bed has an inclination due to the progradation of the river (as seen in Figure 2.2 and Figure 2.3) and the particles are sedimented at the angle of repose.
3. **Topset beds** are laid on top of the foreset bed with varying sizes in a horizontal manner.

In other words, if the structure of a delta can be divided into these three *bed types* where an *upward-coarsening* of the materials is expected.

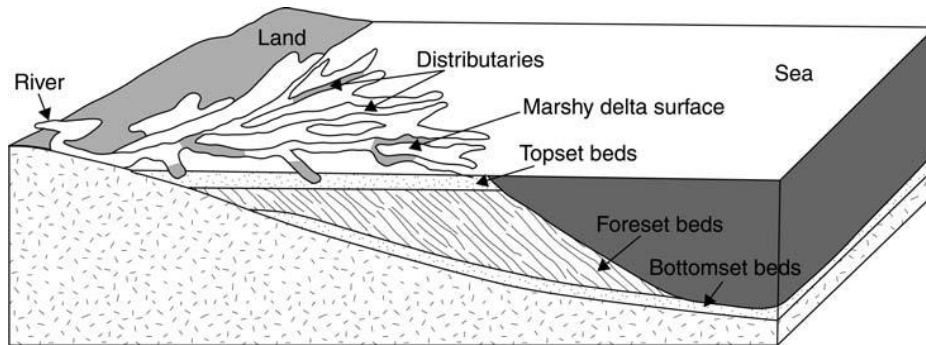


Figure 2.2 – General structure of a delta (Haslett, 2009, p. 118)

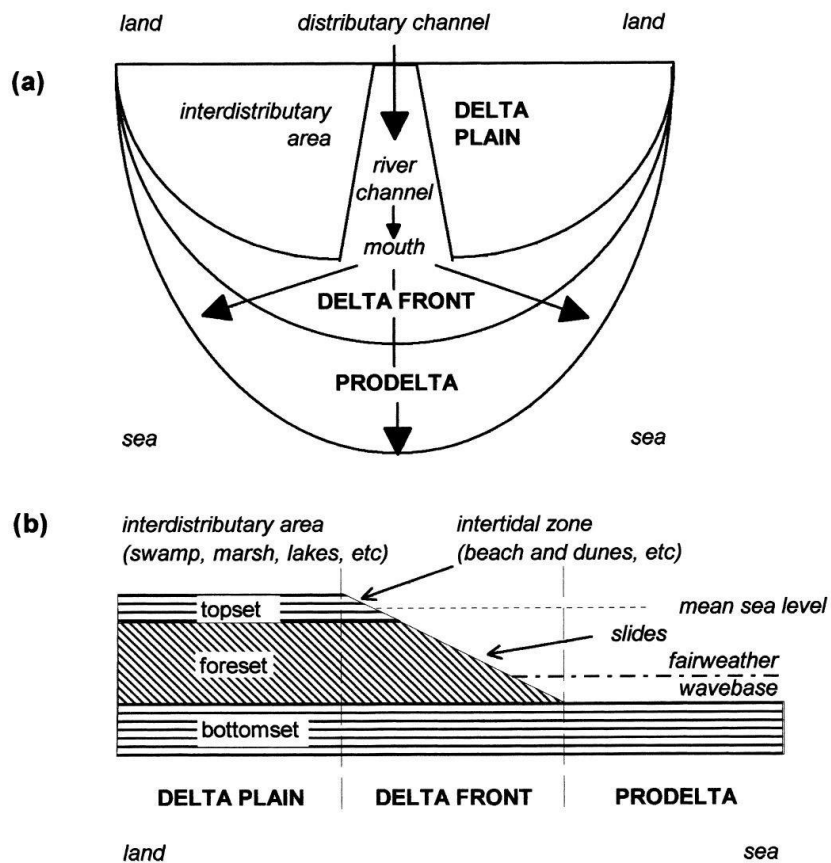


Figure 2.3 – Geomorphology of a river delta, (a) plan view, (b) cross-section (Haslett, 2009, p. 119)

2.3. Characterization of a river delta using CPTUs

The CPTU is a great tool to characterize the complicated structure and mixed soils found in a river delta. Large variations of materials can be expected with varying coarseness, particularly in the foreset bed. In such conditions the pore pressure measurement from the CPTU is believed to be very useful and accurate to determine interfaces. It may well determine whether the behavior of the soil is drained or undrained and thus indicate the soil type (Campanella et al., 1983). With the use of this parameter, preferably in combination with the other two, the CPTU well describes the continuous changes of the stratigraphy vertically. Though, assessments of the horizontal variation of the soil is more demanding. Measurements at the same site may not reflect a matching stratigraphy due to the sedimentation process.

Multiple studies have been performed proving the CPTUs great possibilities to characterize river deltas stratigraphy on a large scale. Among these are studies of the Po Plain in Italy (Amorosi & Marchi, 1999) and (Amorosi et al., 2014) and the Llobregat delta plain in Spain (Lafuerza et al., 2005) and the Aliakmon River delta in Greece (Styllas, 2014). Common for these is a rather geological focus, covering large distances, often tens of kilometers. The spacing of CPTUs in these articles is of mostly a hundred meters to a kilometer, which can be said to be high resolution in geological terms. The CPTUs are used to characterize layer units which are then connected to the layer units of neighboring tests.

In geotechnical terms however, the parameters of the soil at a more specific area of the site is often of greater interest, e.g. for a moderate sized construction site at a river delta. Furthermore, due to the sedimentation process previously described, interpolation between CPTUs can be very inaccurate. The potential using signatures in the CPTUs to discover connections between neighboring tests was also done for a soft clay site (J. Powell & Quarterman, 1995) with good results. These signatures are characteristic variations and size of CPTU measurements. This article contained tests more than 40m apart, though due to the homogenous conditions it still gave good results. Studies focusing on interpretation of CPTUs at a small grid has been done, though with a rather statistical focus of determining the spatial variability properties. A study using CPTUs of 2m distance in a river delta in Denmark concluded that bedding inclination should be considered for statistical calculation in deltaic soils, though this was not done in the article (Firouziandbandpey et al., 2014). Another study of a Danish river delta covered almost seven kilometers with 25m distance between CPTUs to determine spatial variability, concluding that each soil type must be considered independently (Bombasaro & Kasper, 2016). No article was found for any soil type where procedures of adjusting for depth trends were presented. To enable comparison of measurements, values must resemble each other, thus it is crucial to remove these trends.

2.4. Accuracy of CPTU parameters

To be able an evaluation of measurement accuracy, the definition of accuracy for CPTUs must be given. In metrological terms, accuracy relates to the true quantity of a measurand (Peuchen & Terwindt, 2014). The accuracy of a measurement may be defined as a quantified value of the systematic errors or the measurement bias. Precision is used together with the accuracy to describe the *degree of repeatability*. Applied to the case of CPTUs, the precision is defined to be how similar different CPTU profiles using the same measurement equipment is when the properties of the soil it encounters is assumed to be equal. The bias of the equipment is then the difference between the mean CPTU profile and the true profile. Figure 2.4 illustrates this meaning of accuracy for the CPTUs.

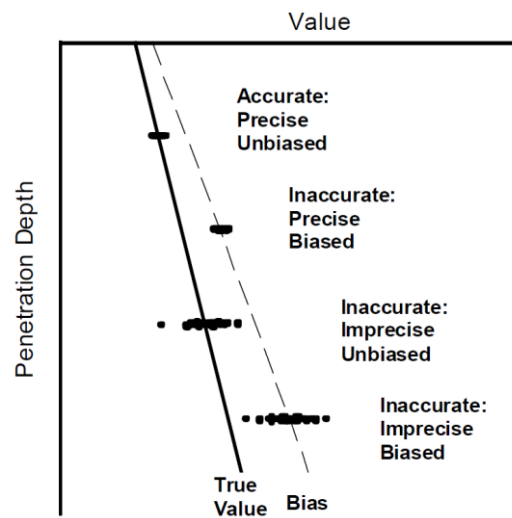


Figure 2.4 – Definition of accuracy of CPTU measurements (Peuchen & Terwindt, 2014)

The European standard of the piezocone penetration test (ISO 22476-1:2012) defines the requirements for CPTUs. That includes equipment, execution and data treatment. Requirements to accuracy is defined through application classes, which are dependent on the soil and intended use. Equipment must be controlled against the requirements of the application class. A cone penetrometer has a certain load capacity, where higher capacities gives a poorer load cell resolution, thus limiting the accuracy. Other aspects that influence on data quality are probe geometry and tolerances, temperature and zero shifts or misuse (Sandven, 2010). The latter will not be considered in this study, while possible misuse include insufficient saturation of pore pressure system, lack of maintenance and or errors in the user operation of the test.

The values measured is by itself not the only information that can be extracted from the CPTU – the variation of the values may be of equal importance. In this study the shape characteristics of the profiles with depth will be called *fluctuations*, while the size characteristics is referred to as the *magnitude*. If the fluctuations are of good precision while the magnitude is off compared to the true value, values may be shifted. A such behavior is potentially caused by zero drift or temperature effects and results in a bias.

2.5. Corrections of CPTU measurements

Standard corrections that should always be done before analysis, when possible, of the CPTU data includes correction for values due the unequal area and temperature effects and corrected depth due to rod curvature. The unequal area effect causes a decreased tip resistance depending on the area of the inner cone geometry, due to a net larger pore pressure acting on the tip. This correction depends on the factor a , presented as a -nom in Table 3 and is presented in equation (2.1).

$$q_t = q_c + u_2 \cdot (1 - a) \quad (2.1)$$

As the CPTU is advancing through the soil, the cone tends to follow the direction of least resistance. In cases of non-horizontal bedding it can have a significant influence, especially when the penetration resistance is high and at big depths. The deviation of the vertical path causes a change in the penetration depth that should be corrected for. It should also be controlled that the inclination of the cone does not exceed the recommended limit of 2° . The inclination with a single axis inclinometer is called α , and a single corrected depth, z_{cor} is given in equation (2.2), where l is the total length.

$$z_{cor} = \int_0^z \cos \alpha \cdot dl \quad (2.2)$$

The influence of corrections for temperature effects vary with equipment and air temperature, though it might have a crucial effect. Particularly when the measured values are low. The corrected pressure due to temperature is given in equation (2.3), assuming a constant relationship between temperature change and change in measured value.

$$X_{cor} = X_0 + X_{temp} \cdot \Delta T \quad (2.3)$$

Here X is a general term for the three measured values. X_{cor} is the corrected value and X_0 is the measured value. X_{temp} is the pressure rate of change depending on the difference in temperature. The temperature change, ΔT , is defined as the temperature of the cone penetrometer, normally air temperature, minus the temperature in the ground.

After the corrections, the data was interpolated with a constant depth distance of $10mm$. This was done through linear interpolation based on the depth values to enable easier data processing. These corrections were performed on all the data used in this study. Presented data of q_t , f_s , u_2 as well as depth in this study is corrected for all the factors mentioned here. Though the data is corrected it is still referred to simply as *measurements*.

3. The Øysand research site

3.1. About the site

The site evaluated in this study is at the Øysanden river delta, formed of fluvial material with deltaic and marine deposits underneath. The Øysand site is one of five research sites in the Norwegian Geo-Test Site (NGTS) project established in 2016, where each site represents an important characteristic of Norwegian soils. The sites are used as for benchmarking of testing, calibrating and verifying new soil investigation equipment and methods in geotechnical engineering (L'Heureux et al., 2017). The Øysand research site is described as the sand site, where the other four are soft clay, quick clay, silt and permafrost.

Only the top 25 meters of soil at Øysand is evaluated through measurements in this study. These 25m may be roughly separated into one upper unit of about 5m depth with coarse sand to gravelly sand followed by a unit of fine silty sand (Quinteros et al., in press). The cited article describes an in-depth characterization of the research site with the geotechnical properties from extensive in-situ, sampling, laboratory and geophysical tests at the site. This will henceforth be referred to as the Øysand characterization article and should be used for further information about the site.

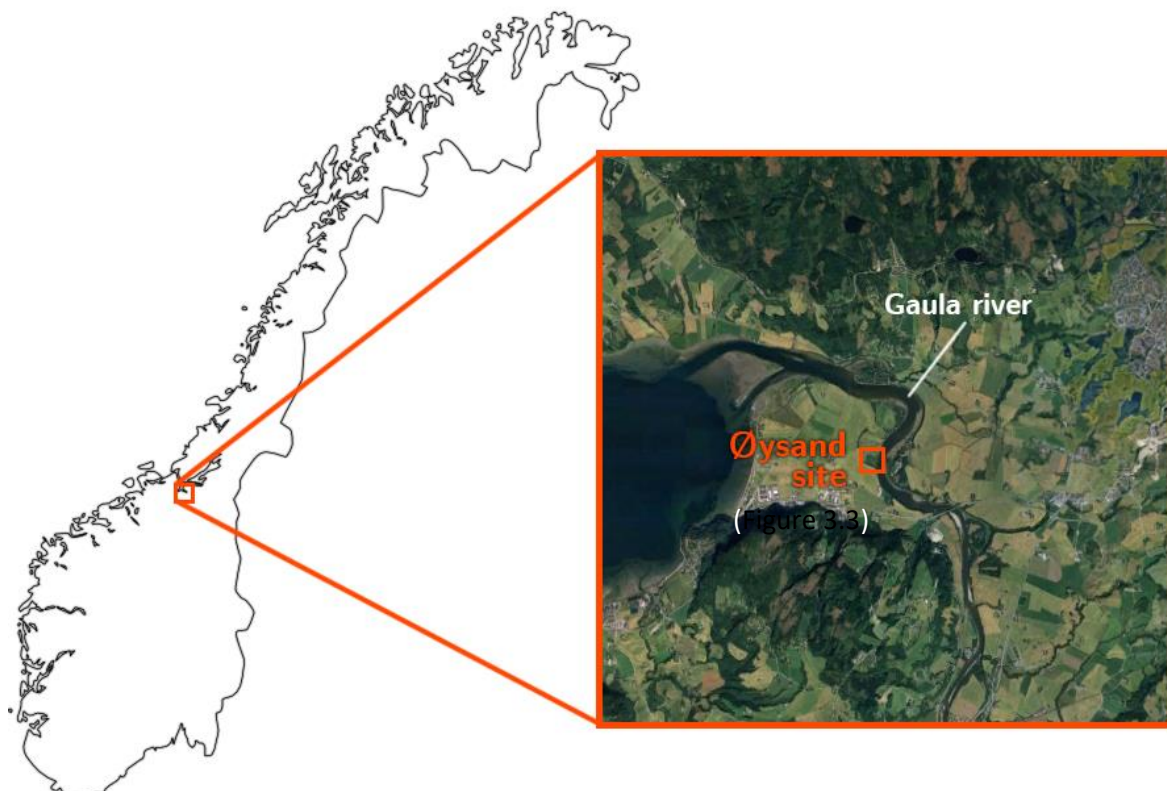


Figure 3.1 – Location of the Øysand research site

Though much more geotechnical data is gathered from the site, only the CPTU data will be used in this report together with a single borehole profile and a GPR profile. Results from the bore hole is presented in Figure 3.2. Here, multiple layers are determined using engineering judgement. From measurements presented in the Øysand characterization, the ground water table is found to be at a constant 2m below terrain level.

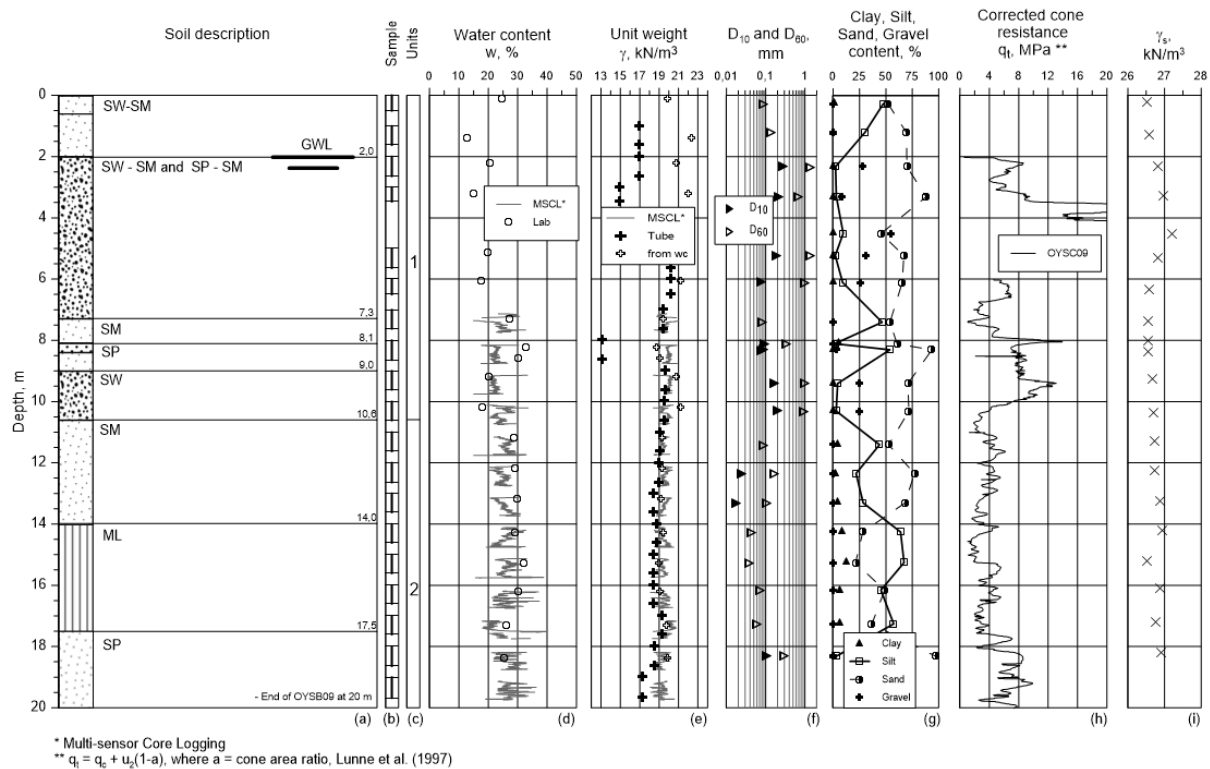


Figure 3.2 – Data found from a bore hole at Øysand (Quinteros et al., in press)

As seen on Figure 3.1, the site is located close to the estuary where the river Gaula meets the Trondheim Fjord. The deltaic sediments at Øysand is fairly young as the area emerged from the sea only about 1,000 years ago (Reite et al., 1999). Furthermore, as stated in the article by Quinteros et al., 2019:

Following their emergence from the sea, the deltaic deposits were covered by coarser river deposits as the Gaula River meandered in the valley. Coarse sands and gravels are therefore expected to occur in the upper portion of the soil stratigraphy at Øysand.

The layer structure of Øysand is naturally a result the geological history of the river delta, the sedimentation theory as previously described.

3.2. Performed CPTUs at Øysand

3.2.1. Overview

In the timespan between 2016 and 2018, more than 40 piezocone tests were performed at the Øysand site. These were executed using multiple different rigs and cone types. Most of the CPTUs are concentrated in a cluster at the southern part of the site (Figure 3.3) covered in the box.



Figure 3.3 – Map of Øysand with the CPTU locations with a box that covers the cluster

Only the tests inside the box considered in this study, which includes the 31 points listed in Table 2. The CPTU tests will be referenced to the ID in this table. Some of the CPTUs were performed in two parts, A and B, due to limitations of capacity in the gravelly parts. Similarly, for the test number 43 through 62 were predrilled to below the gravel layer.

An in depth characterization using CPTUs together with other in situ tests and laboratory results has been done at the site (Gundersen et al., 2018). This study does not cover soil characterization as it has been presented in both the prior mentioned article as well as the Øysand characterization article.

The borehole presented was performed close to CPTU 09. Only the visual stratigraphy of the borehole, which will also be referred to as B09, will be used in this study. The position of the most densely packed tests in the cluster are presented in Figure 3.4 with the cone type in parenthesis. The position of the CPTUs are given in distances to B09 for simplicity.

Table 2 – List of the performed CPTU that will be evaluated in this report

CPTU ID	UTM 32, EUREF89 [m]			Cone type	Depth at end of test [m]	Test date	Manufacturer
	Northing	Easting	Elevation				
02	7022895.043	562573.888	2.74		20.94	28.09.2016	
09A	7022898.245	562569.982	2.77		4.19	22.03.2017	
09B	7022898.245	562569.982	2.77		20.01	22.03.2017	
21	7022895.436	562573.258	2.609	12	25.45	21.09.2017	A
22	7022895.502	562573.703	2.618	5	25.31	21.09.2017	A
23	7022895.512	562574.183	2.634	3	25.75	21.09.2017	A
24	7022895.602	562574.688	2.622	11	25.31	21.09.2017	A
25	7022895.702	562575.141	2.617	5	25.46	21.09.2017	A
26	7022895.814	562575.610	2.630	4	25.33	21.09.2017	A
27	7022895.856	562576.157	2.632	12	25.34	21.09.2017	A
28	7022895.921	562576.652	2.625	5	25.29	21.09.2017	A
29	7022896.013	562577.135	2.659	11	25.35	21.09.2017	A
30	7022896.053	562577.734	2.660	3	24.92	21.09.2017	A
31	7022896.149	562578.112	2.646	5	24.32	21.09.2017	A
32	7022896.222	562578.715	2.664	4	25.3	21.09.2017	A
34	7022897.246	562574.705	2.653	1	20.75	27.09.2017	B
35	7022897.475	562576.160	2.654	1	20.59	27.09.2017	B
37	7022897.816	562579.202	2.681	1	20.77	28.09.2017	B
38	7022897.967	562580.712	2.681	1	20.83	28.09.2017	B
39	7022898.495	562572.970	2.662	6	25.9	28.09.2017	C
40	7022898.598	562574.455	2.701	6	20.31	28.09.2017	C
41A	7022898.956	562575.887	2.693	6	4.46	28.09.2017	C
41B	7022898.956	562575.887	2.693	6	20.27	28.09.2017	C
42A	7022899.176	562577.382	2.698	6	4.75	28.09.2017	C
42B	7022899.176	562577.382	2.698	6	20.35	28.09.2017	C
43	7022900.641	562573.441	2.782	7	25.7	03.05.2018	D
44	7022900.961	562575.395	2.862	7	20	03.05.2018	D
45	7022901.217	562577.405	2.822	7	20.34	04.05.2018	D
50	7022911.037	562566.048	2.743	2	19.38	31.05.2018	E
51	7022913.128	562566.817	2.720	2	19.46	31.05.2018	E
52	7022912.375	562568.746	2.716	2	19.58	31.05.2018	E
60	7022894.396	562558.195	2.399		19.84	24.09.2018	
61	7022894.217	562573.648	2.617		19.84	24.09.2018	
62	7022892.051	562573.175	2.614		13.82	25.09.2018	

The terrain at Øysand is almost entirely flat, however there are some small elevation differences. These height differences are partially caused by furrows, as the site is located on a field. Furthermore, these positions of the tests are determined through GNSS equipment with possible user operating errors. Effects caused by this is not considered. Except for CPTU 60, the maximum elevation difference is about 25cm. Elevation differences were considered in depth adjustments.

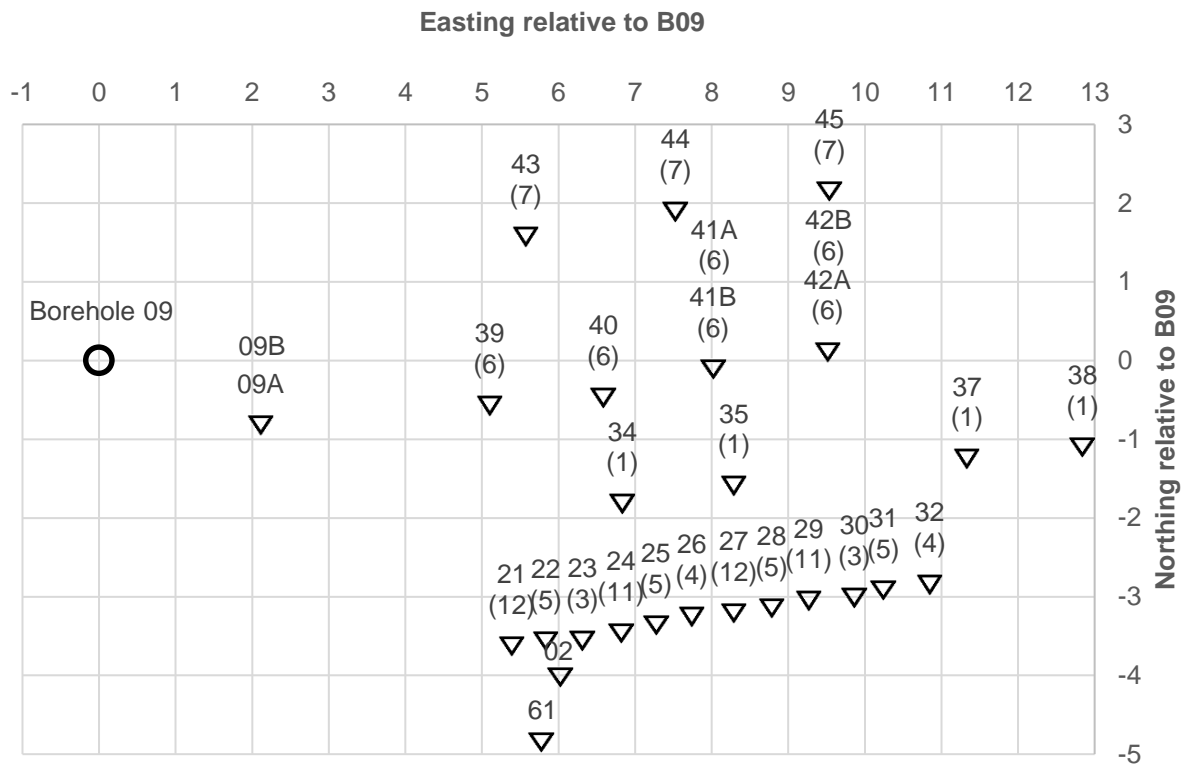


Figure 3.4 – CPTUs in the cluster, with the cone type in parenthesis

3.2.2. Example of a CPTU measurement at Øysand

Characterization of soil materials is as stated not included in this study, as it is already done in the two prior articles from Øysand. In these articles it was found that the results indicate an upward coarsening sequence. It was concluded that the CPTU failed to identify the occasional high content of gravel based on the used interpretation method (Gundersen et al., 2018). Figure 3.5 presents the profiles from CPTU 21, which reflect typical results from Øysand. High gravel contents are expected to be found at the parts with very high cone resistance measurement, i.e., in this case about between 1m and 5m. The pore pressure profile includes the hydrostatic pore pressures, u_0 . At the mentioned depth the values of u_2 is seen to match the value of u_0 , which indicates coarse materials. Below depth 5,5m, a large fluctuation of measurements of all three parameters is seen, indicating a very mixed layering. Pore pressure measurements significantly larger than u_0 is a sign of fine materials, thus it seems like a larger content of fines is found at larger depths. As described in the Øysand characterization article, a sandy-silty mix is found at these depths.

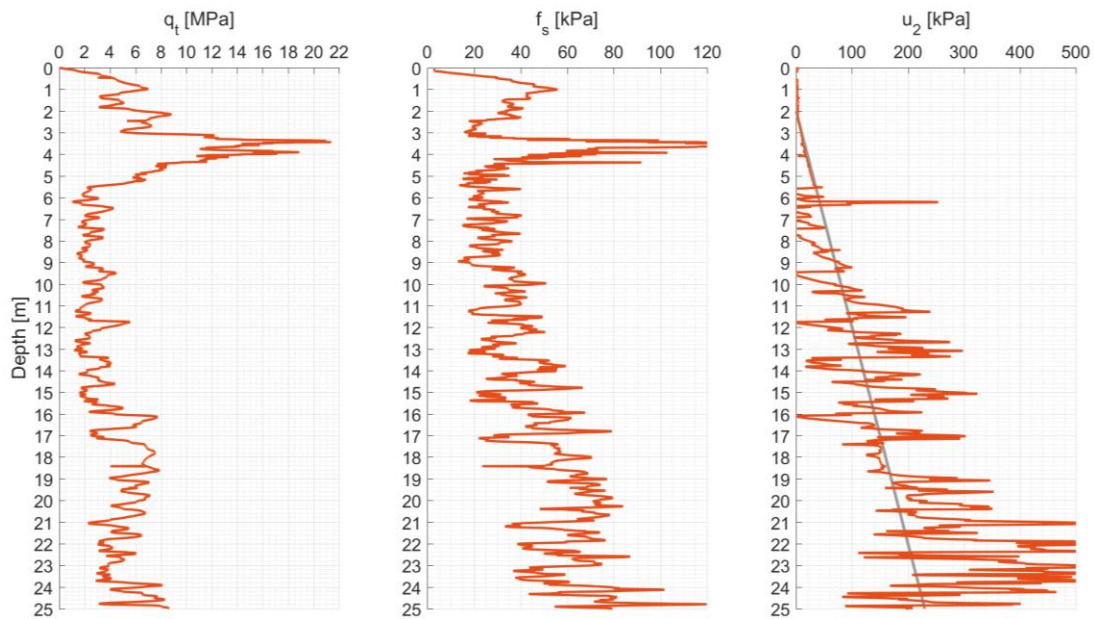


Figure 3.5 – A characteristic CPTU profile at Øysand, CPTU 21

3.2.3. Cone types

All CPTUs are performed to the requirements given by international standards (ISO 22476-1:2012). The CPTUs marked in grey in the table are performed with an unknown cone type without detailed information. 9 different known cone types have been used for the evaluated tests, these are numbered 1-7, 11 and 12 as seen in Table 2. These cone piezocones are from different manufacturers, except for cone type 3, 4, 5, 11 and 12 which are from the same manufacturer. All these cone types are a part of the NGTS research project. A detailed report of all properties of the piezocones used are presented in an article (L'Heureux et al., 2019). Table 3 and Table 4 present a list with the information about the different cone types.

Table 3 – List of cone types and their properties (L'Heureux et al., 2019)

Cone type	D ₁	D ₂	h	L ₁	A _c	A _{sb}	A _{st}	A _s	a-nom	b-nom	Cone type	Cone capacity		
												q _c	f _s	u ₂
1	35.8	35.8	10.0	134	1004	200	200	15015	0.8	0	Comp	50	1.6	2.5
2	35.9	36.0	10.0	134	1012	163	163	15155	0.85	0	Comp	25	0.5	2
3	36.0	36.1	10.0	135	1000	219	219	15000	0.8	0	Subtr	100	1	2
4	36.0	36.1	10.0	135	1000	219	219	15000	0.8	0	Comp	100	1	2
5	36.0	36.1	10.0	135	1000	219	219	15000	0.8	0	Comp	50	0.5	2
6	36.0	36.0	10.0	135	1017	297	168	15268	0.69	0.008	Comp	50	1	2
7	35.7	35.9	7-10	134	1000	263	263	15000	0.75	0	Comp	75	1	2
8	35.7	35.9	7-10	134	1000	263	263	15000	0.75	0	Comp	7.5	0.15	2
9	35.9	36.0	10	134	1012	163	163	15155	0.85	0	Comp	100	0.5	2.5
10	35.9	36.0	10.0	134	1012	163	163	15155	0.85	0	Comp	50	0.5	2
11	44.1	44.2	12.2	165	1500	309	309	22500	0.8	0	Subtr	100	1	2
12	44.1	44.2	12.2	165	1500	309	309	22500	0.8	0	Comp	100	1	2

Table 4 – List of filter types for each cone type (L'Heureux et al., 2019)

Cone type	Filter type	Saturation fluid
1	Bronze	Silicone ISOVG 100
2	Bronze	Glycerine
3	Brass 38 micron	Silicone oil 200 fluid 50 cSt
4	Brass 38 micron	Silicone oil 200 fluid 50 cSt
5	Brass 38 micron	Silicone oil 200 fluid 50 cSt
6	Slot	Grease/Oil
7	Stainless steel, S/S 10 μ	Silicone oil, DC200, 50 cSt
8	Stainless steel, S/S 10 μ	Silicone oil, DC200, 50 cSt
9	Bronze	Glycerine
10	Bronze	Glycerine
11	Brass 38 micron	Silicone oil 200 fluid 50 cSt
12	Brass 38 micron	Silicone oil 200 fluid 50 cSt

From this there are four important factors that may influence the result – these are the cone diameter (giving an area of either 10mm^2 or 15mm^2), the cone design (compression or subtraction), the cone capacity and the filter properties. Other factors are the how the cones are affected by temperature, the pore pressure measurement system. These are all factors that might influence the results and should therefore be corrected when possible. Correction for temperature will be performed and there are possibilities for scaling due to different cone area. The latter will not be done here, deviations that might be caused by this and other the remaining factors are only commented in this study. Most of the cone types have a measurement distance of either every 10mm or every 20mm , though data of CPTUs 21 to 32 are recorded between every 2mm to 4mm .

Table 5 presents the values of X_{temp} , the pressure rate of change due to temperature change for the cone types which are used for temperature correction in equation (2.3). Temperature effects for the cones used for the CPTUs in this study have been carefully included and is presented in detail in the article discussing the cone types (L'Heureux et al., 2019). It is noted in this article that care should especially be taken for subtraction cone types due to how the temperature effects will influence both the side friction and the tip resistance combined. The correction for temperature effects should thus be done before subtraction. Corrections for temperature was done based on calibrations shown in the same article. The measurements implied that there was a linear relationship between temperature change and pressure change in the sensors. Table 5 presents the pressure rate of change. The ground temperature is assumed to be at a constant 4° . Table 6 presents the zero drifts recorded for the CPTUs. Measurements with large zero drifts were not excluded in the results. The zero drift will be considered in the discussion.

Two articles about the effect of cone type on CPTU measurements has been published based on data from two of the NGTS sites. These are the Onsøy soft clay site (Lunne et al., 2018) and the Tiller-Flotten quick clay site (Lindgård, 2018). Both sites are classified as uniform and homogenous (L'Heureux et al., 2017), thus trend removal was not needed, unlike that of the Øysand site. Both articles concluded that u_2 gave the most repeatable results and that q_t varies somewhat more than u_2 . Sleeve friction

measurements varied significantly at both sites. Both sites contain clay, so as expected the values of q_t is far smaller than that measured at the deltaic soil at Øysand. The f_s -values are also a bit smaller, while the values of u_2 was significantly larger due to the undrained conditions.

Table 5 – List of pressure rate of change (L'Heureux et al., 2019)

Cone type	Pressure rate of change [kPa/Δ°C]		
	q_c	f_s	u_2
1	11.70	0.120	0.120
2	0.60	0.011	0.021
3	5.50	0.490	-0.800
4	5.50	0.490	-0.800
5	5.50	0.490	-0.800
6	NA	NA	NA
7	2.10	0.040	0.680
8	2.10	0.040	0.680
9	0.55	0.008	0.021
10	0.75	0.016	0.056
11	5.50	0.490	-0.800
12	5.50	0.490	-0.800

Table 6 – Summary of zero drifts for CPTUs at Øysand (L'Heureux et al., 2019)

Test ID	Cone Type	Zero drifts			Test date	Temp. ¹⁾ °C
		q_c , kPa	f_s , kPa	u_2 , kPa		
OYSC21	12	-71.4	0.2	-5.8	2017-09-21	12
OYSC22	5	9.8	0.4	-11.1	2017-09-21	12
OYSC23	3	5.1	-3.9	-20.2	2017-09-21	12
OYSC24	11	-48.5	0.9	14.9	2017-09-21	12
OYSC25	5	-44.5	0.0	-0.7	2017-09-21	12
OYSC26	4	-28.5	-0.5	-33.2	2017-09-21	12
OYSC27	12	-41.6	-0.5	2.8	2017-09-21	12
OYSC28	5	-4.5	0.0	-4.5	2017-09-21	12
OYSC29	11	-127.3	-6.4	15.6	2017-09-21	12
OYSC30	3	-19.4	-0.9	-31.1	2017-09-21	12
OYSC31	5	-21.7	-0.1	-0.9	2017-09-21	12
OYSC32	4	-62.2	-1.1	7.5	2017-09-21	12
OYSC34	1	5.4	0.6	0.0	2017-09-27	18
OYSC35	1	21.7	0.1	0.2	2017-09-27	17
OYSC37	1	21.7	0.2	0.2	2017-09-28	18
OYSC38	1	16.3	0.2	0.1	2017-09-28	17
OYSC39	6	168.0	80.3	2.0	2017-09-28	17
OYSC40	6	64.0	-1.1	-19.5	2017-09-28	17
OYSC41	6	56.0	-0.9	-12.8	2017-09-28	17
OYSC42	6	26.0	62.6	-23.1	2017-09-28	17
OYSC43	7	6.1	0.5	-1.9	2018-05-03	10
OYSC44	7	-13.4	-1.5	0.4	2018-05-03	10
OYSC45	7	-20.2	0.0	13.1	2018-05-04	10
OYSC50	2	4.2	0.3	1.0	2018-05-31	16
OYSC51	2	-18.9	0.3	-1.0	2018-05-31	16
OYSC52	2	-26.3	0.5	-1.1	2018-05-31	16

¹⁾ Representative air temperature used to correct measured results

4. Processing of CPTU data

4.1. Sections

To properly use the spatial information from the CPTUs, it is normal practice to present the test results in sections making a plane of one horizontal direction and the vertical direction. It is important to consider the proximity of the test to the chosen horizontal line to achieve an accurate presentation of the selection.

The positions of the tests in this study made it natural to select sections where the tests were aligned, as seen in Figure 3.4. These are the four “lines” with multiple tests at about the same latitude. As the intention was discover trends in different horizontal directions, it was desired to create sections in multiple directions. Therefore, as many as 11 sections were made in different directions in the cluster together with two sections covering the remaining CPTUs. The directions of the sections are presented in Figure 4.2.

The sections are listed in Table 7 and presented in Figure 4.1. Three groups were made depending on the section’s direction. These are *West to East*, *South to North* and *Other*. The CPTUs included in the section are listed in respect to the direction of the section. Each section has a *reference* CPTU, marked in bold in the table. The reference CPTU was selected with the criteria of having continuous measured data of good quality from close to the surface to a sufficient depth. Data from other CPTUs in the section were to be related to the reference. The importance of this will be covered in the coming chapters. The lines in which the sections follow are northing values as functions of the easting values (x), relative to borehole 09. Figure 4.2 simply presents an overview of the directions of the sections.

Table 7 – List of sections

Section	Group	CPTUs	Line	Notes
1	W-E	21 , 22, 23, 24, 25, 26, 27, 28, 29, 30, 31, 32	$0.148x - 4.421$	
2	W-E	34 , 35, 37, 38	$0.118x - 2.582$	
3	W-E	09, 39, 40 , 41, 42	$0.126x - 1.120$	
4	W-E	43 , 44, 45	$0.145x + 0.799$	
5	S-N	26, 34 , 40, 43, 52	$-2.45x + 15.399$	
6	S-N	28, 35 , 41, 44	$-4.083x + 32.581$	
7	S-N	29 , 42, 45	$15.622x - 147.85$	
8	Other	09, 34 , 30	$-0.270x + 0.184$	Section going through the borehole
9	Other	62, 61, 02, 23, 34 , 44	$3.791x - 27.072$	
10	Other	21, 34 , 41, 45	$1.396x - 11.231$	
11	Other	60, 34 , 35, 37, 38	$0.162x - 2.582$	
12	Other	50 , 52	$0.496x + 12.896$	
13	Other	60 , 50, 51	$2.151x + 16.142$	

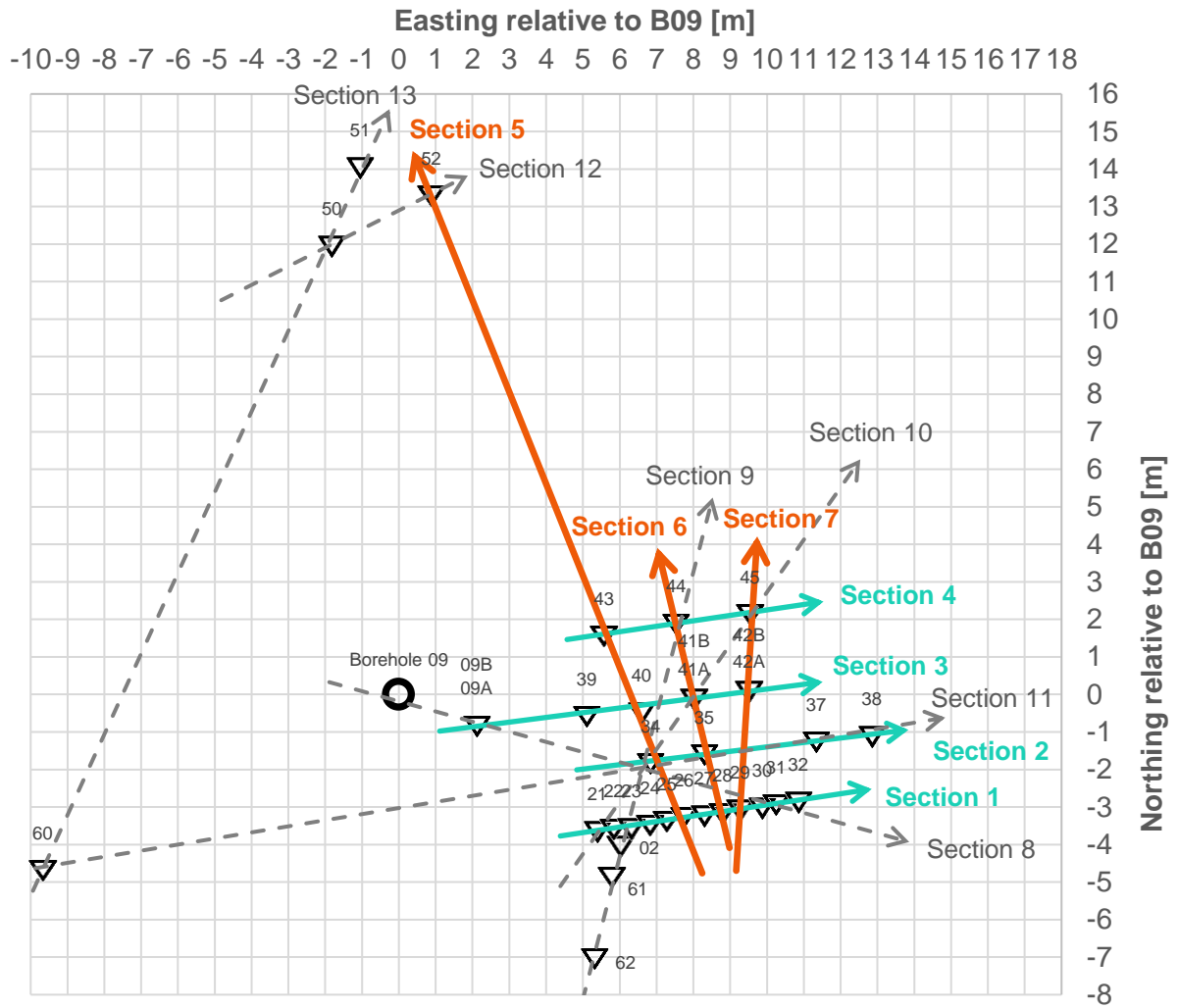


Figure 4.1 – Map with section lines

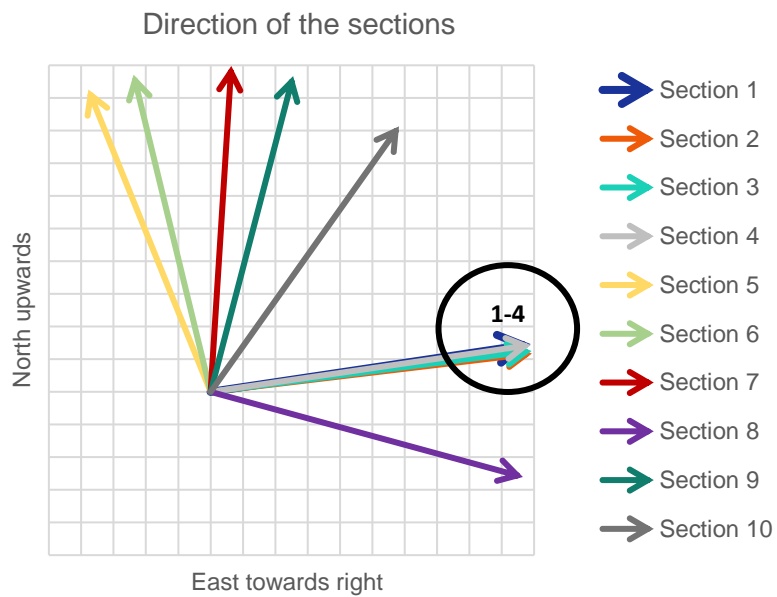


Figure 4.2 – Direction of section 1 through 10

Data from each section in this study is presented as in Figure 4.3. Here, the cone resistance measurements of three illustrational CPTUs are presented, $t1$, $t2$ and $t3$. For clarity, each individual q_t -profile within a section is referred to as a *set*. The figure presents the q_t -profiles of the CPTUs with their name listed on top. Next to the name is a number in parenthesis which is the perpendicular distance to the section line in meters. For this case that means the location of the CPTU tests in this figure are all less than $0.1m$ from the section line. The q_t -data is in general described by its shape in these figures, however the values can be found from the local gridlines for each set. Each has 5 gridlines with a spacing of 2 MPa. The vertical thick dotted lines represent the depth axis of each of the sets. At the top there is a strong line which marks the surface level.

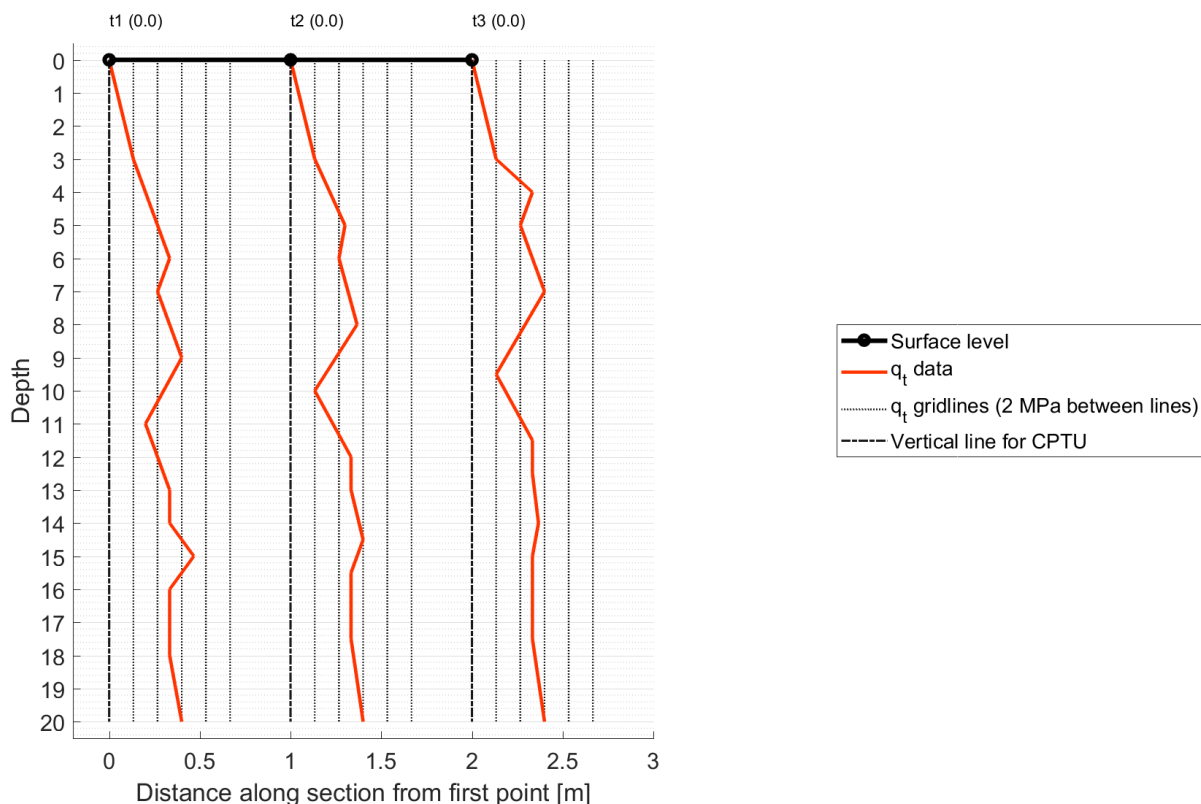


Figure 4.3 – Illustration section plot

The presentation in Figure 4.3 is in a way a 3D presentation as it shows the values for q_t , depth and horizontal distances. A more basic form of presentation in 2D includes only the first two of these. An example of this is shown in Figure 4.4 with the actual data from Section 1. Data from the 12 CPTUs of section 1 is presented which seem to match poorly. From this data one can note how the first 5 meters seem to conform somewhat while the remaining parts seem to have a large scatter.

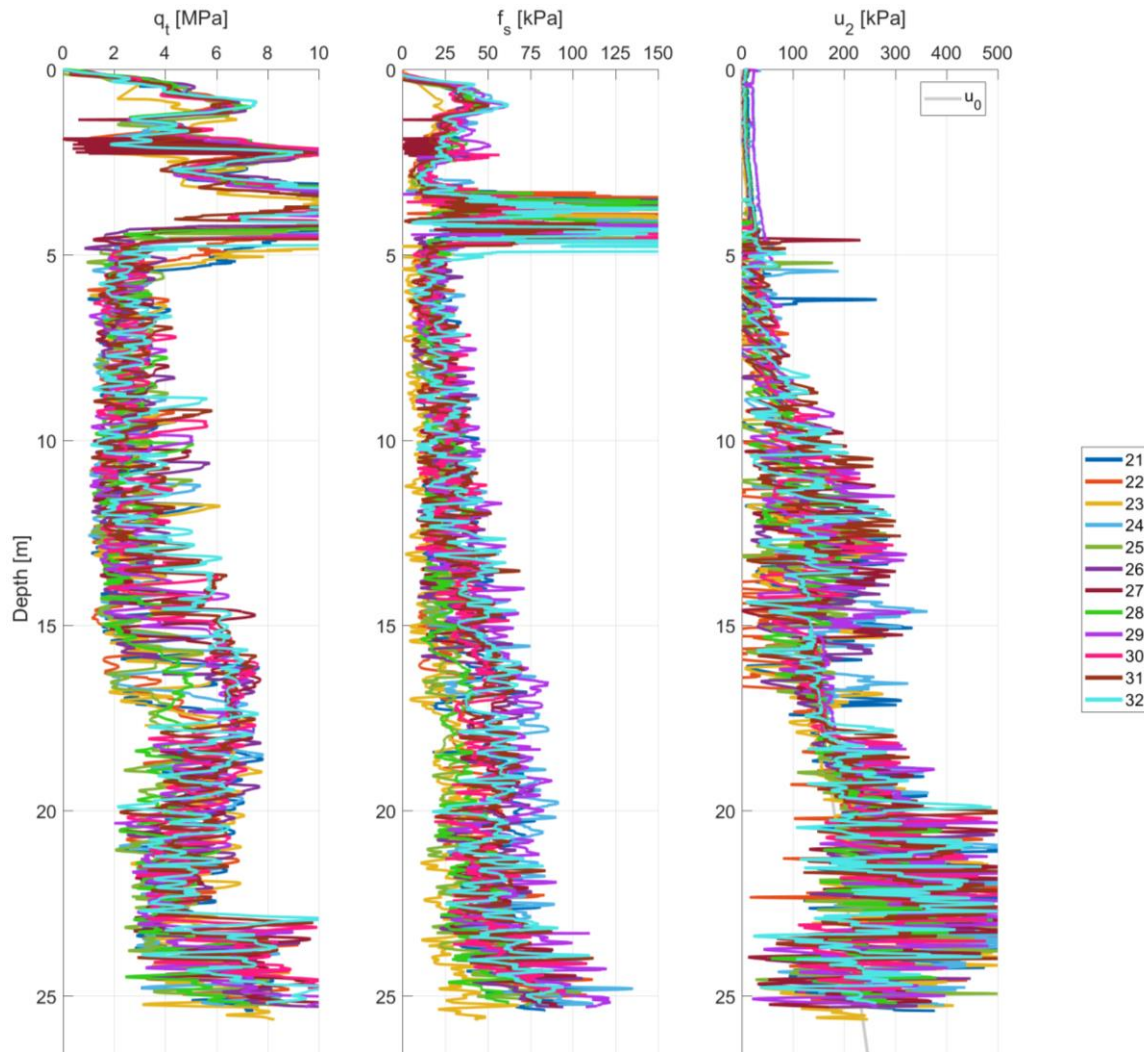


Figure 4.4 – CPTU data of Section 1

However, if the values are presented including the horizontal distances as the section plot Figure 4.5 or the color map in Figure 4.6, it becomes apparent that there are trends that should be accounted for. This will be covered in chapter 4.2 and 4.3. The colormap in Figure 4.6 presents a connected data of all the CPTUs in the section, with the vertical line of each CPTU also presented.

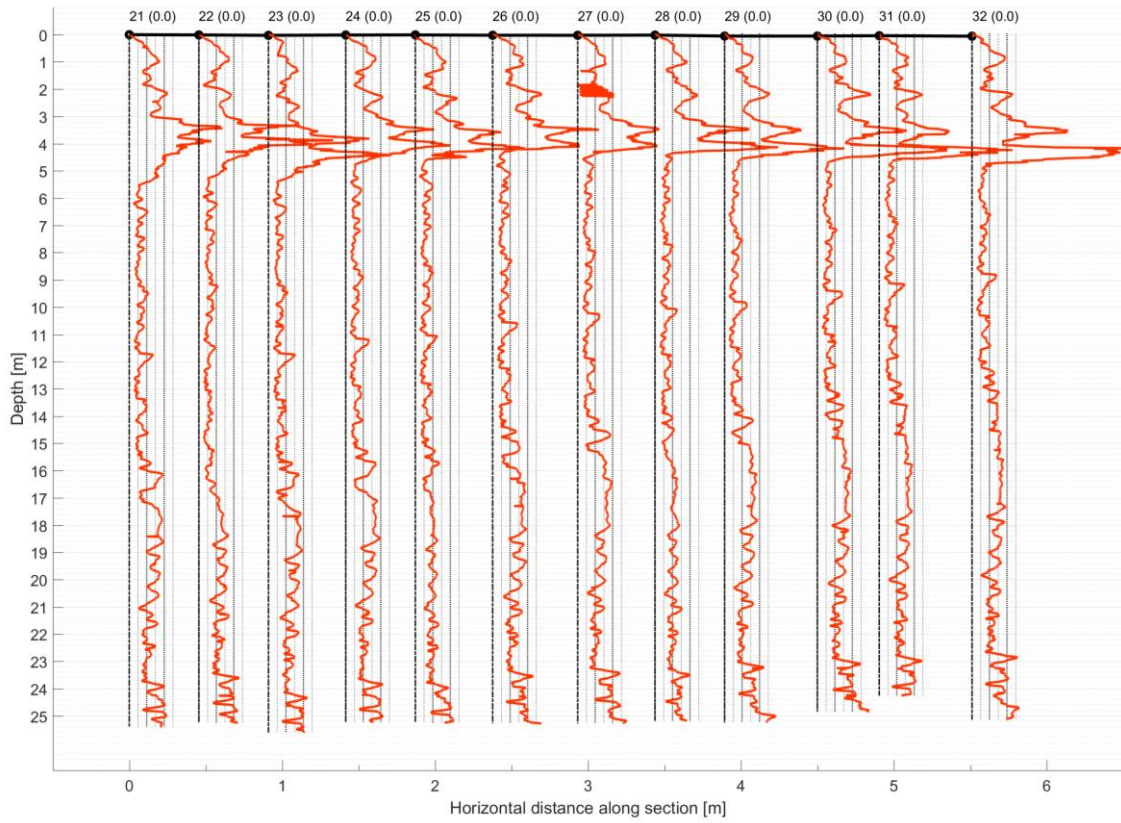


Figure 4.5 – Section plot of Section 1

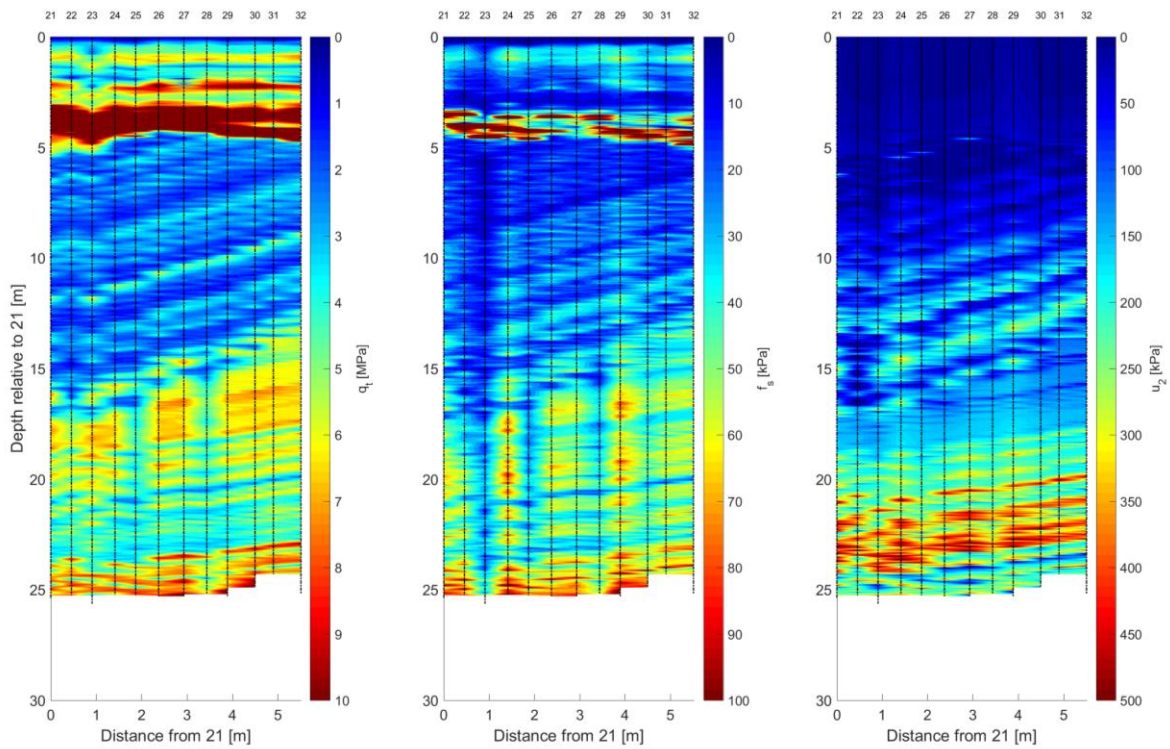


Figure 4.6 – Color map of Section 1

4.2. Determination of stratigraphic isolines along a section

4.2.1. Stratigraphic isolines

CPTUs were performed with a very high density at the Øysand site, e.g. distances between the tests in section 1 is only half a meter. With such small distances, it should be expected that the same characteristics of the measured profiles appear at neighboring CPTUs. However, these characteristics may not necessarily appear at equal depth. One may then form connections between these, from neighbor to neighbor. The term stratigraphic isoline is here made to describe the general idea of this connection. Isoline refers to a line, in this case along a section, where ideally conditions and properties are equal. Here, properties are rather close to equal. The assumption is supported by the geologic law of super-position. The properties of the soil are depth dependent, so these effects must be accounted for.

An illustration of the stratigraphic isolines along a section is presented in Figure 4.7. The colormap represents the gradual and continuous change of properties and how they connect to the neighboring sides. The black lines are stratigraphic isolines, though these are merely contour lines of the colormap. In this example the isolines at the top remain horizontal while at lower parts there is a downwards trend towards right. If one were to for example perform a CPTU test of the soil in the figure, both the leftmost side and the rightmost side, the lines represent the connection between the depth in which characteristics would appear. I.e., the CPTU on the left would show the equal characteristics at *smaller depths* than the CPTU on the right.

It must be emphasized that these stratigraphic isolines are not the layer boundaries, but rather a continuous link throughout the depth. However, after a discretization into a certain number of layers at one place along the section, the stratigraphic isolines at the top and bottom of each selected layer are layer boundaries.

The same materials will be found in an almost horizontal manner forming a continuous plane. Due to sedimentation, these planes will form on top of each other. Connections of points with the exact same characteristics can be made if spatial variability in the plane of equal material is neglected. These characteristics are determined from the combination of the magnitude and the fluctuation of the CPTU data measurements. The determination of these lines will be presented later.

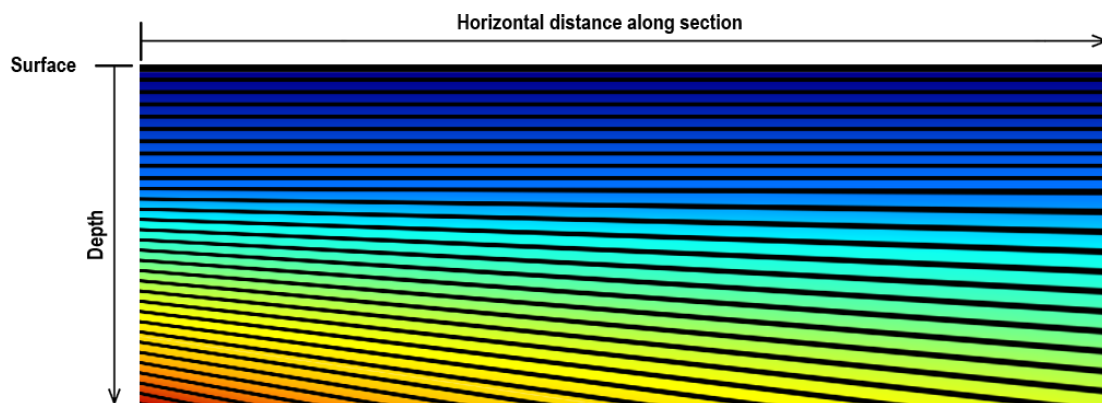


Figure 4.7 – Illustration of stratigraphic isolines

4.2.2. Using the cone resistance data to determine isolines

The CPTU does as stated give great stratigraphic resolution with the recorded values for q_t , f_s and u_2 . When multiple tests are performed one may use these values for each point to compare the tests. It is desired to use one of the three parameters to characterize the variation, so the quality of the measured parameters must be considered. The f_s value is known to be less reliable than the other parameters (Cabal & Robertson, 2014), thus it will not be chosen. Transitions between layers can be displayed by excess pore-pressure from the u_2 parameter and may be a good option. However, the q_t parameter has been found to be more effective in distinguishing the sedimentary facies than the u_2 measurement (Lafuerza et al., 2005). From Figure 4.6 it is evident that trends are visible for all three measurements, however trends such as for the coarser layers are more noticeable from the q_t data. Therefore the q_t data will be used to determine the soils characteristics.

4.2.3. Stratigraphic reference isolines

Trends along sections were characterized by effectively matching similar measurement points between sets of a section plot. By similar measurement points it is meant that the q_t -profiles have almost identical variations and value, for example peaks of similar shape and size. Similar variations and size can also be called the signature of the measurement (J. Powell & Quarterman, 1995). Lines were then drawn between these matched points. A such line is here called a *stratigraphic reference isoline* which is given the abbreviation SRL. The SRLs are only a part in the process of depth adjustment.

Making layer boundary lines is a normal procedure for geotechnical engineer when evaluating a section. However, isolines are as stated not equal to layer boundaries and neither are the SRLs. Layer boundary lines in practices is rarely made to this degree of accuracy as desired in the selection of these SRLs. The SRLs are assumed links between sets and merely a step in the process to accurately link all the CPTU results to the reference. The number of SRLs are not necessarily of importance, though the accuracy of the selected SRLs are. Selection of SRLs were done manually in this study, carefully and with and good understanding of the measurements. The following principles were used to ensure reasonable results:

- Pronounced points should preferably be selected, such as significant peak or valley points.
- One must not be determined to find a link when there might not be one. SRLs should only be made between obvious links.
- No SRLs may cross each other due to the nature of the sedimentation process (law of superposition).
- The SRLs should have a reasonable shape that conforms with the sedimentation process.
- Datapoints between selected SRLs should have the same characteristics.

The degree to which one can obey these principles largely depends on the distance between CPTU tests. This procedure is only applicable for rather densely spaced CPTUs, in the order of less than 20m.

SRLs for the illustration section presented in Figure 4.3 is added in Figure 4.8. Here, t_1 is chosen as the reference test which means that the depths of the SRLs at t_2 and t_3 will be given relative to t_1 . The SRLs were saved with absolute depths for the reference set and relative depth to the reference for the remaining sets. This was done to better keep track of depths due to the later inclusion of *depth*

adjustment. Note that this example includes a very crude set of datapoints and that the uppermost SRL does not follow the first principle mentioned above. It is included none the less for illustrational purposes.

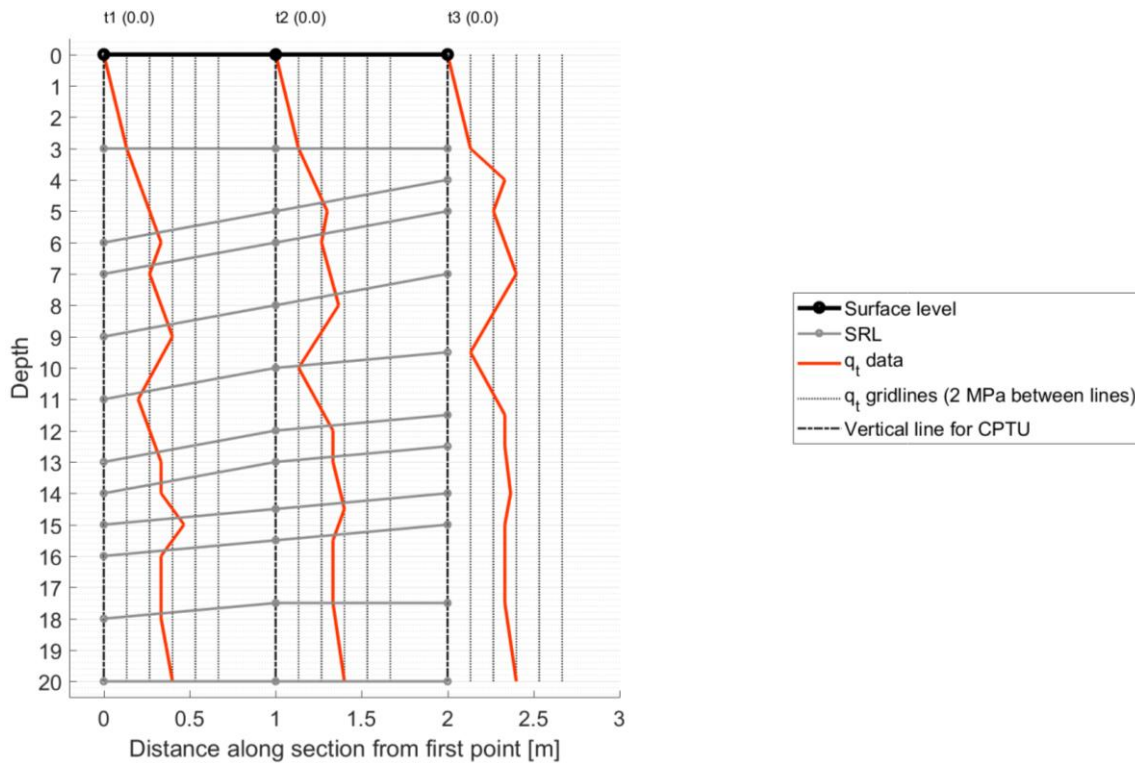


Figure 4.8 – Illustration section plot with chosen SRLs

From the SRLs the isoline inclination was determined. The inclination was denoted $I(z_{ref})$ where z_{ref} is the depth at the reference measurement. For example, from Figure 4.8 the inclination of the second SRL from the top is $I(z_{ref} = 6m) = 1$. If the SRL is not linear the inclination is found through regression. The direction of the river progradation was found from these isoline inclinations. According to the river description of Gilbert (1885), the direction is the opposite direction to where the foreset bed inclination is the greatest. The determined inclination of the foreset bed together with the direction of the section was used to find the river progradation direction. The direction of the section was called θ , which is the angle between the east direction and the evaluated section, going counterclockwise. E.g., a section towards east has $\theta = 0$ while a section towards north has $\theta = 90^\circ$. The sections evaluated in this study are very closely spaced and many sections are overlapping. Thus, it was reasonable to assume a constant linear foreset inclination rather than a fan shape showing in Figure 2.3 (a). The assumed one-directional foreset slope inclination was defined by equation (4.1) where I_f indicates the inclination of the foreset bed.

$$I_f(\theta) = I_{f,max} \cdot \cos(\theta - \theta_{shift}) \quad (4.1)$$

Here, $I_{f,max}$ and θ_{shift} are respectively the maximum expected foreset slope inclination and the direction of the maximum slope inclination. These are both fitted to the data points.

4.3. Depth adjustment

4.3.1. Concept

A procedure was made to adjust multiple measurements to match a selected reference measurement using the selected SRLs. This was necessary to be able to determine the accuracy of the CPTUs. The depth adjustment is not a correction procedure but is rather a method to remove trends and allow for comparison of measurements where equal properties are encountered.

Figure 4.9 illustrates the concept, showing how the measured, non-adjusted values (a) are to be adjusted to match the selected reference (b) which is here *t1*. This is done through what is called the z_{rel} values (c), the relative vertical distances at each depth between the evaluated profile and the reference profile. The relative vertical distance is explained in the next chapter.

The three recorded values q_c , f_s and u_2 are measured with depth with a certain vertical distance. Values are in this study interpolated to a vertical distance of every 10mm, as mentioned. So, the data from each CPTU after corrections is four vectors; a depth vector, \bar{z} , and a vector for each of \bar{q}_t , \bar{f}_s and \bar{u}_2 . The bar implies that these are vectors. The depth vector is then going from the start depth to the end depth with an interval of 10mm. The other three vectors are directly related to the depth vector and has the same number of values. By simply adjusting the depth vector \bar{z} without changing the other measurement vectors, one can go from (a) to (b) in Figure 4.9. The adjusted depth is then found through equation (4.2):

$$\bar{z}_{adj} = \bar{z} - \bar{z}_{rel} \quad (4.2)$$

Here, \bar{z}_{adj} is the adjusted depth vector, where the depths of the measurements are adjusted to fit the reference measurement. \bar{z} is the original depth vector and \bar{z}_{rel} is the relative vertical depth vector.

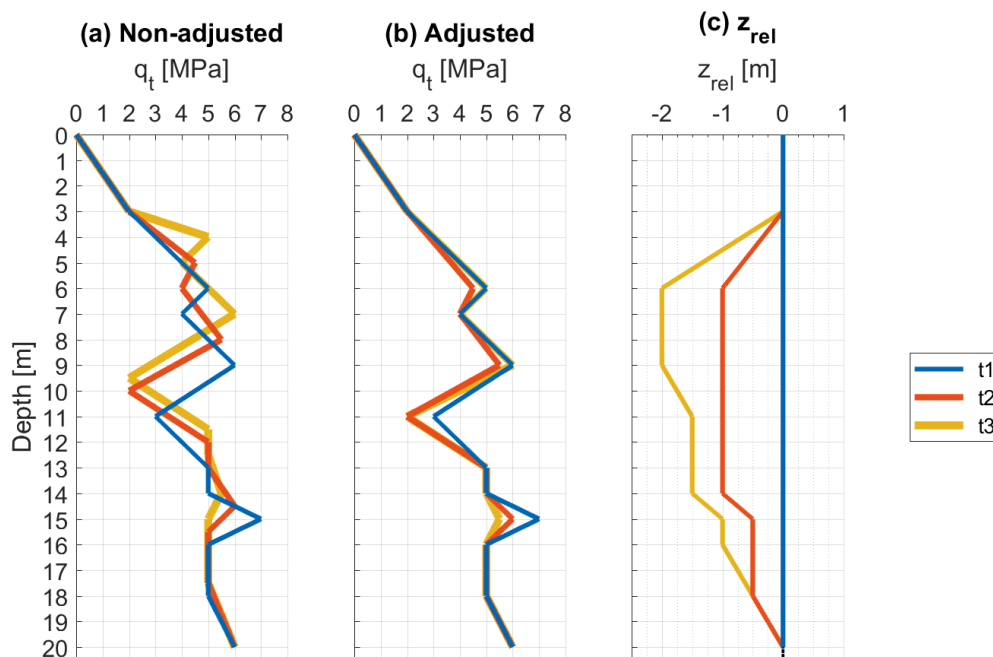


Figure 4.9 – Illustration section set with and without depth adjustment relative to *t1*

4.3.2. Relative vertical distance, z_{rel}

The stratigraphic reference lines described in 4.2.3, where data points at certain depths were linked together, were used to find the z_{rel} value.

Figure 4.3, Figure 4.8 and Figure 4.9 present the same three demonstration data series $t1$, $t2$ and $t3$. These are combined in Figure 4.10 which is used to better describe the procedure. From this figure 11 SRLs were defined. For each SRL, a value for z_{rel} can be defined per CPTU the SRL includes. The general formula for a value of z_{rel} is presented in equation (4.3).

$$z_{rel,n}(z_{ref}) = z_{SRL,n}^j - z_{SRL,ref}^j \quad (4.3)$$

Here, $z_{SRL,n}^j$ is the depth of the at SRL number j for CPTU n and $z_{SRL,ref}^j$ the depth of the same SRL for the reference measurement. I.e., z_{rel} is a value of *how much deeper* the evaluated point is compared to the reference.

E.g., looking at the first SRL in Figure 4.10, at $3m$ depth for $t1$, $t2$ and $t3$ the z_{rel} values are found to be:

$$z_{rel,t1}(3m) = z_{rel,t2}(3m) = z_{rel,t3}(3m) = 3m - 3m = 0 \quad (4.4)$$

Note that the z_{rel} is a function of the depth of the reference set, i.e. in this case $t1$. It can be seen on the z_{rel} figure below that at depth $3m$ all values are 0. Then, looking at the fifth SRL, which is at depth $11m$ for $t1$, the values are

$$z_{rel,t2}(11m) = 10m - 11m = -1m \quad (4.5)$$

$$z_{rel,t3}(11m) = 9.5m - 11m = -1.5m \quad (4.6)$$

These values can be seen in the z_{rel} plot in Figure 4.10 for each of the three tests. Naturally, when using this method for the $t1$ set all values for z_{rel} become 0 as it is the reference. Between the values of the SRLs a linear interpolation is performed such that z_{rel} becomes a vector of equal length as the depth vector z . What this means in practice is that measurements are stretched or compressed between the assumed known positions that the SRLs link together. The value of z_{rel} can be assumed to be 0 at the surface.

The found relative depth vector, $\bar{z}_{rel,n}$ is then used for depth adjustment as presented in equation (4.2) as visualized in Figure 4.9. Depth dependent expressions, such as z_{rel} is hereafter considered as functions of depth rather than vectors when there is no accent to the symbol. The adjusted depth as a function of the non-adjusted depth, $z_{adj}(z)$ from equation (4.2) becomes equal to the reference depth function, z_{ref} . This is the case since the depth adjusted measurement is transformed into the reference measurement. There are some identities with the function z_{rel} that is useful to be aware of. When the derivative of this function is zero, $\frac{dz_{rel}}{dz_{ref}} = \frac{dz_{rel}}{dz_{adj}} = 0$, the measurement is neither stretched or compressed when depth adjusted, i.e. it is either unchanged or translated. Where the derivative is negative the measurement will be stretched, while where the derivative is positive, the measurement is compressed.

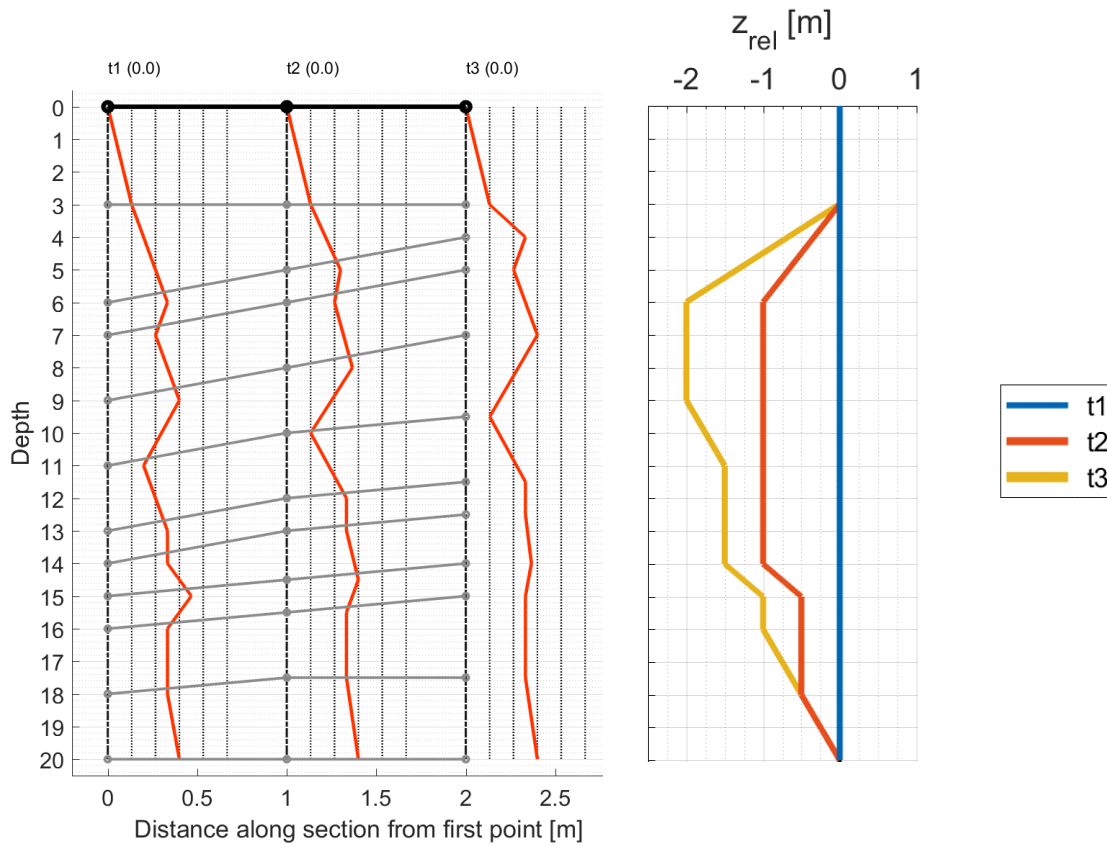


Figure 4.10 – Combination of Figure 4.8 and Figure 4.9, section plot to the left and z_{rel} to the right

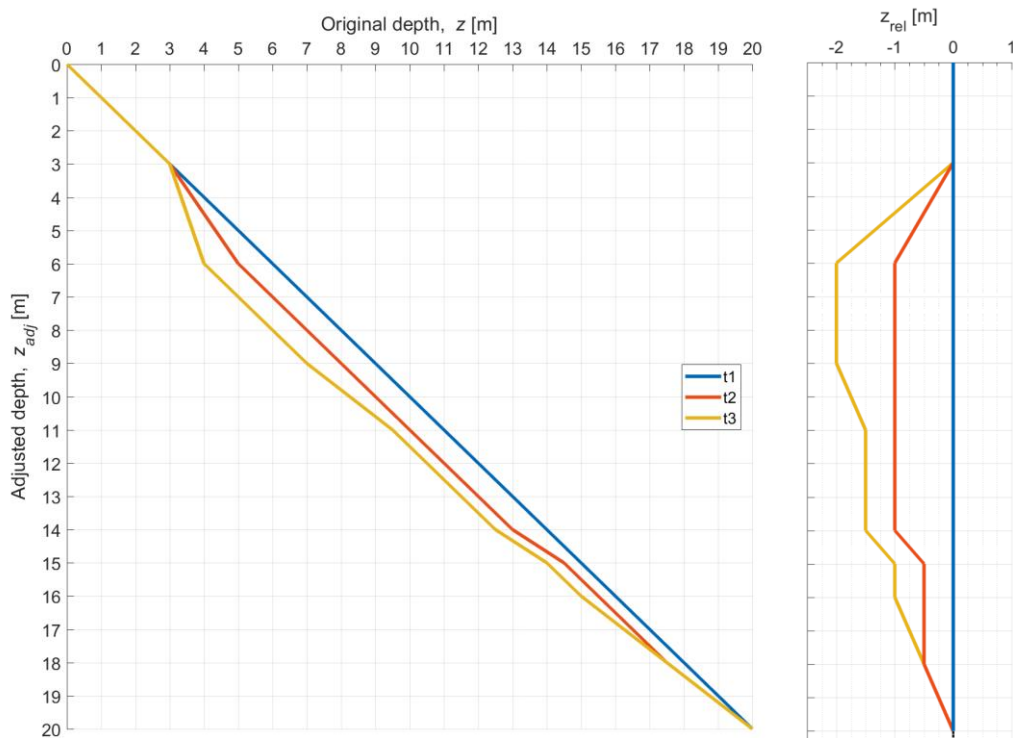


Figure 4.11 – Original depth vs adjusted depth (left) and z_{rel} plot (right)

Figure 4.11 presents the adjusted depth as a function of the original (non-adjusted) depth on the left and the z_{rel} plot to the right. The function of the adjusted depth is known from equation (4.2) to be the original depth minus the z_{rel} . From the figure it can be seen how the z_{rel} function and the adjusted depth as a function of the original depth is the same when the reference depths are subtracted. If the value of z_{rel} is constant and equal to zero, then the adjusted depth will be increasing at a constant 1:1 ratio, which is the case for $t1$.

An important property of the adjusted depth as a function of the original depth is that it is *monotonic increasing*, since SRLs cannot cross each other (due to the law of super-position). Therefore, the largest possible slope inclination in the left of Figure 4.11 is close to a vertical line, while the minimum slope inclination is close to a horizontal line. These two requirements can be expressed with $0 < \frac{dz_{adj}}{dz} < \infty$. The two boundary cases are (I) $\frac{dz_{adj}}{dz} = 0$ and (II) $\frac{dz_{adj}}{dz} = \infty$. Case (I) implies that while with an increasing original depth, the adjusted depth remains the same. I.e., there will be a large compression of values to an almost singular point. Case (II), on the other hand is when there is a large stretching of what originally is an almost singular point. These two cases can be found from the relative vertical depth function with the adjusted depth, $z_{rel}(z_{adj})$. As previously mentioned, the adjusted depths convert the measured profile into the reference profile, thus z_{adj} is equal to z_{ref} . The relationship between the slope of $\frac{dz_{adj}}{dz}$ related to $\frac{dz_{rel}}{dz_{adj}}$ is presented in through the three equations below.

$$\frac{dz_{adj}}{dz} = \frac{d}{dz}(z - z_{rel}) = 1 - \frac{dz_{rel}}{dz} = 1 - \frac{dz_{rel}}{dz_{adj}} \cdot \frac{dz_{adj}}{dz} \quad (4.7)$$

$$\frac{dz_{adj}}{dz} \cdot \left(1 + \frac{dz_{rel}}{dz_{adj}}\right) = 1 \Leftrightarrow \frac{dz_{adj}}{dz} = \frac{1}{1 + \frac{dz_{rel}}{dz_{adj}}} \quad (4.8)$$

$$\frac{dz_{rel}}{dz_{adj}} = \frac{1}{\frac{dz_{adj}}{dz}} - 1 \quad (4.9)$$

The resulting slopes of $\frac{dz_{rel}}{dz_{adj}}$ for the two cases will then become:

$$\begin{aligned} \text{(I)} \quad \frac{dz_{rel}}{dz_{adj}} &= \frac{1}{0} - 1 = \infty \\ \text{(II)} \quad \frac{dz_{rel}}{dz_{adj}} &= \frac{1}{1/\infty} - 1 = -1 \end{aligned} \quad (4.10)$$

This means that if the function z_{rel} increases very rapidly, $\frac{dz_{rel}}{dz_{adj}} \approx \infty$, the values will be compressed when depth adjusted. If the function z_{rel} decreases with a slope of close to -1 , then values will be stretched greatly.

To further emphasize these two cases, a rather extreme example is presented in Figure 4.12 and Figure 4.13. These may be called extreme cases due to the amount of stretching and compressing being done. The two cases are apparent and marked in the figures.

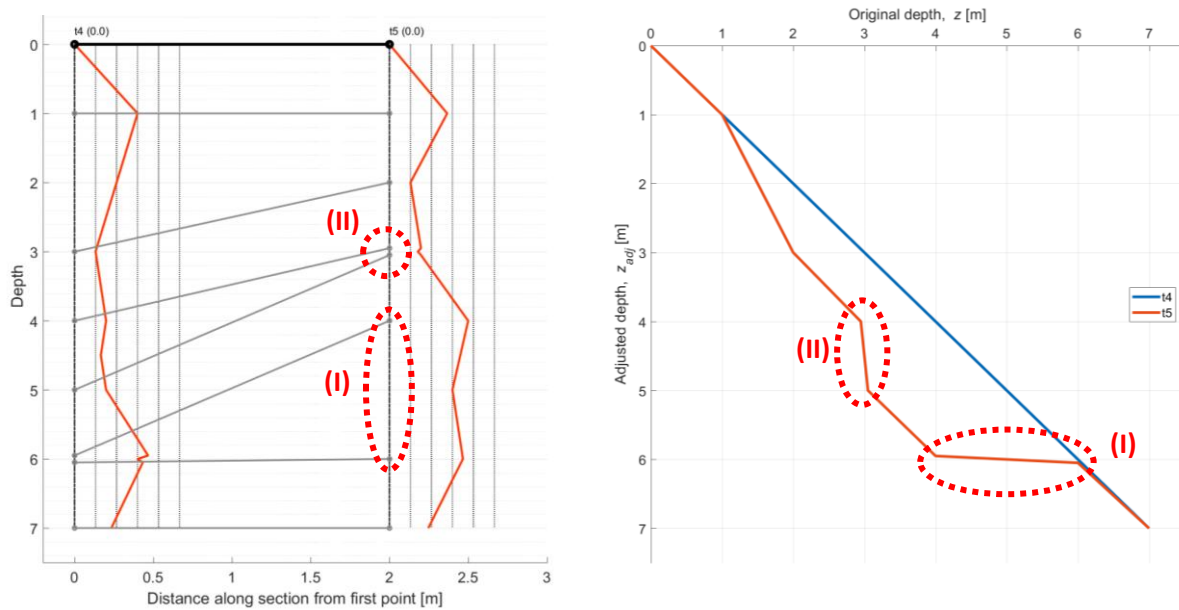


Figure 4.12 – Illustration section plot (left), original depth vs adjusted depth (right)

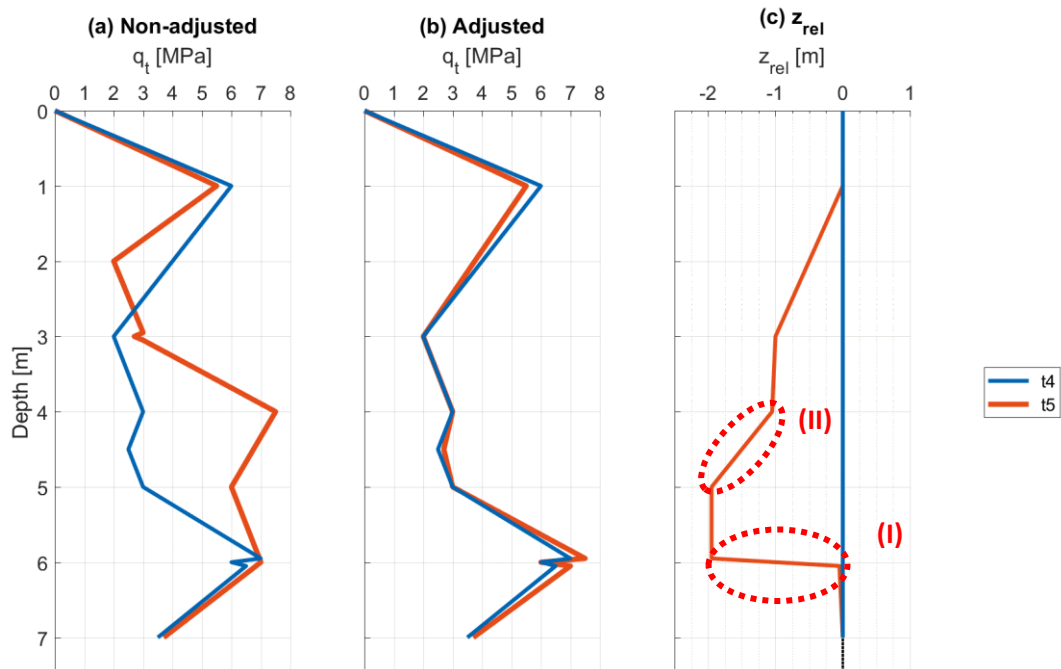


Figure 4.13 – Illustration section set with and without depth adjustment relative to t4

4.3.3. Depth normalization

The values of q_t and u_2 are expected to be dependent on parameters that vary with depth and should thus be normalized when adjusted with depth. CPTU measurements should be corrected for the overburden stress and there are multiple procedures to do so. Sophisticated methods are available for such a normalization (Moss et al., 2006). However, this study did not use the CPTUs for parameter determination and a simpler normalization was used.

The normalized value of the tip resistance is q_{net} , the excess pore pressure, Δu or Δu_2 , is used for the pore pressure measurement, while the side friction, f_s , is not depth normalized. The formula for these parameters is presented below.

$$q_{net} = q_t - \sigma_{v0} \quad (4.11)$$

$$\Delta u = u_2 - u_0 \quad (4.12)$$

σ_{v0} is the overburden total stress and u_0 is the hydrostatic pore-pressure. At Øysand the groundwater table is found to be at 2m depth. The total stresses were determined using the found unit weights at the site, presented in Figure 3.2. From the Øysand characterization article, the average unit weight was chosen as $20kN/m^3$. The resulting stresses at Øysand are presented in Figure 4.14.

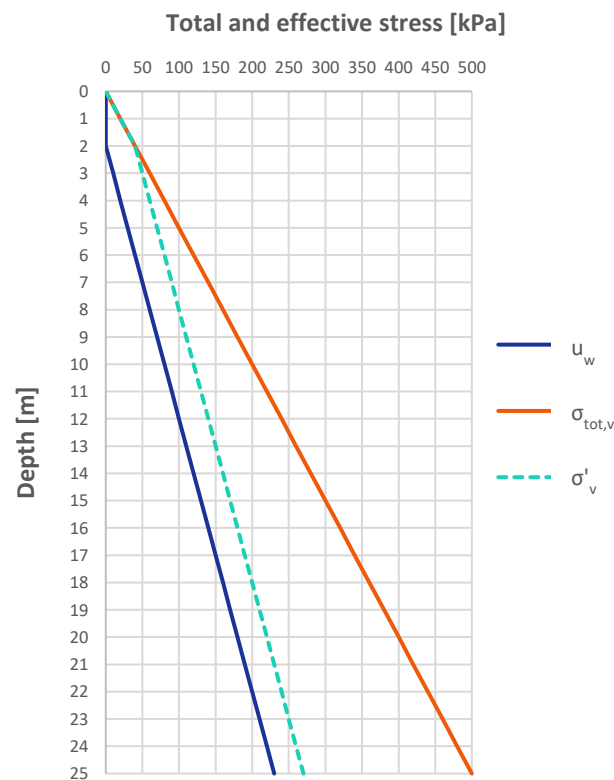


Figure 4.14 – Total and effective stresses used at Øysand

4.3.4. Interpolated adjusted values

After the values were adjusted for depth, the data was interpolated such that the adjusted data again contained data with a constant 10mm spacing. This was done through linear interpolation where the values of q_{net} , f_s and Δu were interpolated based on the adjusted depth vector, z_{adj} .

Figure 4.15 (a) illustrates a realistic set of measurements with data values X for both a reference and the evaluated test. The dots represent the values in the measurement, with lines drawn in between. The horizontal grey lines represent the chosen sampling distance. Figure 4.15 (b) show the adjusted values through the procedure presented in 4.3.2 and fit well. Note how the adjusted depths of the data points in (b) does not fit the horizontal grey lines. The interpolation is done in Figure 4.15 (c). The values then fit with the constant distance of 10mm . The significance of performing this interpolation is that it allows data to be related and compared through vector calculations.

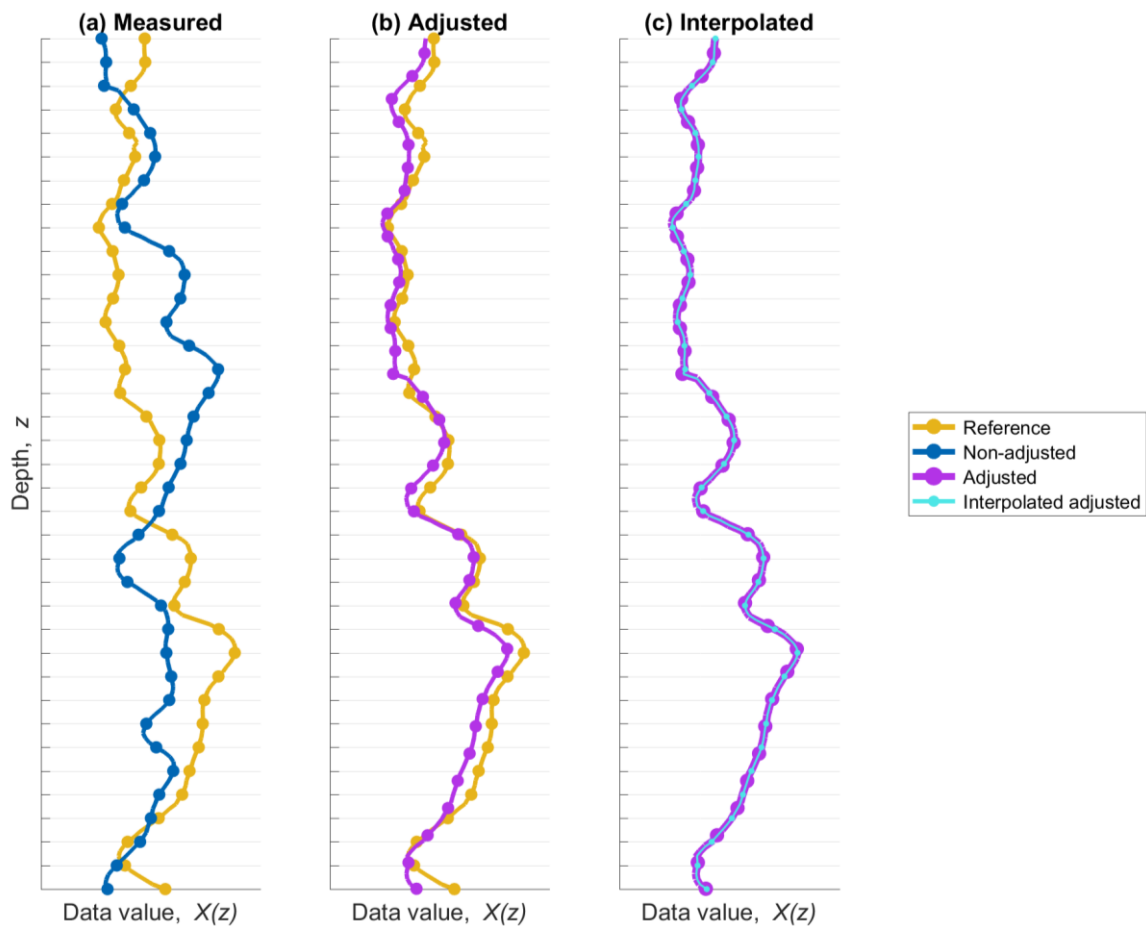


Figure 4.15 – Explanation of the depth adjustment

4.4. Accuracy of depth adjusted CPTU measurements

The quality of the q_t , f_s and u_2 measurements were evaluated after depth adjustments were done. The intention was to find the most reliable and reproducible parameter of the three in deltaic sands, as well as determining the effect of using different cone types. This was done with the assumption that the depth adjusted data represents the exact same material at the same depth. Differences in the measurements was then assumed to be due to the equipment.

The evaluation of the accuracy of the equipment was done with respect to the cone type, as the inaccuracy was expected to be different between cone types. Nine different cone types were used at Øysand. Section 1 includes five different types while section 2 and 4 each uses a unique cone type, as shown in Figure 3.4. If CPTU 09 is excluded from section 3, only a single cone type was used for this section as well. The last cone type was only used for CPTU 50, 51 and 52, though these tests were not evaluated as the tests were performed somewhat far away from the other cones. Thus, section 1 through 4 was used to determine the influence of the cone type on the results. Table 8 presents the CPTUs for each cone type that will be compared. The horizontal distances between the CPTUs with the same cone type are small, as seen in the table. An assumption of little or no property variation over this distance is reasonable for such distances after the trend removal through depth adjustment.

Table 8 – List of CPTUs for each cone type

Cone type	Section	CPTUs (reference CPTUs in bold)	Max. horizontal distance between CPTUs
3	1	23, 30	3,6m
4	1	26, 32	3,1m
5	1	22, 25, 28, 31	4,5m
11	1	24, 29	2,5m
12	1	21 , 27	2,9m
1	2	34 , 35, 37, 38	6,0m
6	3	39, 40 , 41A, 41B, 42A, 42B	4,5m
7	4	43 , 44, 45	4,0m

Comparisons between different cone types were done for section 1, since five different types were used in this section. The evaluation of the results of these cone types consisted of two measures – their *accuracy* and their *precision*. Precision was here considered as the similarity between tests using the same cone type, and accuracy as the similarities between different cone types. The accuracy was measured by how the *representative profiles* of each cone type compares to the others. This representative profile was found in the same way as in the other NGTS articles, however depth adjustments were not found in those. The formula of the representative value is presented in equation (4.13), where the symbol X is used as a general sign for the tree values q_{net} , f_s and Δu . Furthermore, a superscript c was used to indicate that the parameter relates to cone type c . I.e., the representative value is the mean of values of the m number of CPTUs with the same cone type at each depth, z_{adj}^i . As described in the previous chapter, it was important to interpolate the values at a constant vertical distance after depth adjustment. Then the representative values were found through vector multiplication.

$$X_{rep}^c(z_{adj}^i) = \frac{1}{m} \cdot \sum_{n=1}^m X_n^c(z_{adj}^i) \quad (4.13)$$

The precision was in this case a measurement of how similar the different CPTU profiles with the same cone types were. This was measured by the standard deviation, s , of the values of the same cone type at each depth, z_{adj}^i , as shown in equation (4.14).

$$s^c(z_{adj}^i) = \sqrt{\frac{1}{m-1} \cdot \sum_{n=1}^m (X_n^c(z_{adj}^i) - X_{rep}^c(z_{adj}^i))^2} \quad (4.14)$$

The values of the precision, s^c , was then averaged for the entire bed type, i.e., the topset, foreset or bottomset bed. The transition zones (case (I) and case (II)) between the bed types were disregarded. Assumption of bed type boundaries was done based on the characteristics of the different beds. The measurement of the precision was then done in a comparative form for each of these three parts. The average standard deviations of the bed type are given in equation (4.15). s_{avg} is the average standard deviation, l is the length of the bed (topset bed, foreset bed or bottomset bed) and i_1 and i_2 are the first and last depth index of the bed, respectively. The s_{avg} was found for each of the parameters q_{net} , f_s and Δu .

$$s_{avg}^c = \frac{1}{l} \cdot \sum_{i=i_1}^{i_2} s^c(z_{adj}^i) \quad (4.15)$$

The intention was to find the most precise cone type for each of the three parameters at each of the three beds. Similar to the evaluated precision, the resulting accuracy was measured for each parameter and bed.

The expected true profile was found from the average profile of the representative profiles, $X_{rep,avg}$. The value is given as presented in equation (4.16), where p is the total number of cone types evaluated.

$$X_{rep,avg}(z_{adj}^i) = \frac{1}{p} \cdot \sum_c X_{rep}^c(z_{adj}^i) \quad (4.16)$$

The accuracy was then determined for each cone type based on the representative profile. This accuracy was determined as the average value of error for a bed type and was called e_{avg}^c . The value was found as presented in equation (4.17). $\hat{X}_{rep,avg}$ is a non-depth normalized parameter, e.g. q_t instead of q_{net} for the cone resistance. The accuracy is quantified by e_{avg}^c since a lower means a better accuracy.

$$e_{avg}^c = \frac{1}{l} \cdot \sum_{i=l_1}^{i_2} \frac{|X_{rep}^c(z_{adj}^i) - X_{rep,avg}(z_{adj}^i)|}{\hat{X}_{rep,avg}(z_{adj}^i)} \quad (4.17)$$

A qualitative evaluation of the precision was done for the remaining sections (2, 3 and 4). The most reliable and reproducible parameter in deltaic soils was found through comparison of the five representative profiles of section 1.

5. Results

5.1. Determined SRLs

The method of selecting SRLs was followed for section 1 to 10 and 12. Figure 5.1 presents the section plot for section 1 including the selected SRLs, while the remaining section plots are found in the AppendixA1. As many as 33 SRLs were selected for section 1, and arguably even more lines could have been selected. However, the objective with the method is to select enough SRLs such that clearly matching parts of the sets were connected rather than to find possible matches. The resulting SRLs have trends that seem to conform with each other. The confidence in the selection is therefore satisfying.

A measure of the quality of the SRLs is that the values between the SRLs should be matching. In the case of section 1, this is satisfied with the exceptions of the discontinuous parts, on the boundary between the topset and foreset bed as well as between the foreset and bottomset bed. Looking at the two SRLs close to a depth of 17m at set 21, it is evident that there is an interface between these. At set 21, the distance between these two SRLs is about 0.3m, though at set 32 the distance is 2.6m. This is likely due to that the interface between the foreset and bottomset bed lies here. The interface between the topset and foreset bed seems to lie at about 4.5m depth.

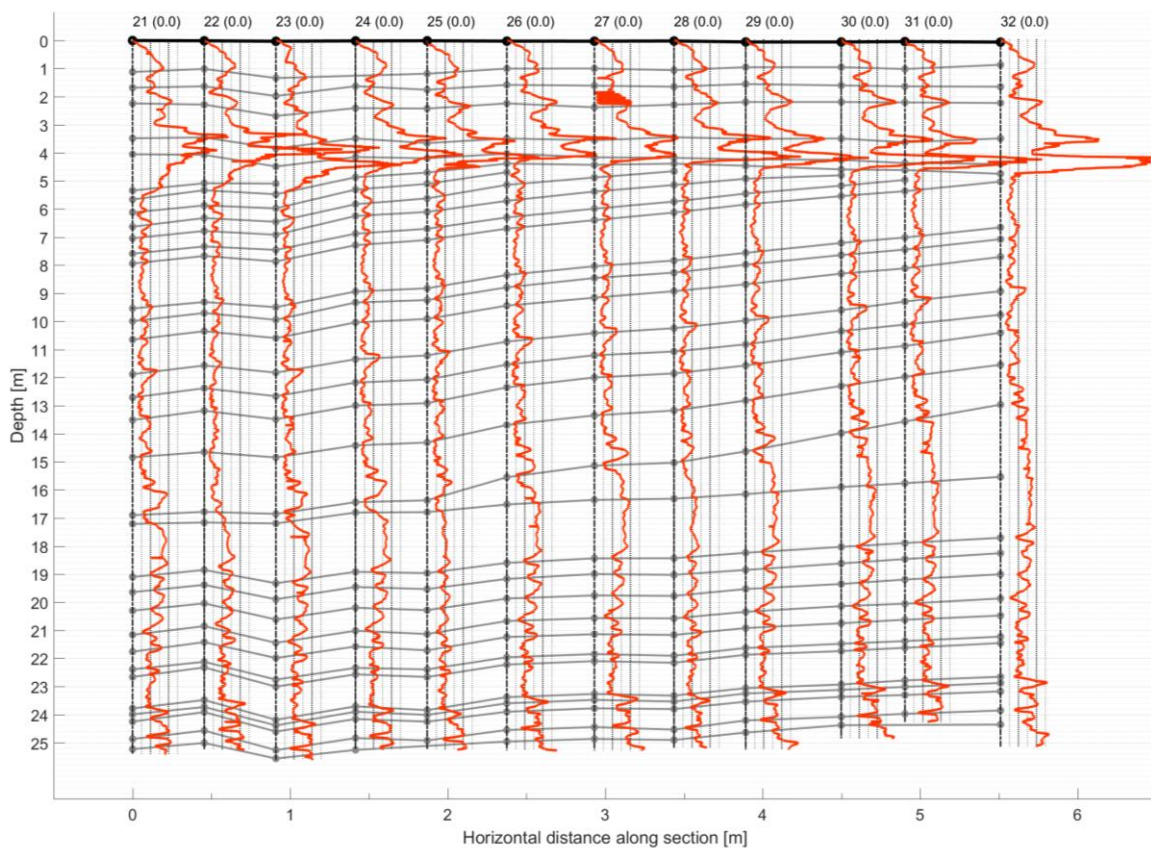


Figure 5.1 – Section plot of section 1 with SRLs

5.2. Depth adjusted data

The procedure of depth adjustment was followed with the determined SRLs for each section. Figure 5.2 presents the depth adjusted data for section 1. Depth adjusted data for the remaining sections is presented in the Appendix.

From the z_{rel} values of Figure 5.2 one can see how there are three different parts with close to constant z_{rel} value with depth. One from the top to about $4m$ depth, the next from between $4m$ and $8m$ to $17m$ and the last below $17m$. The value of z_{rel} for the first is close to zero, the middle has a decreasing value for increasing distance to the reference set. The last also decreases with increasing distance to the reference, though much less than the middle part. These three parts reflect the properties of the topset, foreset and bottomset, respectively.

Between these beds, i.e. $4m - 8m$ and at $17m$ are intermediate zones. The values between $4m$ and $8m$ have values of z_{rel} that decreases with an almost constant slope of about -1 . As presented in equation (4.10), this reflects boundary case (II), i.e. a slope of -1 means that values are stretched significantly. At about $17m$, all z_{rel} lines have a sudden increase, making this a case (I), where values are greatly compressed compared to the reference.

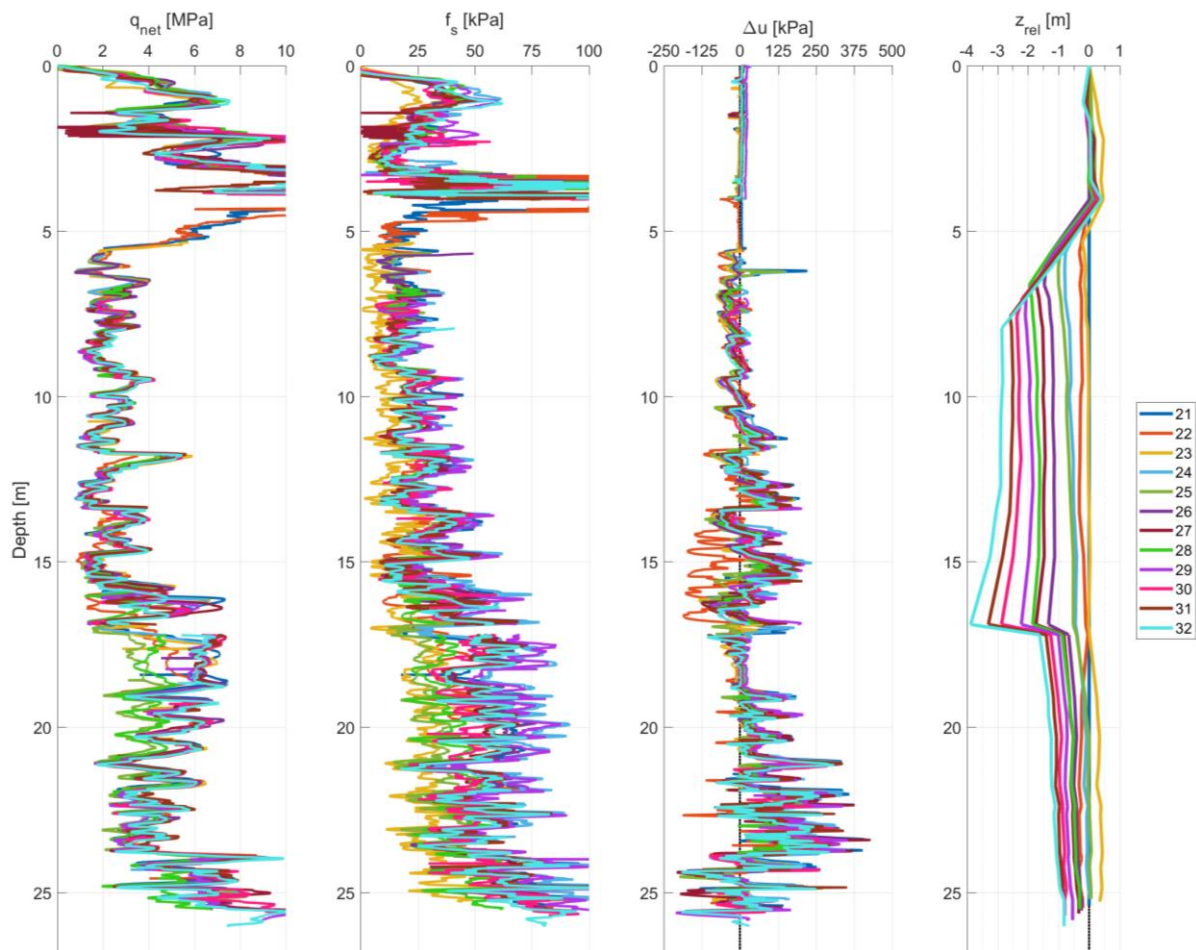


Figure 5.2 – Depth adjusted data for section 1

The values where the slope of z_{rel} is close to either of the two boundary cases are hidden in these figures. This is done to avoid the disordered information caused by large stretching and compressing that occurs in these two intermediate zones. Some measurements are therefore broken up.

A colormap of the depth adjusted data of section 1 is presented in Figure 5.3. In line with the concept of depth adjustment, this figure shows how there are no non-horizontal trends along the section. The exception is the transition zone between the topset and foreset beds, at about 5m and increasing along the section. Unlike in Figure 5.2, the values at the boundary cases (I) and (II) are shown, though these values should be regarded due to the fact of stretching mentioned above.

The colormap of the q_{net} (or q_n) in Figure 5.3 demonstrates how the depth trends are adjusted for compared to the non-adjusted data of section 1 seen in Figure 4.6. Values of f_s and Δu express the same.

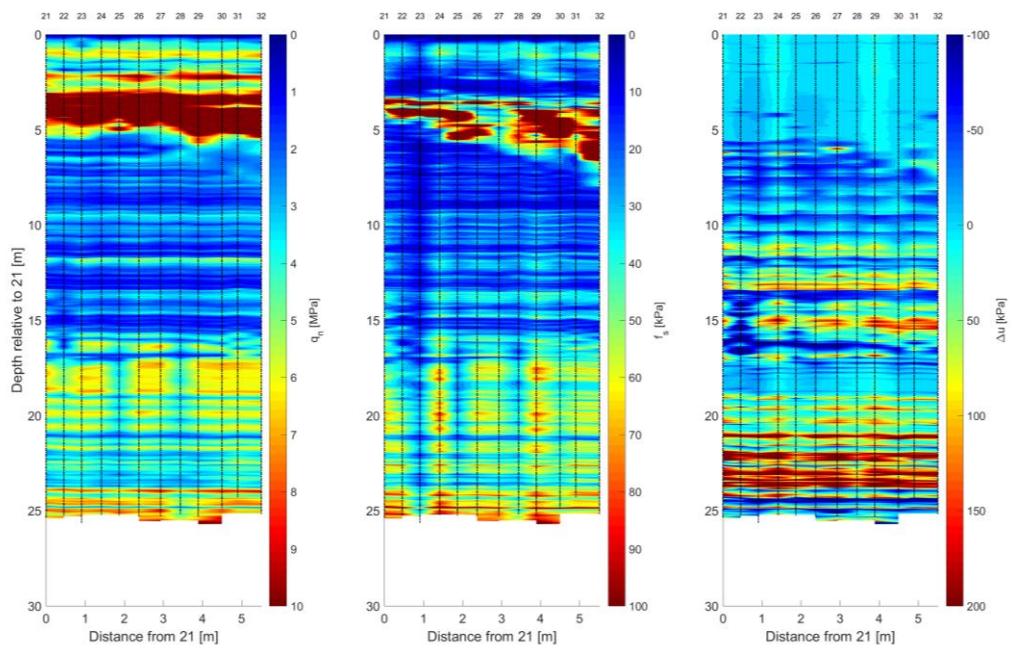


Figure 5.3 – Adjusted colormap plot of section 1

5.3. Trends along sections

5.3.1. Isolines for sections

Colormap of isolines was made for each section based on the z_{rel} functions. Equation (4.2) was used to find the relationships between the depths forming isolines. It was used by subtracting the z_{rel} value for the reference depth values, i.e. a reformulation of the equation. Contour lines were then drawn on top, forming isolines. The vertical distance between the isolines are constant at the reference measurement since the z_{rel} function is constant and equal to zero.

Figure 5.4 presents three of these isoline plots, from section 1, 2 and 5. The vertical dashed line represents the location of the reference measurement. Three section groups were presented, the East-West containing section 1 to 4, the South-North containing 5 to 7 and the rest, 8 to 12. Figure 5.4 includes two from the East-West direction and one from the South-North direction. The isoline for section 1 and 2 show a very evident trend below about 5m, and they appear to merge at this depth on the right side. On the other hand, isolines of section 5 shows no well-defined trend.

5.3.2. SRL inclination for sections

From Figure 5.4 it is evident that the inclination in the layers are different in the two different directions. The top 4 – 5m, which is characterized as the topset, are horizontal for both. However, the below this the sections in the E-W direction show a much stronger tendency of an inclination in the direction of the sections. These tendencies of inclination of the isolines were quantified through the slope inclination of the SRLs, which was defined as the function $I(z_{ref})$, found through regression. A positive inclination means that the slope is increasing in the direction defined for the section in 4.1. The slope inclination of each of the three groups, East-West, South-North and the rest are presented in Figure 5.5, from top to bottom respectively. These plots clearly show different characteristics indicating that the direction influence the bedding inclination.

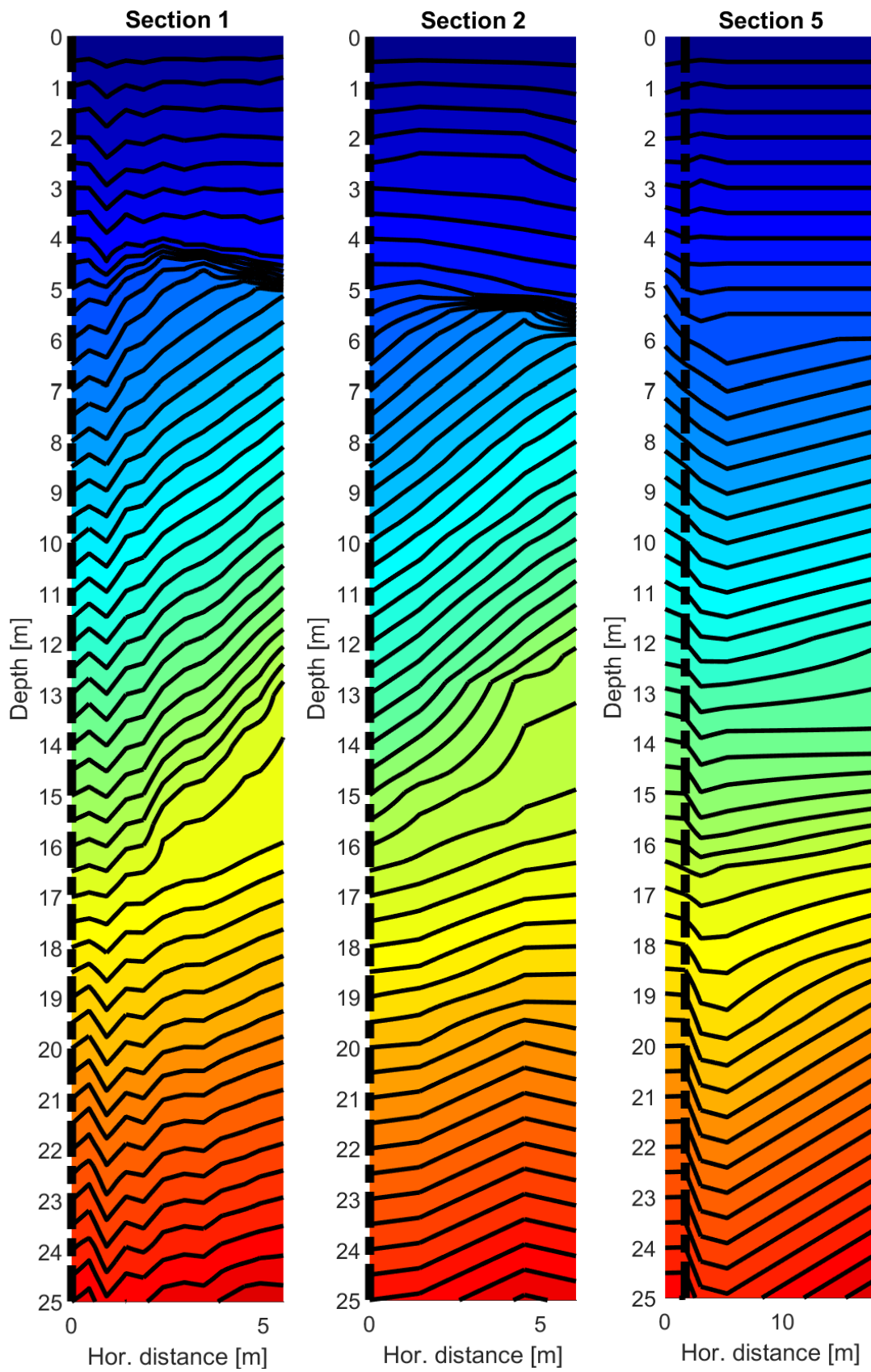


Figure 5.4 – Stratigraphic isolines along the sections 1, 2 and 5

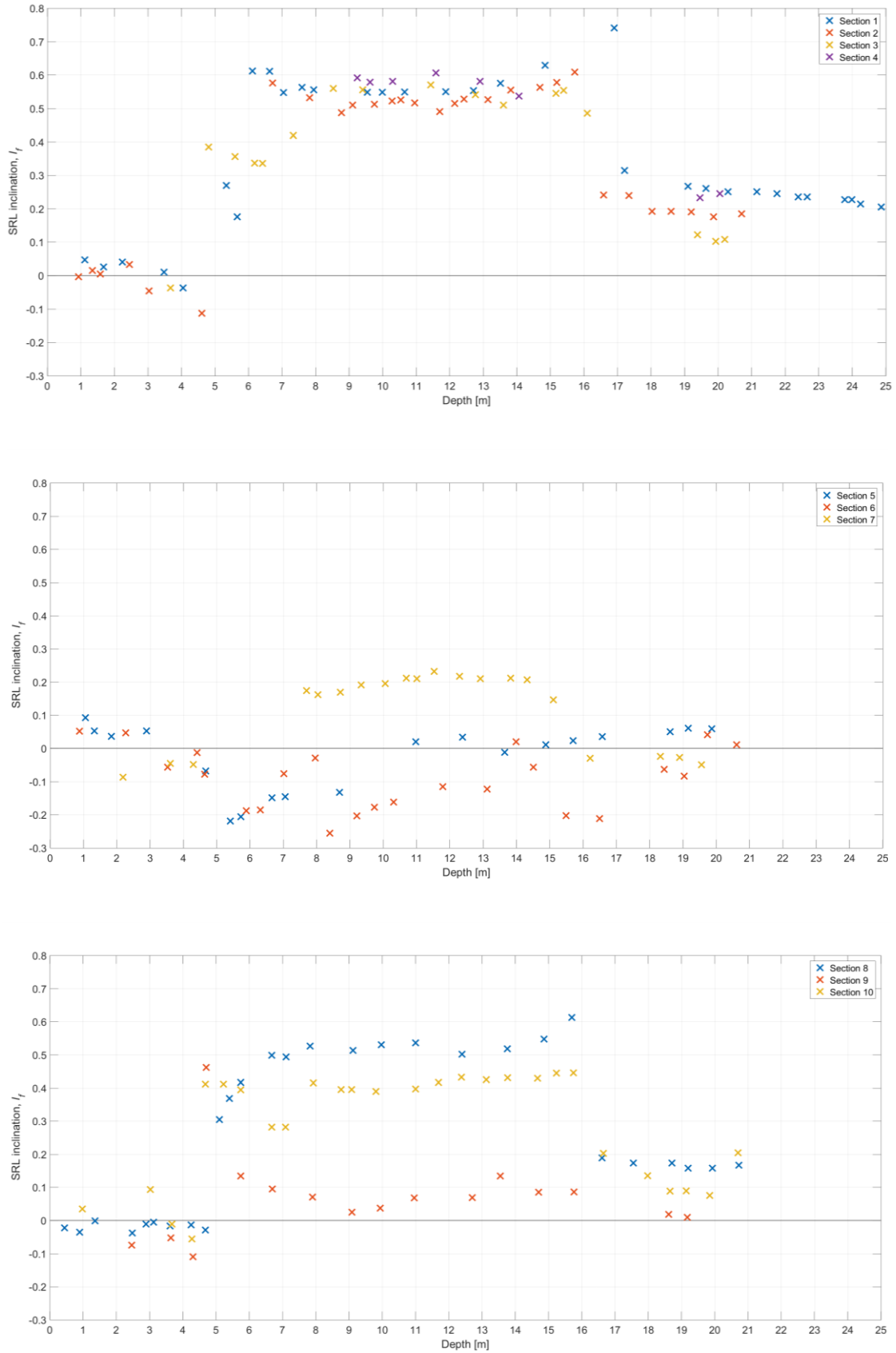


Figure 5.5 – Slope inclination for section 1-4 (top), 5-7 (middle) and 8-10 (bottom)

5.3.3. The direction of progradation at Øysand

The foreset bed slope inclination of each section was found using the values from Figure 5.5. This value, which was called I_f in equation (4.2), is the average of these SRL inclinations along the foreset bed. The depth of the foreset layer varies with each section but is selected between depths of about 6m and 16m. The values of I_f was plotted together with the direction of the section forming datapoints, where the angle, θ , can be found from Figure 4.1 and Figure 4.2.

Figure 5.6 shows these datapoints of I_f values for section 1 – 10 together with the equation (4.1). The values of $I_{f,max}$ and θ_{shift} that gave the best fit was found. The resulting values of $I_{f,max}$ was 0,55 and the angle of the steepest inclination, θ_{shift} , was found to be 0.

The direction of the river propagation was from this found to be directly towards west. The foreset bed slope inclination, which reflect the angle of repose, is about 29°.

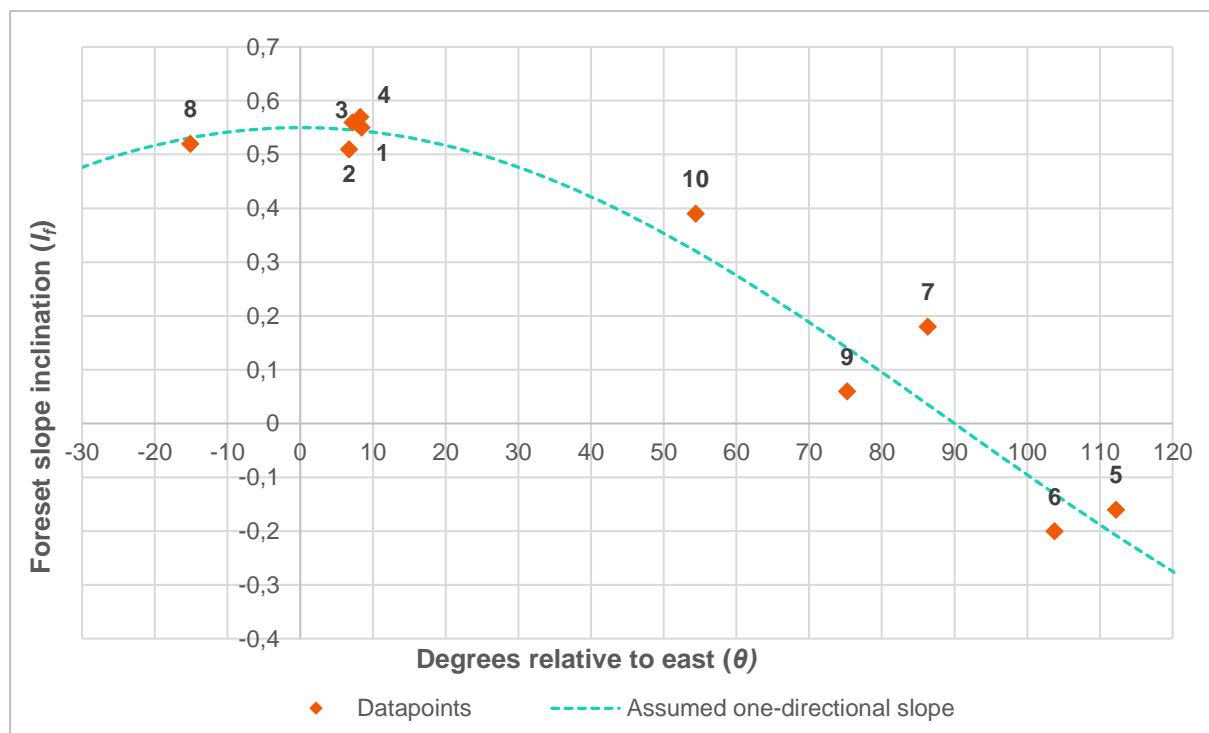


Figure 5.6 – Foreset bed slope inclination of sections by direction

5.4. Determined precision for cone types on depth adjusted CPTU measurements

The precision of the cone types was found as described in chapter 4.4. The evaluation of precision for each cone type in section 1 was done to differentiate between the repeatability of data from one cone type to the other. The results for the five cone types in section 1 were found through statistical calculation. For the three cone types used in section 2 through 4, their precision was found through visual inspection. As described in chapter 5.2, the boundary zones between the topset and foreset, and foreset and bottomset are hidden for some of the CPTUs due to large stretching and compression. The topset of section 1 is 0 – 4,5m, the forest 8 – 17m and the bottomset 17m and below.

Precision of cone types in section 1

Figure 5.8 and Figure 5.9 presents plots of the depth adjusted data in section 1 for each of the five cone type separately. A varying degree of conformity between the CPTU tests can be seen from these figures. The assessment of the precision was done through the procedure earlier explained, where the average standard deviation, s_{avg} was found. These results, for q_{net} , f_s and Δu at the topset, foreset and bottomset are presented in Figure 5.7. This figure shows the precision of cone types compared to each other for the same parameter and bed type.

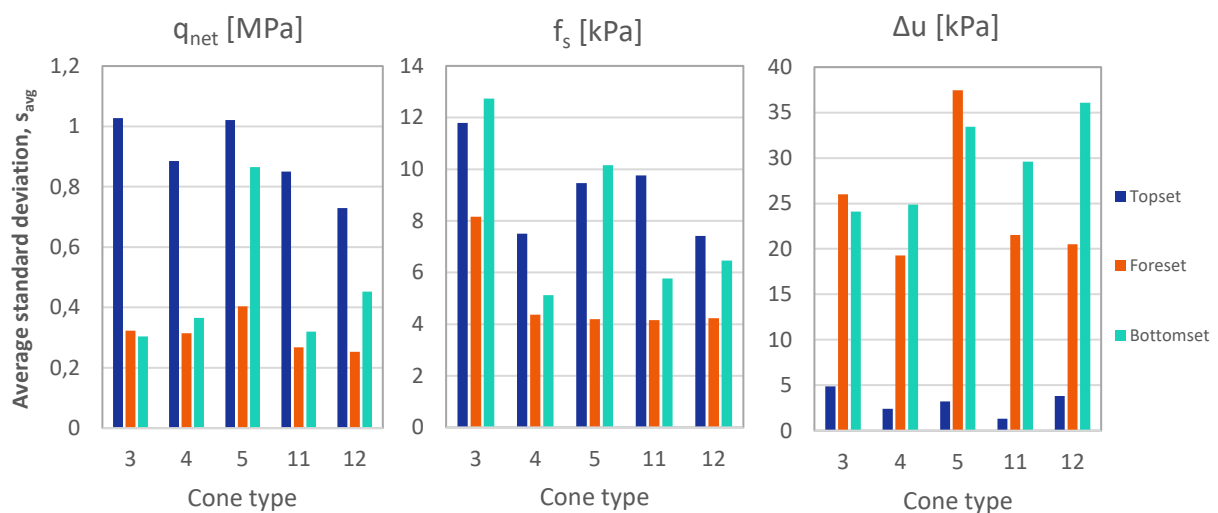


Figure 5.7 – Plots of standard deviation for the cone types in section 1

The magnitude of s_{avg} is naturally largely dependent on the magnitude of the evaluated value. E.g., all q_{net} values at the topset are measured as up to 30MPa compared to an average value of about 3MPa in the foreset. Larger values of s_{avg} may therefore be expected in the topset. Figure 5.7 shows that the s_{avg} values of cone type 5 is higher than the other cone types for both foreset and bottomset. The s_{avg} values for the friction sleeve are also largest at the topset. Cone type 3 has the greatest deviation of f_s at the foreset and the bottomset, while cone type 5 shows large deviation primarily at the bottomset. The Δu values are close to 0 at the topset, and the deviations are small. In the foreset, the greatest deviation was seen for cone type 5, while in the bottomset cone type 5, 11 and 12 have the largest values of s_{avg} .

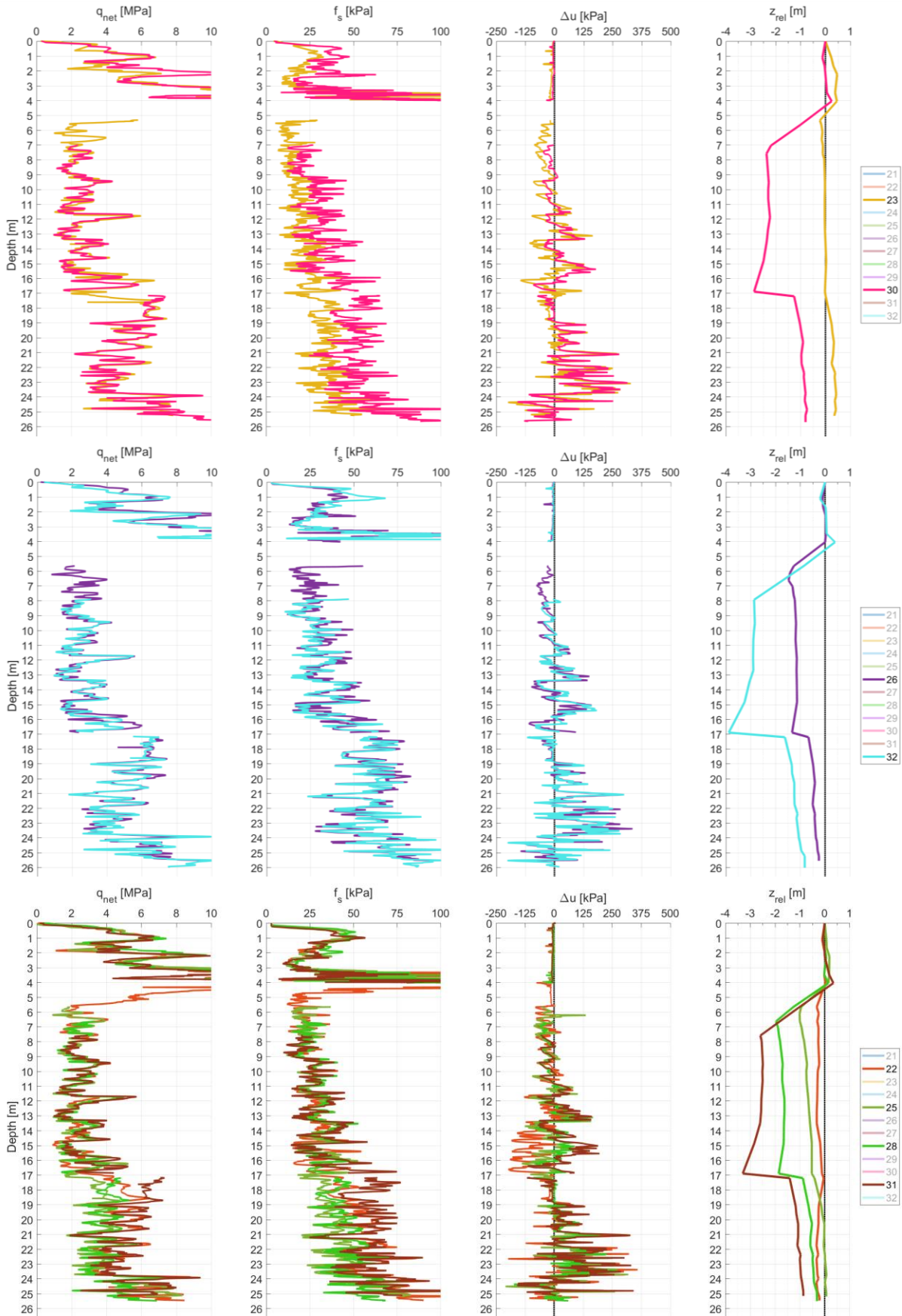


Figure 5.8 – Depth adjusted data for cone type 3 (top), 4 (middle) and 5 (bottom)

5. Results

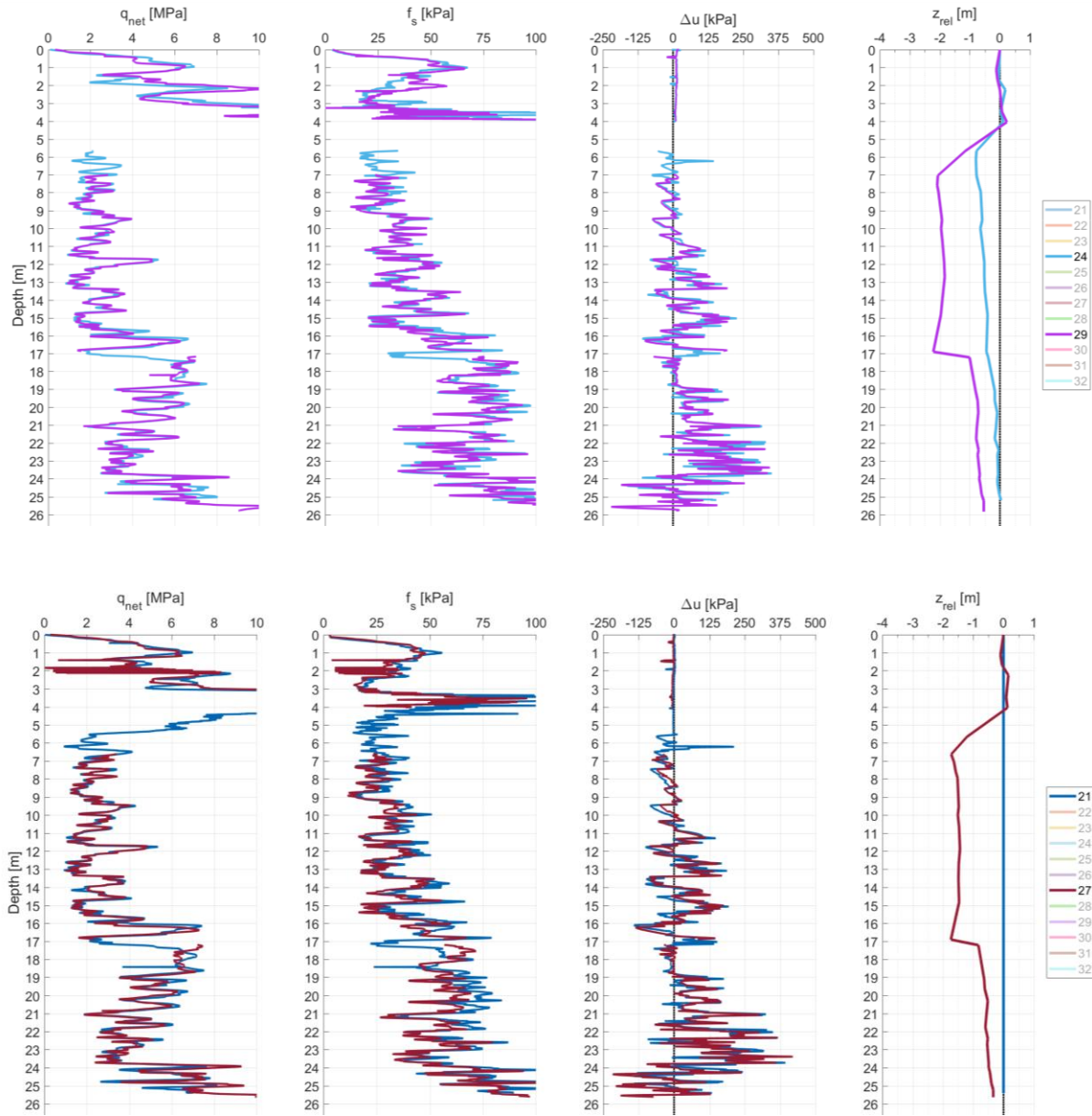


Figure 5.9 – Depth adjusted data for cone type 11 (top) and 12 (bottom)

Precision of cone types in section 2 – 4

The precision of the three different cone types used in section 2, 3 and 4 was evaluated qualitatively based on the depth adjusted plots presented in Figure 5.12, Figure 5.11 and Figure 5.12. Each of these sections have a different reference measurement than section 1, thus values at these depths may not be compared directly to those of section 1. This includes the transition zones between topset, foreset and bottomset beds given to section 1, which does not apply at exact same depths for section 2 - 4. However, the transition zones were found at similar depths as for section 1.

Cone type 1 (section 2)

The q_{net} and f_s measurements of CPTU 38 are very low at the topset, it is possibly due to a predrilling that was not logged. Values of CPTU 37 are slightly lower at the bottomset compared to the other three. This cone type shows noticeable variations at the topset. With these exceptions, the q_{net} and f_s values at the foreset and bottomset shows very good similarity. The Δu profile matches poorly in the foreset while the similarity is very good for the bottomset.

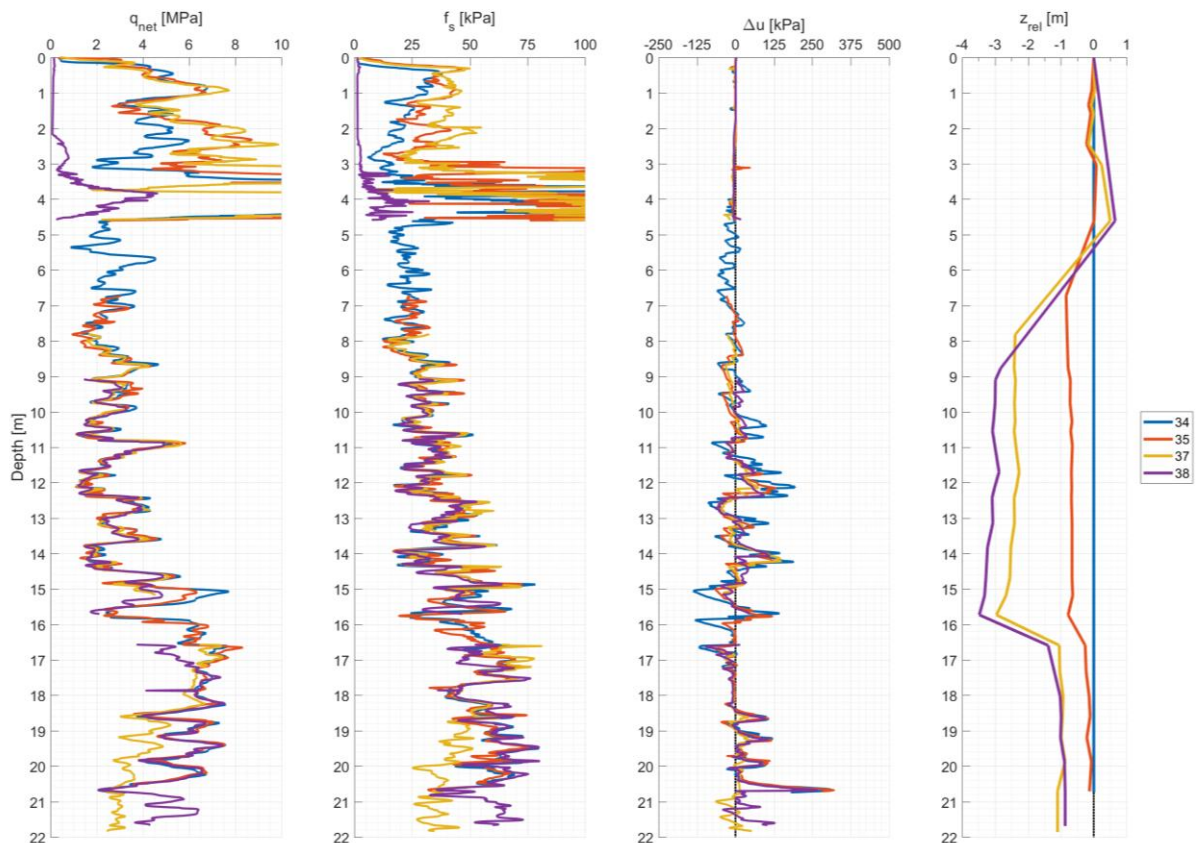


Figure 5.10 – Depth adjusted data for cone type 1

Cone type 6 (section 3)

Figure 5.11 presents the depth adjusted results of cone type 6. For the topset and foreset the values of all three parameters fits well, with the exceptions of the f_s profile of 39 and 42a. As seen in Table 6, these have large zero drifts. Values of Δu fits well for the foreset bed. Values at the bottomset, below 15m, shows large variations for all three parameters.

5. Results

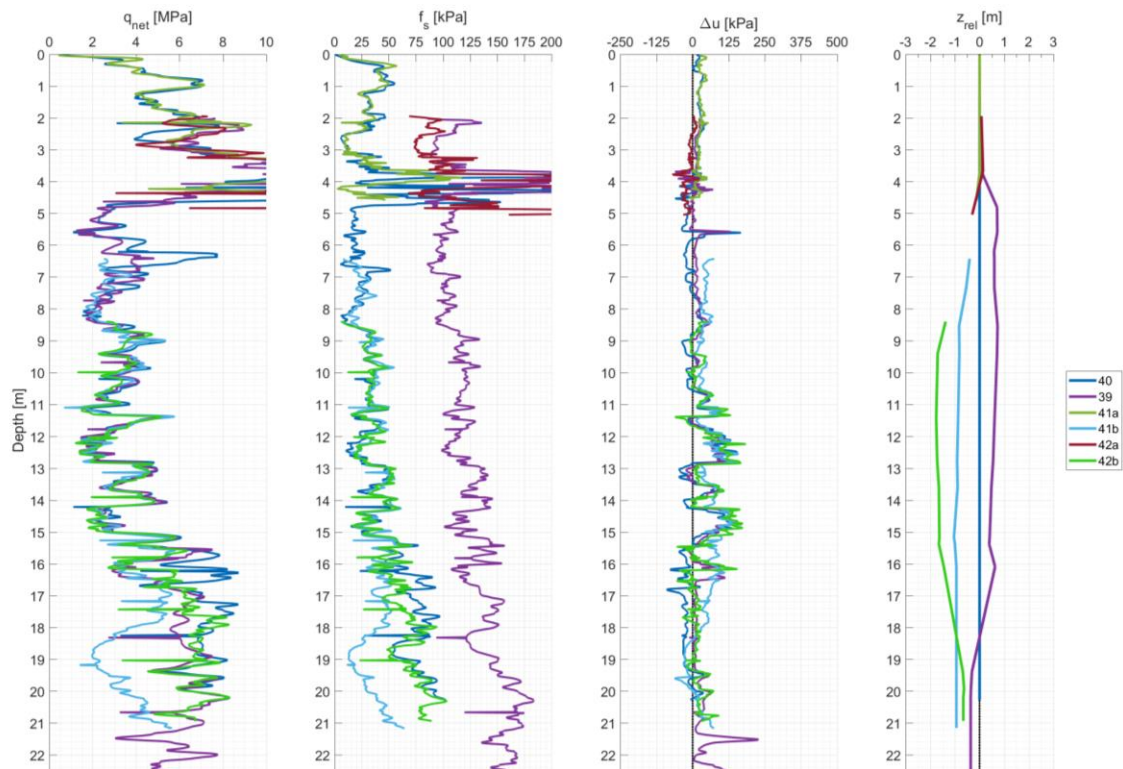


Figure 5.11 – Depth adjusted data for cone type 6

Cone type 7 (section 4)

The quality of the depth adjusted profiles of cone type 7 was poorer than for the other East-West sections, the SRLs of the section is in the appendix. CPTUs with cone type 7 were predrilled to below the topset layer. Values of q_{net} and f_s fits fairly good for all three CPTUs, though for CPTU 44 sudden loss of both tip resistance and side friction is apparent. Note that CPTU 44 was performed with a seismic module explaining this response and the behavior is likely due to how the test was performed. CPTU 43 has a response at about 8m depth that resembles topset values. The pore pressure measurements show significant variations.

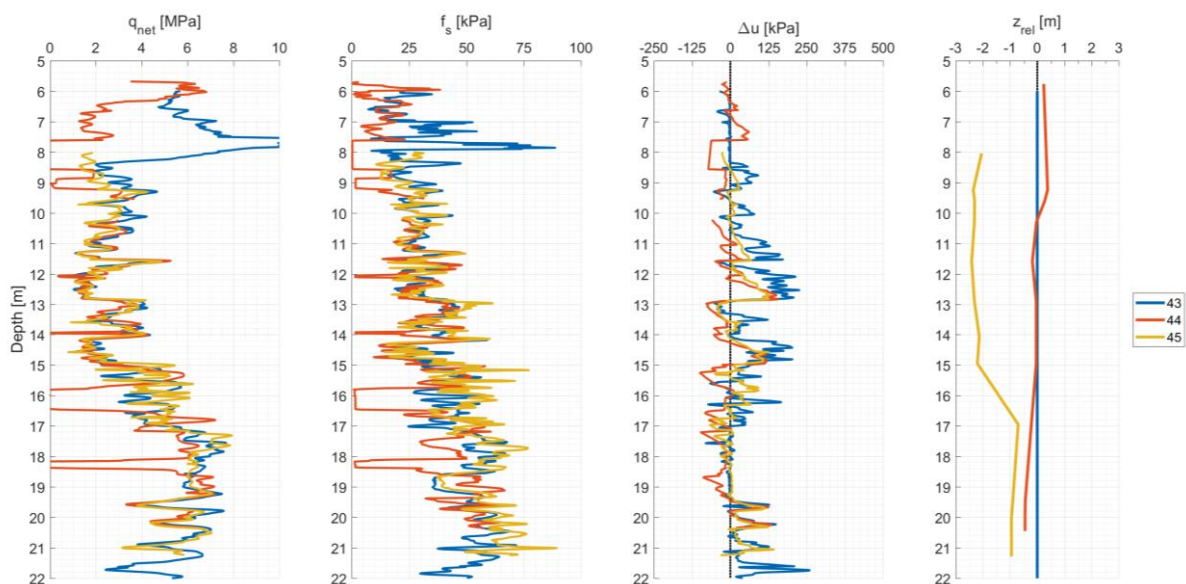


Figure 5.12 – Depth adjusted data for cone type 7

5.5. Determined accuracy of the CPTU parameters in deltaic sediments

The five cone types of section 1 were compared to evaluate which parameter is the most accurate and to find the bias of the cone types. Representative profiles for the five cone types are presented in Figure 5.15 including the average of the representative profiles, $X_{rep,avg}$. The average error, e_{avg} , was found as described in equation (4.17), the results are shown in Figure 5.13. The s_{avg} values in Figure 5.7 presents the precision or the repeatability of the same results using the same cone type. Values of e_{avg} shown in Figure 5.13 on the other hand presents the error between measurements of the evaluated cone type to the average representative value. Pore pressure measurements at the topset is not included due to coarse materials and values of Δu close to zero. However, looking at the Δu profiles of cone type 11 for the topset, the s_{avg} value is low. That means good precision and that the Δu profiles on this cone type matched well. Then, the accuracy of Δu measurement for cone type 11 in the topset is poor, as can be seen from Figure 5.15. Potential causes for this will be mentioned in the discussion.

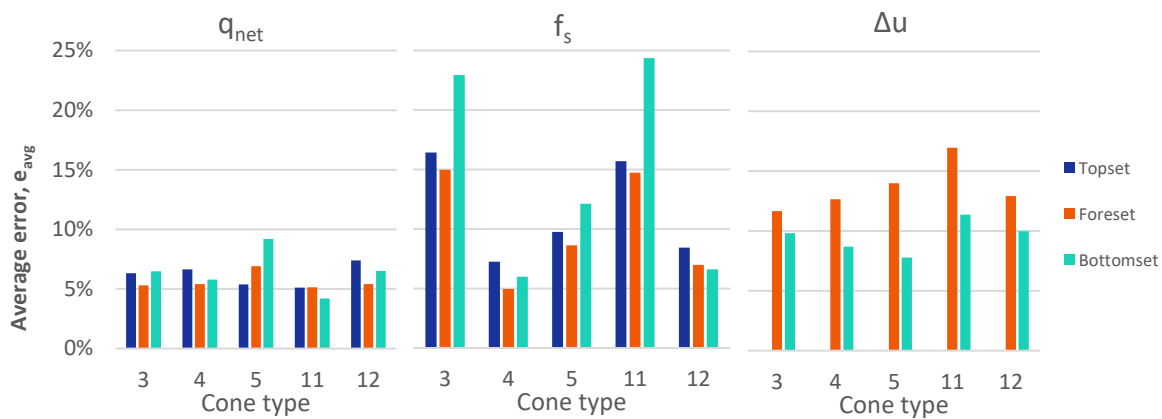


Figure 5.13 – Average error

The accuracy of the q_{net} measurement was found to be the lowest for cone type 5 in the foreset and bottomset. Representative f_s profiles show significant variation, as seen in Figure 5.15. Cone type 3 and 11 is seen to have the largest error values. From Figure 5.15 these can be seen to have the lowest and largest representative f_s values, respectively. The e_{avg} value for the pore pressure measurements mostly reflect differences in the extreme values measured while the variations are quite similar for all cone types. Cone type 11 shows throughout the largest e_{avg} values for the pore pressures. Average values of e_{avg} for all cone types is shown in Figure 5.14. The cone resistance has evidently the best accuracy of the three parameters.

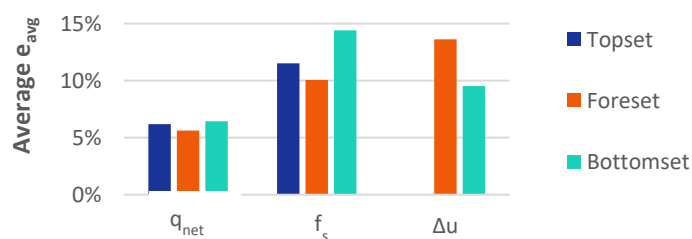


Figure 5.14 – Average of average errors

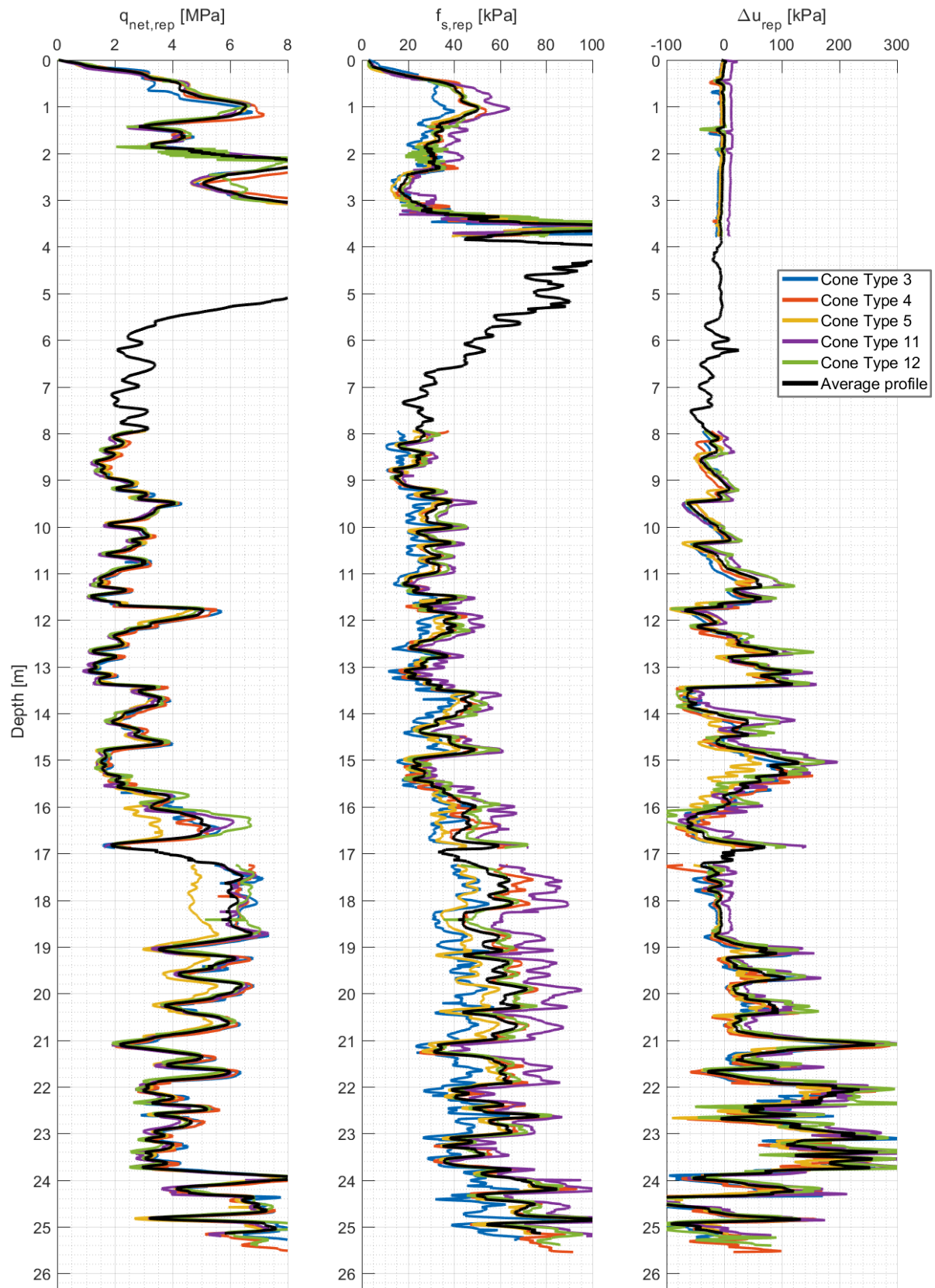


Figure 5.15 – Comparison of representative profiles for cone types 3, 4, 5, 11 and 12

6. Discussion

6.1. Comparison between isolines and GPR data

Multiple ground penetrating radars were performed at Øysand. The purpose of GPRs are to measure the positions of the layer boundaries along a line. The technique has limitations on both the resolution and accuracy. Results from GPR will be compared with the isolines from the CPTUs to find the informational value of the GPR. Only one GPR is presented here, which is called GPR1. The position of GPR1 compared to the CPTUs is presented in Figure 6.1. The total length of the section for GPR1 is 184m and the result of the GPR is shown in Figure 6.2. Results from GPRs show a map with black and white lines. These lines represent interfaces in the measured soil. Depths are not exact as they are determined from the signal travel time.

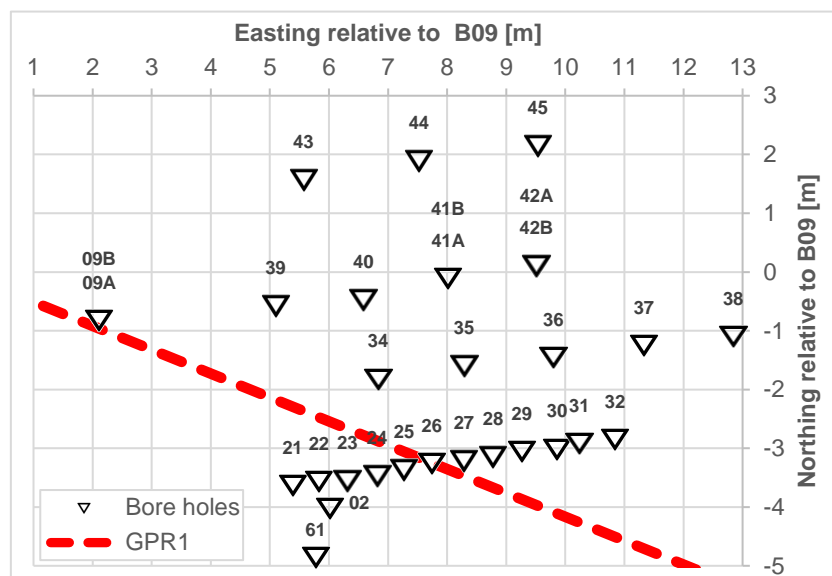


Figure 6.1 – Map of GPR1

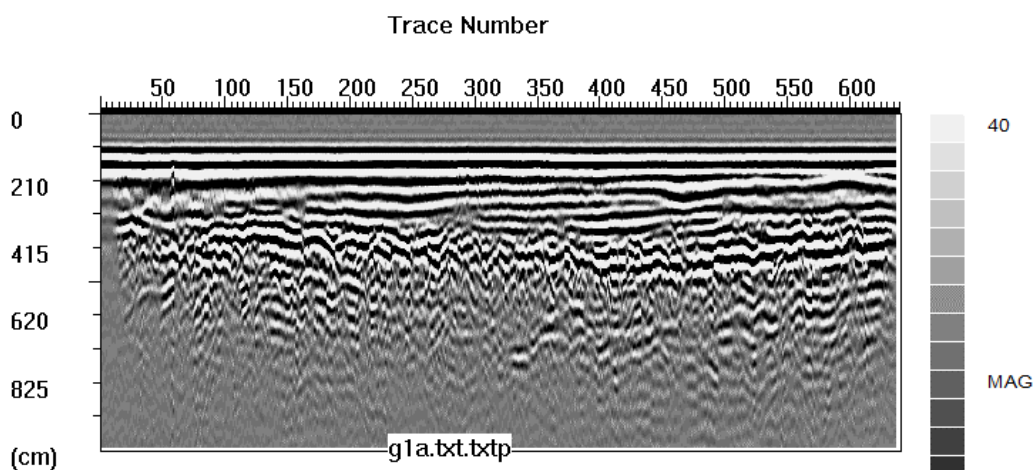


Figure 6.2 – Data from GPR1

The direction of GPR1 is -22° compared to east as seen in Figure 6.1. Equation (4.1) then gives an estimated foreset bed inclination of $I_f = 0,51$. Note that the GPR1 covers a much larger distance than any sections evaluated and that the foreset bed inclination is found using data for only a small part of the site. Figure 6.5 presents the GPR1 data together with stratigraphic isolines assuming a constant foreset bed inclination. At the transition zone between the topset and foreset is indicated with a yellow line, where the horizontal isolines from the topset meets the inclined isolines of the foreset. Isolines are merging in a such transition zone. The two vertical lines presented in the figure shows where the two CPTUs of 09 and 26 are intersected. The boundaries of topset and foreset, and the foreset bed inclination are validated between these two CPTUs.

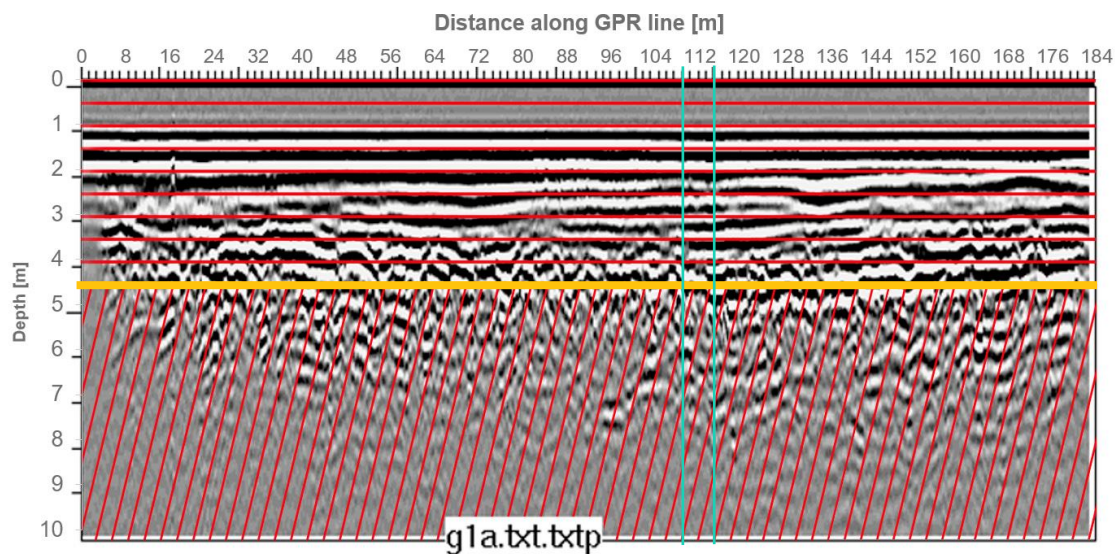


Figure 6.3 – Data from GPR1 with expected isolines in red

When the assumed isolines are compared with the GPR it is evident that the only information provided by the GPR is for the topset. The GPR shows here correctly horizontal interface lines matching with the horizontal isolines at the topset. It also finds an appropriate depth of the interface between topset and foreset, judged from how the interface lines almost disappears below about 4,5m. However, the GPR interface slopes at the foreset is does not reflect the correct orientation and the GPR does not indicate the direction of river progradation. A possible explanation of poor characterization from the GPR is how measurements partly rely on an increased stiffness with depth, which is not the case here.

6.2. Comparison between borehole and CPTU measurements – detecting thin layers

CPTUs can be used together with geotechnical understanding to characterize the materials it encounters, based on the behavior of the soil. However, data from the CPTU should be used together with other in situ and laboratory tests to accurately characterize the materials and to validate the results.

Figure 6.4 presents a detailed image of the stratigraphy at borehole 09. The sample was taken using a sonic drill. The container is 1m long and contains soil from the surface to a depth of 18m. From the image one can evaluate the coarseness and gradation, the presence of gravel is particularly clear at many depths. The sediments below 9m has homogenous properties from a visual judgement.

To compare the CPTU results with these gradual varying visual properties can be of good help to validate the data. However, the proven inclination of the bedding must be considered before results can be compared. It is here desired to use the technique of stratigraphic isolines to perform a depth adjustment of values to match borehole 09 to compare CPTU data with borehole data.

The dashed circle in Figure 6.4 marks a what looks like a thin layer of clay, at depth of a little less than 9m. This thin layer will be in focus here, as the behavior of the CPTU in clay is easy to predict especially since this clay layer is surrounded by coarse materials. The q_{net} value is expected to be higher for the coarse material above and below the clay layer, while the f_s value is expected to increase when passing the clay layer. The occurrences of clay are most noticeable detected by the pore pressure measurement. It is expected that the Δu value increases significantly in this layer due to the water being incapable escaping the fine grains when loaded quickly, which is the case of a CPTU test. From Figure 6.4 the thin clay layer appears to be about 20cm thick, though this is not exact as sonic sampling is not as precise as piston sampling.



Figure 6.4 – Image of stratigraphy from borehole 09 (Quinteros et al., in press)

Section 8 is almost crossing borehole 09, as can be seen in Figure 4.1. It is therefore assumed that the SRLs may be extrapolated along this section from CPTU 09 to borehole 09. This extrapolation is presented in the section plot in Figure 6.5. The foreset bed inclinations for section 8 is about 0,5 as presented in Figure 5.6. So, even though borehole 09 is only about 2m away from CPTU 09, the vertical difference of the SRLs below the topset is about 1m.

The extrapolation of SRLs was performed between B09 and CPTU 09. Borehole 09 is used for depth reference, i.e. the measurements will be depth adjusted to those of B09. The comparison between the CPTU data and the borehole is done by plotting the depth adjusted measurements on top of the image of stratigraphy from Figure 6.4. Figure 6.6 presents the depth adjusted data with the stratigraphy. The transition zone between the topset and foreset is apparent at 5m depth for CPTU 30. Depth adjustment will cause large stretching of the value for CPTU 30; hence these transition zone values should be omitted.

The Z_{rel} plot shows how the depth adjustments is done without notable stretching or compression of values, except for the topset to foreset transition mentioned above.

A box at the depth of the thin clay layer is marked in the figure, an enhanced presentation of values at this depth is presented in Figure 6.7.

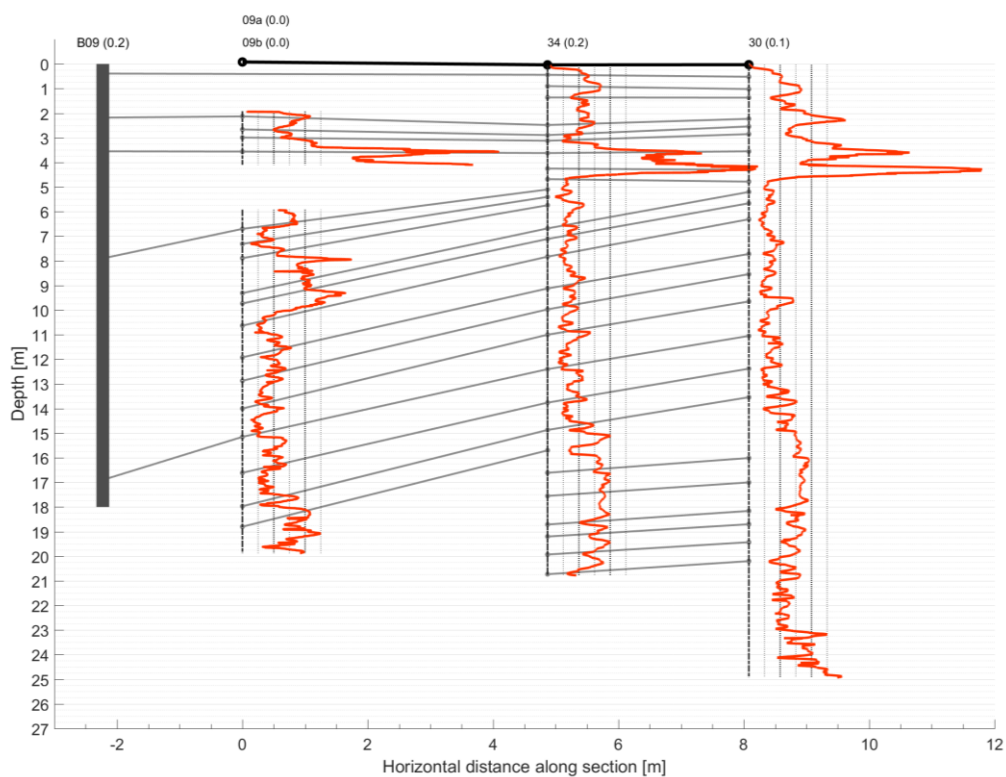


Figure 6.5 – SRLs along section 8 including borehole 09

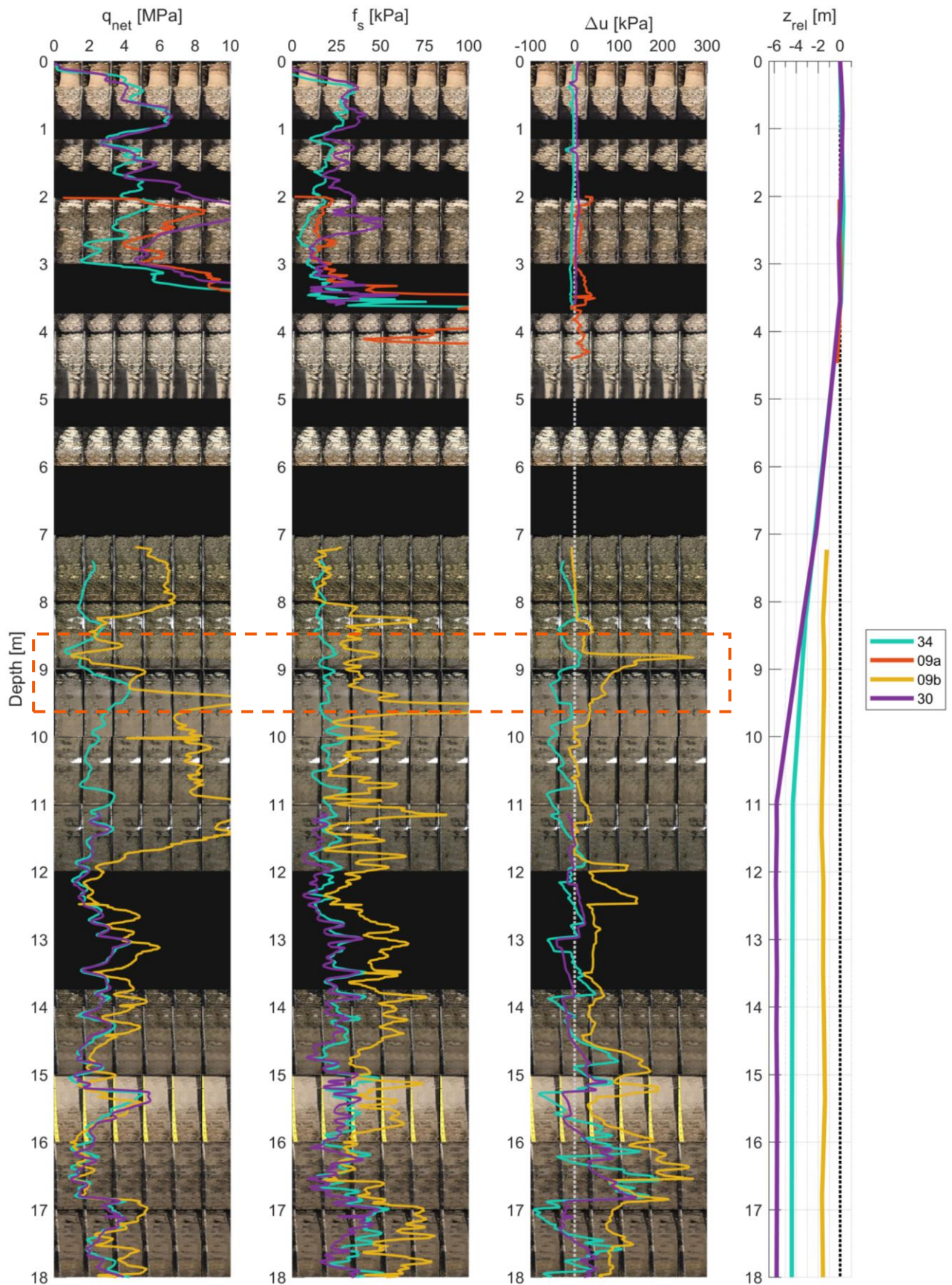


Figure 6.6 – Depth adjusted measurements on top of borehole data

Figure 6.7 presents the comparison between the stratigraphy and depth adjustments at about 9m depth. Here, it can be seen how the selected extrapolation resulted in a good match with the thin clay layer. The dashed lines in the figure represents the interpretation of where a clay layer is encountered due to the response in the measurements. On the other hand, beneath the clay layer in borehole 09 there seem to be a material of coarse grains or gravel where large tip resistance should be expected. CPTU 09b shows what looks to be the response to this layer at about 9,4m depth, though in B09 the material is at about 9m. The dotted lines are the interpreted adjusted depths for the gravel response for CPTU 09b and 34. From the original measurement of CPTU 09b, the vertical distance between the clay response and the gravel response is about 0,8m. That means that if the borehole presents these to materials at the correct depth, i.e. immediately on top of each other, the vertical distance of 0,8m disappears between B09 and CPTU 09. This matter will not be further discussed, however, the discovery of thin layers will.

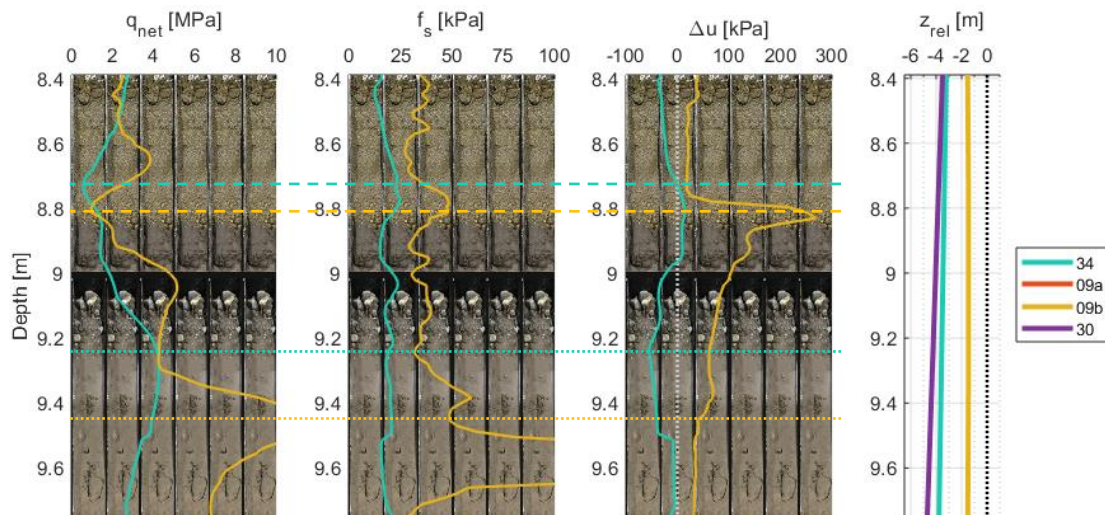


Figure 6.7 – Enhanced presentation of marked depth in Figure 6.6

An interesting observation of the response of CPTU 34 at the expected clay layer is that there is only a very little reaction of the pore pressure measurement compared to CPTU 09b. From the decrease in tip resistance it is assumed that a weak material is encountered. Though, when there are little or no increase in the pore pressure it is likely to not be interpreted as clay. The appearance of this thin clay layer will then be looked further into at other sections to understand whether this lack of pore pressure increase should be expected. In a regular site investigation, the density of CPTUs are not enough to rely on multiple data from other CPTUs to discover a such layer like it is here. Therefore, it is of interest to discover which cone types that most accurately discover such layers.

The clay layer is at 9m depth at B09, and from the z_{rel} plot in Figure 6.7 the depth is found to be about 7,5m at CPTU 09 and 5,5m at CPTU 34. The bottom of the topset bed is at about 4,5m. The one directional increasing slope of the foreset bed is found to be increasing in the direction of directly east with an inclination of about 0,5. Thus, the thin clay layer in the foreset should be assumed to join the topset at about 2m east of CPTU 34. In section 1, CPTU 21 through 27 is expected to contain this thin clay layer.

The colormap presented in Figure 4.6 is a good tool for such a densely spaced section to discover trends. A cut out at depths below the foreset bed of this figure is presented in Figure 6.8. The colormap of the pore pressures, Δu , shows increased values with trend along the section. The dashed lines represent the CPTUs in the section and the peaks in Δu values appear for test number 1, 4, 5 and 7 along the section, i.e., CPTU 21, 24, 25 and 27. CPTU 22, 23 and 26 does not show the same reaction.

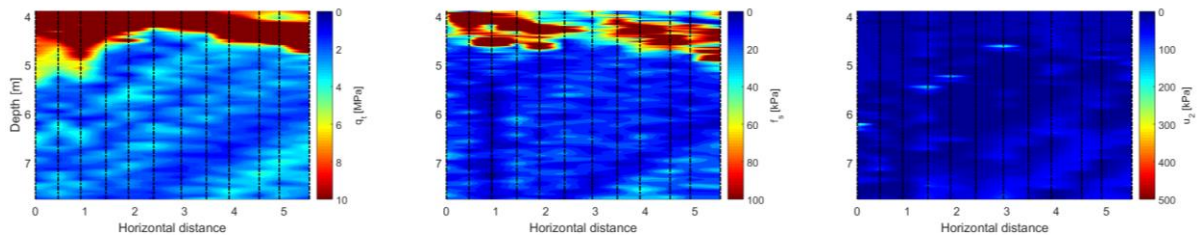


Figure 6.8 – Details of the colormap plot of section 1 presented in Figure 4.6

Similarly, the depths in which the response matching the clay layer is found for other sections. CPTUs shows clay-like behavior at other depths as well, however, as the visual appearance of the clay layer was found in the bore hole this is focused on. Enhanced presentations of the measurements of these sections are presented in Figure 6.9. From these values of section 1 one may again see how CPTU 21, 24 and 25 responds with an increased pore pressure measurement while the well-defined response is lacking for 22, 23 and 26. The measurement of CPTU 27 is hidden in the figure since it is in the transition zone, though the response is seen in the figure above. In section 3, CPTUs 39, 40 and 09 display a distinct peak as a response of the layer, while the same is true for 02, 61 and 62 in section 9. The remaining CPTUs did not show any Δu response in the clay layer.

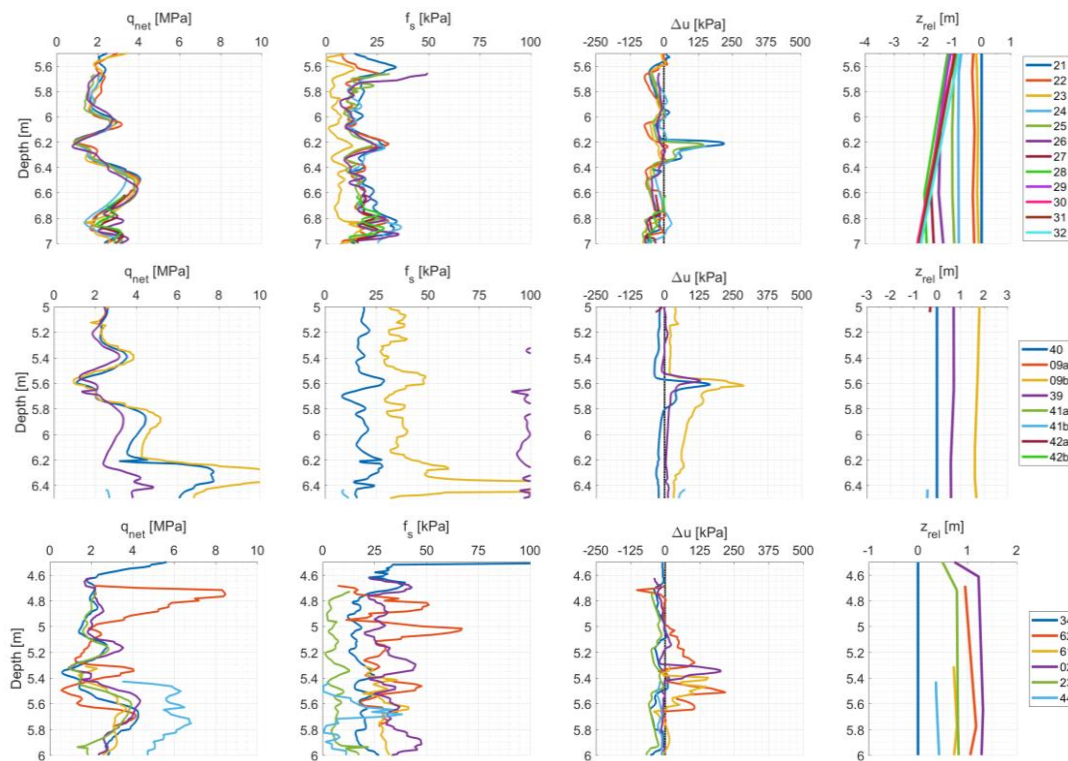


Figure 6.9 – Detection of thin clay layer for section 1 (top), 3 (middle) and 9 (bottom)

6.3. Effect of cone penetrometer type

The resulting accuracy of the cone types are evaluated from the results. All evaluations of data are judged by the depth adjusted measurements. For the CPTUs at section 1, both the precision and the bias has been considered, while cone types 1, 6 and 7 are evaluated in a more qualitative way. From the results and descriptions given in chapter 5.3.3, the performance of the cone types is evaluated based on their properties. Table 9 presents the most important properties of the cone types with emphasize on the differences.

Table 9 – Table of cone type properties

Cone type	Section	Tip area [cm ²]	Compression/subtraction	Filter type	Saturation fluid	Cone capacity [MPa]		
						q_c	f_s	u_2
1	2	10	Compression	Bronze	Silicone ISOVG 100	50	1,6	2,5
3	1	10	Subtraction	Brass 38 micron	Silicone oil 200 fluid 50 cSt	100	1	2
4	1	10	Compression	Brass 38 micron	Silicone oil 200 fluid 50 cSt	100	1	2
5	1	10	Compression	Brass 38 micron	Silicone oil 200 fluid 50 cSt	50	0,5	2
6	3	10	Compression	Slot	Grease/oil	50	1	2
7	4	10	Compression	Stainless steel S/S 10 μ	Silicone oil, DC200, 50cSt	75	1	2
11	1	15	Subtraction	Brass 38 micron	Silicone oil 200 fluid 50 cSt	100	1	2
12	1	15	Compression	Brass 38 micron	Silicone oil 200 fluid 50 cSt	100	1	2

It is believed that the materials encountered in section 1, 2, 3 and 4 can be regarded as equal due to their proximity. This means that the variations in the results reflect the quality of the cone rather than differences in the soil. From the results it is seen that the q_{net} values tend to match very well for the CPTU tests evaluated supporting this assumption. On the other hand, the profiles of f_s and Δu are of more varying quality. For instance, the results presented of thin layer discovery from the pore pressure measurements is assumed to reflect which cones are capable of a such detection and is therefore a sign of its quality. As for the f_s profiles, these have showed in some cases an almost constant difference between measurements of the same cone type, indicating a zero drift. These measurements will here be linked to the properties of the cone type.

Table 10 presents a table with notes to the quality of the data based on the precision (s_{avg}) and accuracy (e_{avg}) of the cone types. The evaluations consist of a rough classification of either good, fair or poor for the precision and accuracy. The values measured in the topset is expected to vary significantly more than in the foreset and bottomset, thus only the latter two are considered here. These are noted with (F) for foreset and (B) for bottomset, or none when the comment is the same for both beds. The classifications are used as a base for the consideration of the cone type which performed the best tests.

Table 10 – Evaluation of cone types quality

Cone type	Precision (good: precise, poor: unprecise)		Accuracy (good: unbiased, poor: biased)	
	1	q_c	(F) Good, (B) Fair	N/A
f_s		(F) Good, (B) Fair		
u_2		(F) Poor (B) Good		
3	q_c	Good	q_c	Good
	f_s	Poor	f_s	Poor - low
	u_2	(F) Poor (B) Good	u_2	Fair - low
4	q_c	Good	q_c	Good
	f_s	Good	f_s	Good
	u_2	Good	u_2	Good
5	q_c	(F) Fair (B) Poor	q_c	(F) Good (B) Fair - Low
	f_s	(F) Good (B) Fair	f_s	(F) Good (B) Poor - low
	u_2	(F) Poor (B) Fair	u_2	Fair
6	q_c	(F) Fair (B) Poor	N/A	
	f_s	(F) Good (B) Fair		
	u_2	Fair		
7	q_c	Fair	N/A	
	f_s	Fair		
	u_2	(F) Poor (B) Fair		
11	q_c	Good	q_c	Good
	f_s	Good	f_s	Fair – high
	u_2	Good	u_2	Fair - high
12	q_c	Good	q_c	Good
	f_s	Fair	f_s	Good
	u_2	Good	u_2	Good

Measurements at the foreset is regularly found to be of better quality than the bottomset. An important factor to this is likely that the materials encountered here are more homogenous for the depth adjusted measurements. The cone types are then primarily compared with respect to the foreset measurements.

Cone resistance measurements

The performance of the tip resistance is proven to be very good for most of the cone types. There are great similarities for tests run with the same cone type as well as good matching of the representative profiles of the cone types. Values of cone type 6 matches well in the forest, while significant variation are seen in the bottomset, with higher peak values than the other cone types as well as a lack of similarities between these measurements. Zero drifts presented in Table 6 had little influence on the resulting accuracy due to the large tip resistances measured. The best results were found from cone types 1, 3, 4, 11 and 12. Thus no significant difference is found between those with cone tip area of 10cm^2 and 15cm^2 or compression type compared to subtraction type. The only property in common is a higher cone resistance capacity, except for cone type 1.

Friction sleeve measurements

Measurements of the sleeve friction varies significantly for most of the cone types. Table 6 shows how the zero drifts vary from none to as much as $80kPa$ for CPTU 39 (cone type 6). When the zero drift is measured as for 39 and 42a, it can be accounted for and the result can be either adjusted or the values can be disregarded. Therefore, the f_s values of cone type 6 is described to be fairly good. In other cases, the sleeve friction measurements from the same cone type show a zero drift-like behavior, i.e. fluctuations appear to be very similar though there is a constant difference in value. When the zero drift-like behavior is not actually measured as a zero drift it weakens the reliability of the measurement. The behavior is evident for instance in cone type 3 plots in Figure 5.10. Similarly, the representative values of the sleeve frictions show the same, almost constant difference in measurement (Figure 5.15). This proves that the difficulty mostly lies in the determination of the size of the value rather than the detection of variations.

The influence of the cone type is partially due to the surface roughness and the wear of the sleeve. Furthermore, if the sleeve is made slightly larger than the tip the sleeve friction measurements has been found to yield significantly larger values of f_s (Cabal & Robertson, 2014). If the sleeve diameter is known and larger than the cone, there has been proposed corrections due to these errors (Holtrigter & Thorp, 2016). However, such detailed properties of the sleeves used on the different sleeves are not known.

Cone type 3 and cone type 11 forms the minimum and maximum values of the f_s profiles as shown in Figure 5.15. Both use the subtraction type, indicating that this type gives less accurate results. It has been pointed out that the subtraction type is more dependent on accurate temperature correction, and that this correction should be done before doing the subtraction to find the f_s value (L'Heureux et al., 2019).

Pore pressure measurements

The pore pressure measurements did for most cone types show the same trends with depth, for instance showing increased excess pore pressure at the same depths. However, the value of the excess pore pressure varied between the cone types. Cone type 1, 3, 5 and 7 has large variations of the excess pore pressures in the foreset, while the values in the bottomset matches well. Especially cone type 5 shows very large differences at the bottom of the foreset bed, where for instance the u_2 for CPTU 22 is close to zero or negative, while the other tests of cone type 5 measure large excess pore pressures. This is possibly due to lost saturation for CPTU 22. The excess pore pressure found using cone type 4, 11 and 12 is consistent within results from the same cone.

The cone types are also compared on their capability of discovering a thin clay layer, as discussed previously. From the isoline trends, the location of the clay layer discovered in borehole 09 is known along the sections. Some of the CPTUs shows an increased excess pore pressures indicating a detection of a fine grained soil, while some encountered the layer without detecting it. Three cone types had one CPTU running through the layer without a significant Δu increase. These were CPTU 34 (cone type 1), 23 (cone type 3) and 26 (cone type 4). Cone type 5 had one CPTU which did not detect the layer, CPTU 22, while another detected it, CPTU 25. Three cone types detected the thin layer at all CPTUs

that encountered it. These are CPTU 39 and 40 (cone type 6), 24 (cone type 11) and 21 and 27 (cone type 12). The penetration speed may influence the ability of the cone to measure large excess pore pressures. The tests performed here are mostly done with a speed of between 15 – 20mm/sec, which is a reasonable pace.

It is worth mentioning that cone type 6 and 11 both have good similarity of its measurements at the topset, while the results show an excess pore pressure of about 20 – 30kPa. The reason for this is not known, though it indicates a measurement bias. From the comparison of representative profiles cone type 11 indicates an almost constant 25kPa bias. The zero drift presented in Table 6 shows that the two tests using this cone type (24 and 29) have zero drifts of about 15kPa, which matches the observations. The results of cone types 11 and 12 is believed to give the best results of pore pressures in the evaluated soils due to their accuracy and ability to detect thin layers. Both these cone types use cones with area of 15cm² while the other cone types have area of 10cm². Both cone penetrometers use the same filter type and saturation fluid, as shown in Table 9.

Cone penetrometer performance

From Table 8 the largest distances between CPTUs of the same cone types is presented together with the number of CPTU of the same cone type. It is natural for closer tests to give better matches in the results, and for some cone types as few as two tests were run. However, the effect of these aspects is difficult to include in the evaluation. The results are expected to be representative for the cone types. Furthermore, it has been assumed for simplicity that the soil properties are independent on the distance between tests when the measurements are depth adjusted.

The cone penetrometer properties that yielded the best results of the cone types used to measure the data evaluated in this study was those with (a) compression type and (b) with a cone area of 15cm². Though the different filter types and saturation liquids did show explicit advantages, it is believed that the best results were given with the *Brass 38 micron* filter type and *Silicone oil 200 fluid 50 cSt saturation* liquid. The capacity of the cone penetrometer was of less influence on the accuracy. These properties reflect those of cone type 12. From the CPTUs performed, this is a reasonable evaluation, however to clearly state the cone type of the best properties more tests of especially cone type 11 and 12 should be performed at Øysand.

6.4. The accuracy of CPTU parameters in deltaic sediments

The calculated accuracy of the CPTU parameters is presented in the results, and the three parameters were compared with an accuracy index. Cone resistance was found to be the most accurate parameter in deltaic sediments and the pore pressure measurement is of comparable accuracy of the in the bottomset bed. While for the foreset bed, pore pressures have similar, lower accuracy as the sleeve friction values in all bed types. This result, that the cone resistance has the highest accuracy, is evident from the figure of representative profiles.

It is important to note the uncertainty of the assumption of “true” profiles from the average representative profiles. However, it was found that the average representative profile and the average profile of all CPTUs in section 1 (cone type 3, 4, 5, 11 and 12) very close to the same results. I.e., the process of finding average profiles of each cone and then taking the average of this (average representative profile) gave approximately the same result as taking the average of the 12 CPTUs altogether. The difference is presented in Figure 6.10, where the average representative values is in black and the average values in cyan. The fluctuations were identical, and the maximum difference was less than 5% for q_t and u_2 and less than 7% for f_s . This supports the assumption of the average representative profile being the true, unbiased profile.

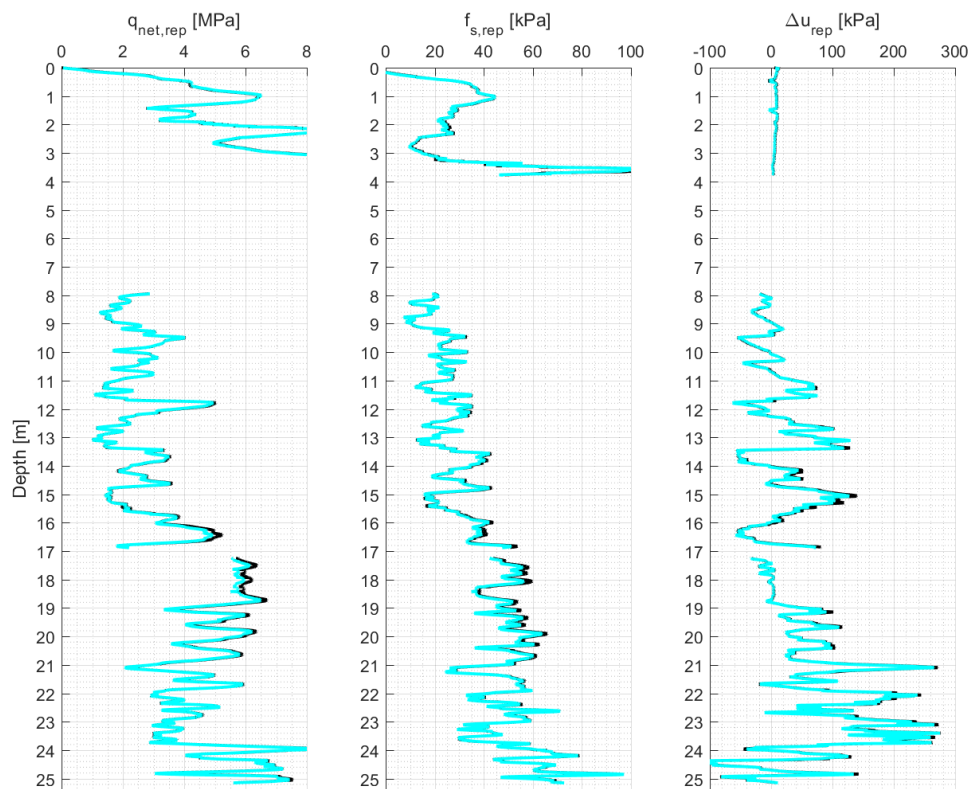


Figure 6.10 – Average of all profiles in section 1 vs average of representative profiles

The required accuracy of the parameters is given in the standard (ISO 22476-1:2012), depending on the soil type. When used to characterize deltaic soils, which can be described as mixed stiff bedded soils, application class 3 is appropriate. This class requires accuracy of at least $200kPa$ or 5% for the cone resistance, $25kPa$ or 15% of the sleeve friction and $50kPa$ or 5% of the pore pressure measurement. The requirement is defined as the larger of the two and is demanded for each measured value when all sources of errors are considered. Thus, less accuracy is allowed for smaller values. The two limits per parameter coincide at $4MPa$ for q_t , $167kPa$ for f_s and $1MPa$ for u_2 , for larger values the minimum accuracy is given as the percentage. Measured values at Øysand is at and above these values for the q_t , while the other two parameters are significantly less, thereby allowing larger span of values. Figure 6.11 shows these required accuracy limits together with the representative profiles of cone type 3, 4, 5, 11 and 12. These limits forms a band with the width of the allowed error on each side. The requirements are related to the non-depth normalized parameters of q_t , f_s and u_2 of the average profiles. These are then depth normalized in the figure.

The requirements are in large parts fulfilled for all these cone types. Due to the dense to medium dense silts and sands throughout the depth, the cone resistance is large while the sleeve friction is mostly low. The figure of the measurement requirements reflects well how larger values creates tighter bands, as seen for q_{net} compared to u_2 and how the accuracy requirements compares well to the achieved results.

All three parameters can be used to define stratigraphy in deltaic soil, though the cone resistance is considered to be the best choice. The cone resistance parameter may as well be used for more than just stratification purposes due to its accuracy. The pore pressure parameter is often believed to be the most reliable parameter in very mixed soils, as interfaces are well detected. However, the peak values of the measurements are proved to be unreliable by itself. Detection of for instance thin, fine grained layers by the pore pressure measurement varies with the cone type, while the fluctuations of the measurement generally responds well to interfaces. As discussed for the cone penetrometer types, there are zero drift-like behaviors occurring for the sleeve friction measurements. In soil characterization for soil behavior types, the f_s must be used with care due to the uncertainty. Often the soil behavior type characterization is done using the logarithmic value of the friction ratio, i.e. the relationship between the sleeve friction and cone resistance. Due to the accurate nature of the cone resistance not much uncertainty is added. Though, the errors of f_s is seen to be of magnitude $\pm 20\%$ which can influence the soil characterization. Furthermore, geotechnical design should not be based on this parameter unless the sleeve friction accuracy of the used cone penetrometer is known to be good.

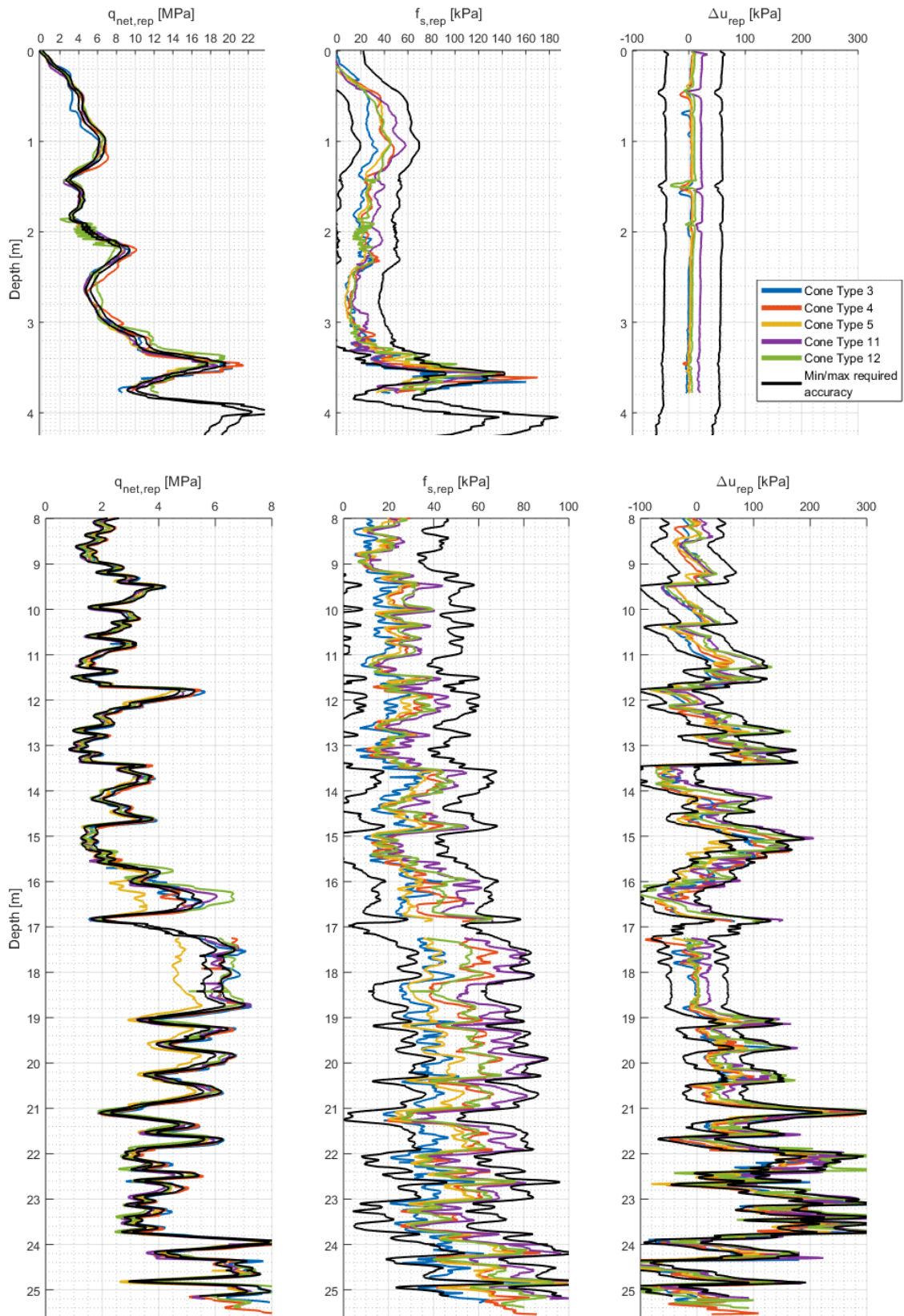


Figure 6.11 – Representative profiles with accuracy requirements

6.5. Stratigraphic isolines and depth adjustments

Through selection of stratigraphic reference isolines and the following depth adjustment, the data along a section was enabled to be compared. The assumption that the cone resistance parameter is best suited for accurate selection of SRLs along sections and thus use for determining facies is to a large extent confirmed through the results.

However, trends along section can only be uncovered using good engineering judgment based on adequate data. If the density of CPTUs is low, the possibility of detecting these trends disappears. Recommended density of CPTUs are discussed later. This study mainly focused on one section with the highest density of CPTUs, section 1. With measurements every 50cm the resolution became very clear, yielding very good data. It can be stated that this study has lacked comparisons between sections. For instance, all profiles between section 1, 2, 3 and 4 could be compared together and analyzed as section 1. However, the reason this was not done is not due to difficulties relating profiles between section. Such a procedure is identical to relating measurements within a section to the reference profile. It is rather due to the already large amount of data and to avoid large effects of depth adjustment, particularly in the transition zones between bet types. If this was to be done, however, z_{rel} profiles from sections covering reference profiles at other sections could be used to perform a depth adjustment toward a "site reference profile". E.g., if CPTU 34 was used as the "site reference profile", profiles in section 1, where CPTU 21 is the reference, could be depth adjusted towards 34. That would be done by using the z_{rel} values for 21 at section 10. CPTU 34 is the reference in section 10 and both 21 and 34 is in this section. When depth adjustment of already depth adjusted data were to be performed, interpolation of values is essential.

The accuracy of the depth adjusted data dependent of the quality of the depth adjustment. Depth adjustment is performed with respect to the selected SRLs. These SRLs were selected manually and carefully, and it is therefore believed that there are minimal systematic uncertainties added due to this.

The depth adjusted measurements show how the relative vertical distances are not constant, e.g. looking at the depth adjusted data of section 1 in Figure 5.2. As presented, a constant value of z_{rel} with depth means that values are only shifted up or down to match the reference value. Where the value varies with depth, either stretching or compression occurs. The procedure presented in this study makes a well-defined connection between the isolines and the depth adjustment which is particularly useful where stretching and compression of values occur. Isolines has by itself a great informational value by describing where the same materials are found, especially in the foreset of a river delta.

Measurements in this study was depth normalized with respect to overburden stress for the q_t measurement and the in situ pore pressure for the u_2 measurement. The f_s measurement was not depth normalized. Many methods of depth normalization, of correction for overburden stress, is available. However, from the depth adjusted and depth normalized data, no clear trends were discovered, for q_{net} , f_s nor the Δu . For the f_s values, there were no obvious trends of greater values of measurements were depth adjusted upwards, which could be expected. Quite the opposite, there

was a weak trend of sleeve friction values depth adjusted downwards to have slightly larger values of f_s . This is not believed to be reflecting the truth but rather a result of measurement inaccuracy of the sleeve friction.

This study has mainly focused on the removal of trends through the isolines and depth adjustment method. A case in which the isolines are used to determine the positions of a thin layer is also presented. This is merely a taste of the possibilities with this way of determining the isolines. A great possibility with the depth adjustment is to use it in reverse. That is, one may use the values of z_{rel} from a reference where the layering is determined and then add the z_{rel} values to add the trends which previously was removed.

6.6. Practical use of CPTUs in a river delta

For optimal characterization, it is important to perform enough test so that that one may assume that all layers are detected along a section. As it has been presented here, with the use of CPTUs to characterize deltaic soils, the foreset bed contains the sediments of the largest variation in stratigraphy. A determined maximum distance between CPTUs is found from the properties of this bed. With the aim to detect all materials along an inclined bedding, two factors determine the needed proximity between tests. These are the inclination and the thickness of the bed. At Øysand, the foreset bed is found to have an of repose of 29° , or inclination of 0,55, and the thickness of the bed is about 10m. Assuming constant inclination and bedding thickness, the maximum distance between CPTU should be less than $10m/0,55 = 18m$ in the direction of the progradation. However, this is much larger distances than for most tests evaluated in this study, which has been mostly less than 2m. Looking at the section plots in the Appendix, trends seems to be noticeable in a section between the first and last set as well. Though, properties may change within the same layer larger distances.

To be able to accurately assess the layering as done here, it is believed that distances should be less preferably not more than 10m parallel to the progradation direction. Perpendicular to this direction, however, the distances between adjacent CPTUs may be bigger.

SRLs were not selected for two sections were not due to large distances between tests for section 11 and 13. SRLs could have been selected, however it would have been selected with much uncertainty and thus impair the purpose. The largest distance within these sections are of 17m and 18m, respectively. Section 11 lies in the direction of the largest foreset slope inclination, where a slope of 0,55 is expected. Section 13 is orientated closer to the north-direction. Section plots for these two sections without SRLs is presented in the Appendix.

7. Conclusion

The study of densely spaced CPTUs in deltaic sediments gave interesting results. The sedimentation process in a river delta has a large impact on the CPTU measurements and should be considered to correctly take trends into account. A good way to do this is by creating sections and use the corrected cone resistance measurement to define connections between measurements of the same characteristics. These connections are here called stratigraphic reference isolines. The q_t -profile is proven to be the most accurate parameter and very well suited to determine the SRLs when CPTUs are performed sufficiently close to one another. When the SRLs are successfully determined, a continuous map of isolines can be drawn to further emphasize the trends along sections. At Øysand it is found that the foreset bed has an inclination of 0,55 or a 29° angle at the steepest. The largest inclination is found in the direction of directly east indicating river propagation directly westwards.

Depth adjustment is the procedure presented in the study for removal of trends. It is based on the trends discovered for the sections, through the SRLs which is called the relative vertical distance, Z_{rel} . The values of Z_{rel} describe how much a value at a certain depth must be shifted vertically to match a reference value. Bedding and layers in river deltas are not necessarily only inclined, they may very well be of varying thickness. This is the case at Øysand, and in these conditions the procedure of the relative vertical distance is a very effective way of accurately adjust and stretch or compress measurements to fit a reference. The depth adjustment resulted in very good matches, particularly where many CPTUs were performed with small distances in between.

Measurements were depth adjusted and enabled to be compared to discover its true accuracy. 23 densely spaced CPTUs of eight different cone types were used to determine the precision of the cones. The accuracy is quantified for five of the cone types, while the remaining three is assessed visually. Due to the different properties of the bedding at a river delta, the accuracy is given for each bed type. The accuracy of the cone resistance values is approximately the same for all bed types, with an error of about 5% and it is also almost independent on cone type. The sleeve friction parameter gives very varying accuracy depending on cone type, with errors ranging from 5% to about 15%. The uncertainty of the accuracy of friction sleeve measurements is a weakness that decreases the reliability for characterization use. Lastly, the pore pressure measurements gave more accurate measurements in the bottomset bed than in the foreset bed. The pore pressure measurements have an average error of about 10%. These results show that the measurements of the CPTU lies within the appropriate requirements in deltaic sediments, given by the European Standard for CPTUs, ISO 22476-1:2012.

The evaluated properties for cone types has been the cone tip area, cone design (compression or subtraction type), the capacity, the filter type and saturation liquid. Results indicated that cone types with a cone area of 15cm^2 give better pore pressure measurements, noticeably in the discovery of thin, fine layers. Compression type cone design gives the most reliable sleeve friction values. Most of the results from the sleeve friction parameter gave large uncertainties due to zero drift behavior of values, even when a zero drift was not measured. The cone resistance is less dependent on the properties.

8. Recommendations

The conclusions made in this study at the evaluated site form the basis for recommendations regarding the use of CPTUs for site investigation in a river delta and the confidence of the data for characterization and design use. The cone resistance measurement has proven to have a very good accuracy. Use of sleeve friction values for characterization by soil behavior type should be done with care due to the large zero shifts. Pore pressure values tend to be somewhat more reliable than f_s .

Firstly, regarding the equipment, it is important to take temperature and zero drift effects into account and correct values when possible. Temperature effects were not significant for most of the evaluated tests at the site due to relatively small corrections. However, the subtraction type cone design is more prone to errors due to temperature effects. These values should be corrected for temperature change for both the cone resistance and sleeve friction before subtraction of the sleeve friction. Zero drift of measurements caused the largest errors for the sleeve friction values. A possible explanation is a difference in diameter between the cone and the sleeve. The effect of this can be substantial, while methods of correction of this is proposed. It is therefore recommended to measure deviation of the sleeve diameter, especially for stiff soils as encountered here.

Different cone penetrometers were used at the site, and from comparison between the results cone types proved to have a better performance in deltaic soils. It was found that larger cones, with cone area of 15cm^2 , yielded the best results for especially the pore pressure measurements in the deltaic sediments. No significant impact due to cone area was found for the cone resistance measurement. Cone penetrometers using of the compression type design gave the best friction sleeve measurement due to less evident zero shifts. Temperature corrections of the subtraction type penetrometer design have as mentioned larger impact than for compression type. Due to the possible differences caused by using different equipment, it is recommended to perform comparison between results when different contractors are used. This should be done by performing CPTUs adjacent to those of the other types to evaluate the measurement agreement.

Exact depth trends can be discovered by determining isolines along a section. The best results are found from the cone resistance measurement. If measurements from CPTUs performed at a river delta are to be compared, the profiles should be depth adjusted. If non-depth adjusted measurements are compared one should be aware of the uncertainties it brings. The procedure of determining isolines can in turn give the layer boundary lines once layers are defined at a single CPTU.

Based on these experiences it is recommended to include geological understanding in the assessment of geotechnical investigation and subsequent characterization, particularly when assessing deltaic sediments. It is important to understand the effect of inclined bedding in the foreset bed of a river delta as it causes a challenge of discovery of materials. The recommended maximum distance between CPTUs is therefore based on the properties of this type of bedding. At \emptyset sand it recommended to have distances between CPTUs of maximum 18m in the direction of river progradation, though preferably no more than 10m . If less dense grids of tests are made, then it is probable that some materials will not be discovered.

9. Further work

This study has covered the assessment of CPTU accuracy in the deltaic sediments at Øysand. The accuracy was only quantified for five of the eight cone types at the site, though the results is believed to reflect the cone types that were assessed qualitatively. It would however be interesting to perform the depth adjustment procedure at another river delta site to further evaluate its usefulness.

Some factors of the CPTUs that were not known in this study can be assessed. This includes calibration and correction methods of the f_s measurement. Values such as the roughness, wear and exact diameter may reveal why the sleeve friction measurements tend to have low accuracy. For the accuracy of the pore pressures, it could be interesting to focus on the penetration speed in relation to the excess pore pressure, particularly for thin, fine layers.

The depth adjusted data may be used to characterize the soil and see how the inaccuracy of for instance the sleeve friction measurement may cause potential errors using soil behavior type characterization. The determined isolines can also be used to form continuous layer boundaries together with selected layering from borehole data to. This can be very useful to evaluate the ability to predict values through interpolation.

There are also great possibilities of geostatistical studies due to the amount of data at Øysand, together with the manually removed trends. This includes determination of the spatial variability, which is already done at Øysand (Liu et al., in press). The original objective of this study, inverse filtering, can be performed with confidence now that the accuracy of the data is validated. This method can be used with an attempt to exclude transitional effects of the penetration values.

References

- Amorosi, A., Bruno, L., Rossi, V., Severi, P., & Hajdas, I. (2014). Paleosol architecture of a late Quaternary basin-margin sequence and its implications for high-resolution, non-marine sequence stratigraphy. *Global and Planetary Change*, *112*, 12-25. doi:<https://doi.org/10.1016/j.gloplacha.2013.10.007>
- Amorosi, A., & Marchi, N. (1999). High-resolution sequence stratigraphy from piezocone tests: an example from the Late Quaternary deposits of the southeastern Po Plain. *Sedimentary Geology*, *128*(1), 67-81. doi:[https://doi.org/10.1016/S0037-0738\(99\)00062-7](https://doi.org/10.1016/S0037-0738(99)00062-7)
- Bombasaro, E., & Kasper, T. (2016). Evaluation of spatial soil variability in the Pearl River Estuary using CPTU data. *Soils and Foundations*, *56*(3), 496-505. doi:<https://doi.org/10.1016/j.sandf.2016.04.015>
- Cabal, K., & Robertson, P. K. (2014). *Accuracy and repeatability of CPT sleeve friction measurements*. Paper presented at the 3rd International Symposium on Cone Penetration Testing CPT14: May.
- Campanella, R. G., Robertson, P. K., & Gillespie, D. (1983). Cone penetration testing in deltaic soils. *Canadian Geotechnical Journal*, *20*(1), 23-35. Retrieved from <https://doi.org/10.1139/t83-003>.
- Firouziandbandpey, S., Griffiths, D. V., Ibsen, L. B., & Andersen, L. V. (2014). Spatial correlation length of normalized cone data in sand: case study in the north of Denmark. *Canadian Geotechnical Journal*, *51*(8), 844-857. Retrieved from <https://doi.org/10.1139/cgj-2013-0294>.
- Gundersen, A. S., Quinteros, S., L'Heureux, J.-S., & Lunne, T. (2018). *Soil classification of NGTS sand site (Øysand, Norway) based on CPTU, DMT and laboratory results*. Paper presented at the Cone Penetration Testing 2018, Delft University of Technology.
- Haslett, S. (2009). *Coastal systems* (Second ed.): Routledge.
- Holtrigter, M., & Thorp, A. (2016). *Correction for CPT fs errors due to variation in sleeve diameter*. Paper presented at the Proc. ISC.
- L'Heureux, J.-S., Carroll, R., Lacasse, S., Lunne, T., Strandvik, S. O., Degago, S., . . . Sinitsyn, A. (2017). New Research Benchmark Test Sites in Norway. In *Geotechnical Frontiers 2017* (pp. 631-640).
- L'Heureux, J.-S., Gundersen, A. S., Lindgård, A., & Lunne, T. (2019). Norwegian GeoTest Sites (NGTS) - Impact of cone penetrometer type on measured CPTU parameters at 4 NGTS sites. Silt, soft clay, sand and quick clay.

-
- Lafuerza, S., Canals, M., Casamor, J. L., & Devincenzi, J. M. (2005). Characterization of deltaic sediment bodies based on in situ CPT/CPTU profiles: A case study on the Llobregat delta plain, Barcelona, Spain. *Marine Geology*, 222-223, 497-510. doi:10.1016/j.margeo.2005.06.043
- Lindgård, A. (2018). Effect of cone type on measured CPTU results from Tiller-Flotten quick clay test site.
- Lunne, T., Powell, J. J. M., & Robertson, P. K. (1997). *Cone Penetration Testing in Geotechnical Practice*. London: CRC Press.
- Lunne, T., Strandvik, S., Kåsin, K., L'Heureux, J.-S., Haugen, E., Uruci, E., . . . Kassner, M. (2018). Effect of cone penetrometer type on CPTU results at a soft clay test site in Norway.
- Moss, R. E., Seed, R. B., & Olsen, R. S. (2006). Normalizing the CPT for Overburden Stress. *Journal of Geotechnical and Geoenvironmental Engineering*, 132(3), 378-387. doi:doi:10.1061/(ASCE)1090-0241(2006)132:3(378)
- Peuchen, J., & Terwindt, J. (2014). *Introduction to CPT accuracy*. Paper presented at the 3rd International Symposium on Cone Penetration Testing CPT14: May.
- Powell, J., & Quarterman, R. (1995). *Engineering geological mapping of soft clay using the piezocone*. Paper presented at the Proc. Int. Symp. Cone Penetration Testing, CPT.
- Powell, J. J., & Lunne, T. (2005). Use of CPTU data in clays/fine grained soils. *Studia Geotechnica et Mechanica*, 27(3-4), 29-66.
- Quinteros, S., Gundersen, A., L'Heureux, J.-S., Carraro, A., & Jardine, R. (in press). Øysand research site: Geotechnical characterization of deltaic sandy-silty soils. *AIMS Geosciences*.
- Reite, A. J., Sveian, H., & Erichsen, E. (1999). Trondheim fra istid til nåtid - landskapshistorie og løsmasser. *Gråsteinen*, 5.
- Robertson, P. K. (1990). Soil classification using the cone penetration test. *Canadian Geotechnical Journal*, 27(1), 151-158. Retrieved from <https://doi.org/10.1139/t90-014>. doi:10.1139/t90-014
- Robertson, P. K. (2016). Cone penetration test (CPT)-based soil behaviour type (SBT) classification system — an update. *Canadian Geotechnical Journal*, 53(12), 1910-1927. Retrieved from <https://doi.org/10.1139/cgj-2016-0044>. doi:10.1139/cgj-2016-0044
- Sandven, R. (2010). *Influence of test equipment and procedures on obtained accuracy in CPTU*. Paper presented at the Proceedings of the 2nd International Symposium on Cone Penetration Testing (CPT'10), Huntington Beach, Calif. Edited by Mitchell et al.

-
- Sarti, G., Rossi, V., & Amorosi, A. (2012). Influence of Holocene stratigraphic architecture on ground surface settlements: A case study from the City of Pisa (Tuscany, Italy). *Sedimentary Geology*, 281, 75-87. doi:<https://doi.org/10.1016/j.sedgeo.2012.08.008>
- Schneider, J. A., Randolph, M. F., Mayne, P. W., & Ramsey, N. R. (2008). Analysis of Factors Influencing Soil Classification Using Normalized Piezocone Tip Resistance and Pore Pressure Parameters. *Journal of Geotechnical and Geoenvironmental Engineering*, 134(11), 1569-1586. doi:doi:10.1061/(ASCE)1090-0241(2008)134:11(1569)
- Standard Norge. (2012). Geotechnical investigation and testing Field testing. In *Part 1: Electrical cone and piezocone penetration test (ISO 22476-1:2012)*.
- Styllas, M. (2014). A simple approach to define Holocene sequence stratigraphy using borehole and cone penetration test data. *Sedimentology*, 61(2), 444-460. Retrieved from <https://onlinelibrary.wiley.com/doi/abs/10.1111/sed.12061>. doi:10.1111/sed.12061

Appendix

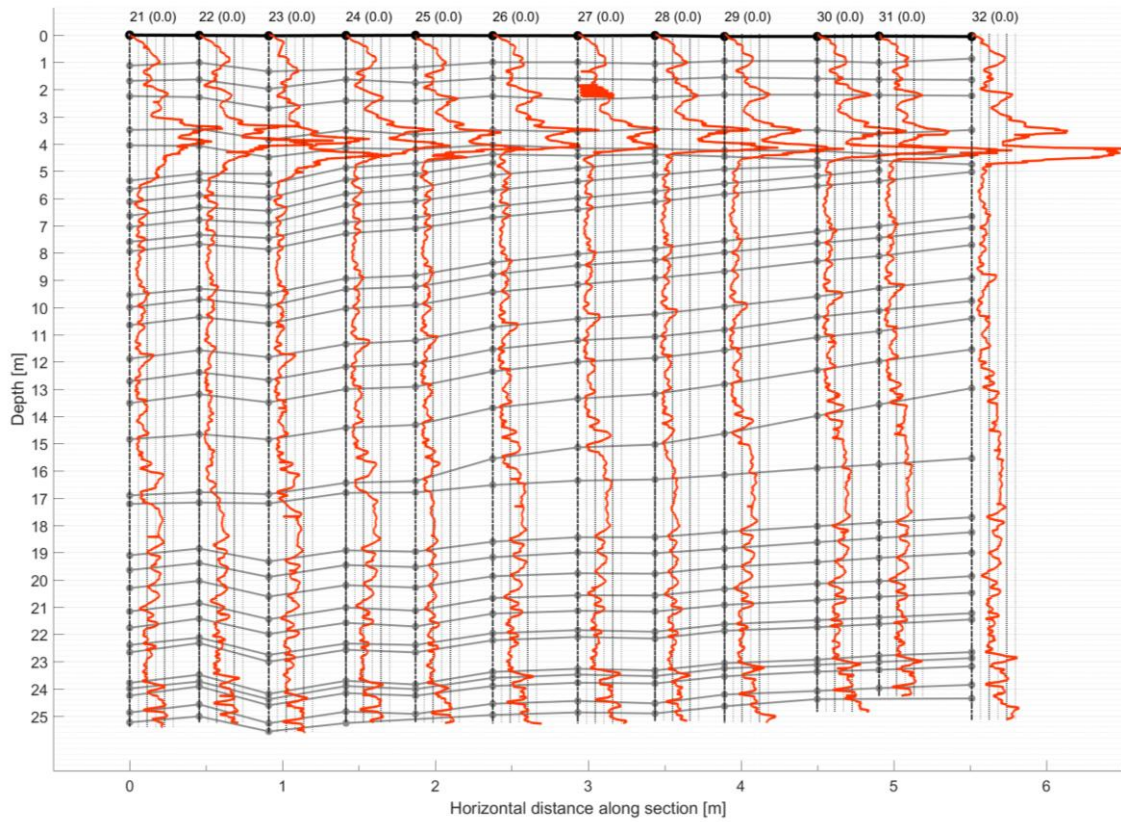
Section plots

A1.	Section plot: Section 1	74
A2.	Section plot: Section 2	74
A3.	Section plot: Section 3	75
A4.	Section plot: Section 4	75
A5.	Section plot: Section 5	76
A6.	Section plot: Section 6	76
A7.	Section plot: Section 7	77
A8.	Section plot: Section 8	77
A9.	Section plot: Section 9	78
A10.	Section plot: Section 10	78
A11.	Section plot: Section 11 (without SRLs)	79
A12.	Section plot: Section 12	79
A13.	Section plot: Section 13 (without SRLs)	80

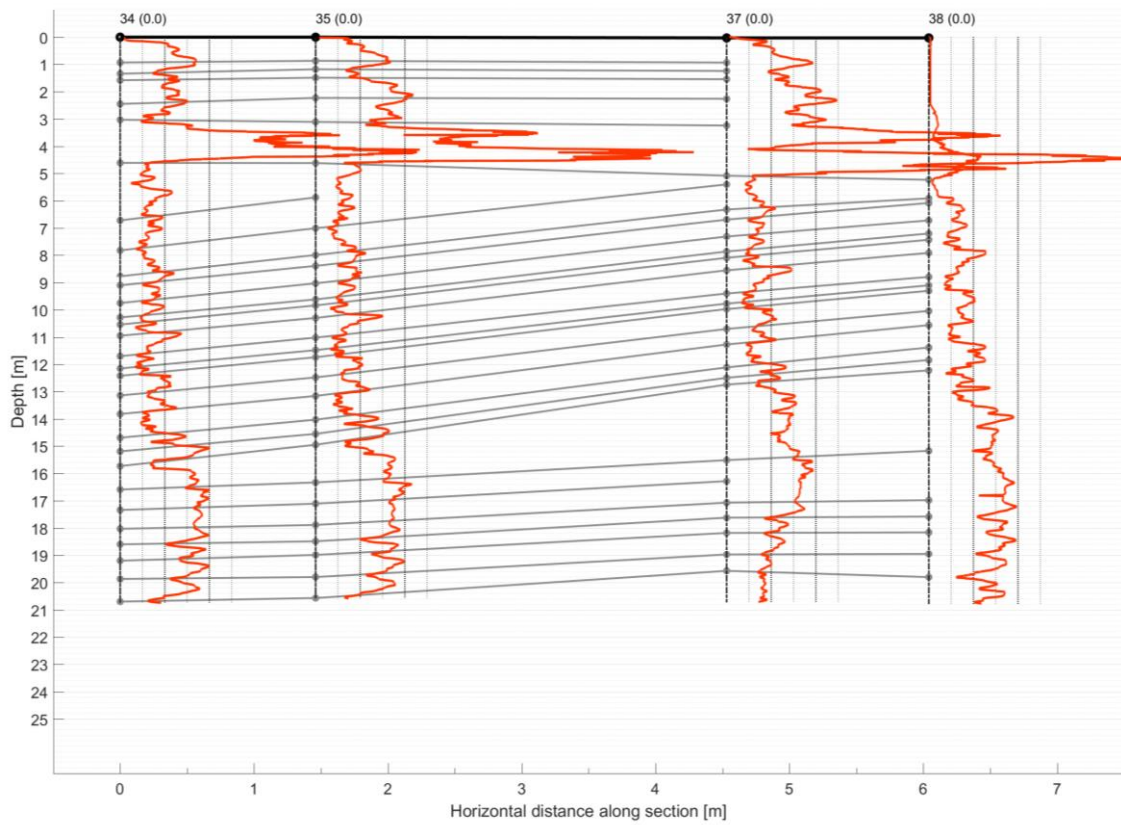
Depth adjusted measurements

A14.	Depth adjusted measurements for section 1	81
A15.	Depth adjusted measurements for section 2	81
A16.	Depth adjusted measurements for section 3	82
A17.	Depth adjusted measurements for section 4	82
A18.	Depth adjusted measurements for section 5	83
A19.	Depth adjusted measurements for section 6	83
A20.	Depth adjusted measurements for section 7	84
A21.	Depth adjusted measurements for section 8	84
A22.	Depth adjusted measurements for section 9	85
A23.	Depth adjusted measurements for section 10	85
A24.	Depth adjusted measurements for section 12	86

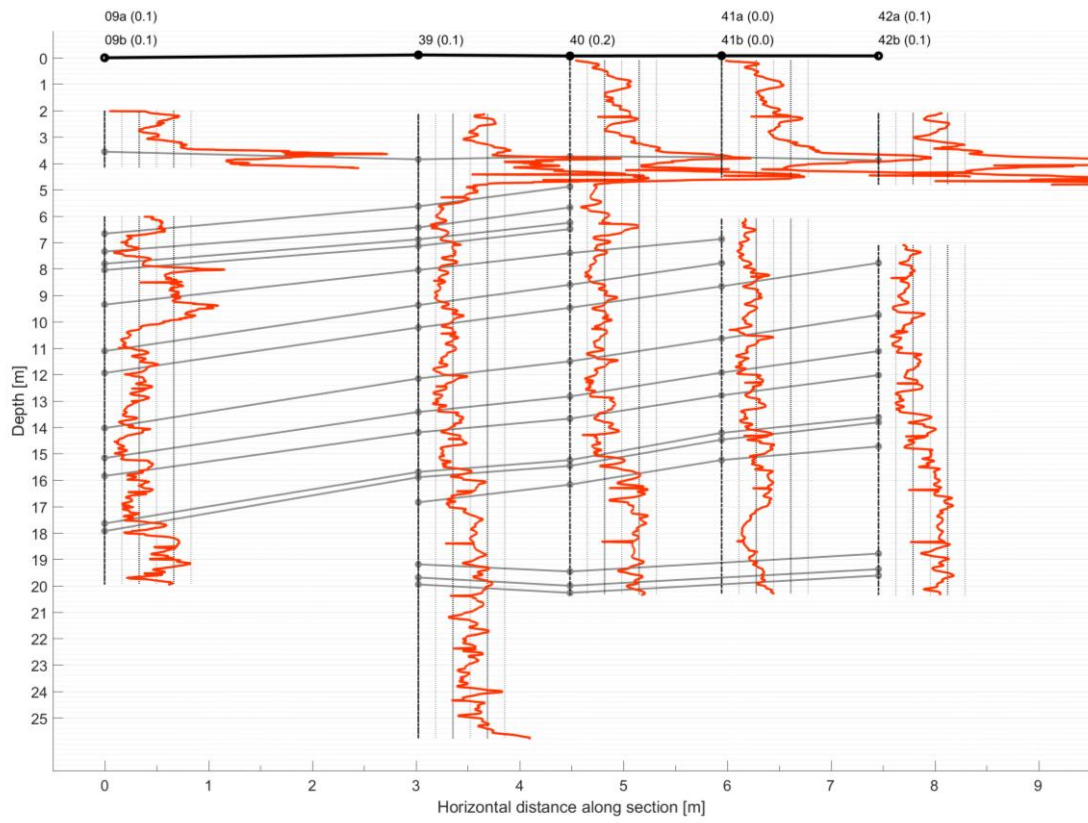
A1. Section plot: Section 1



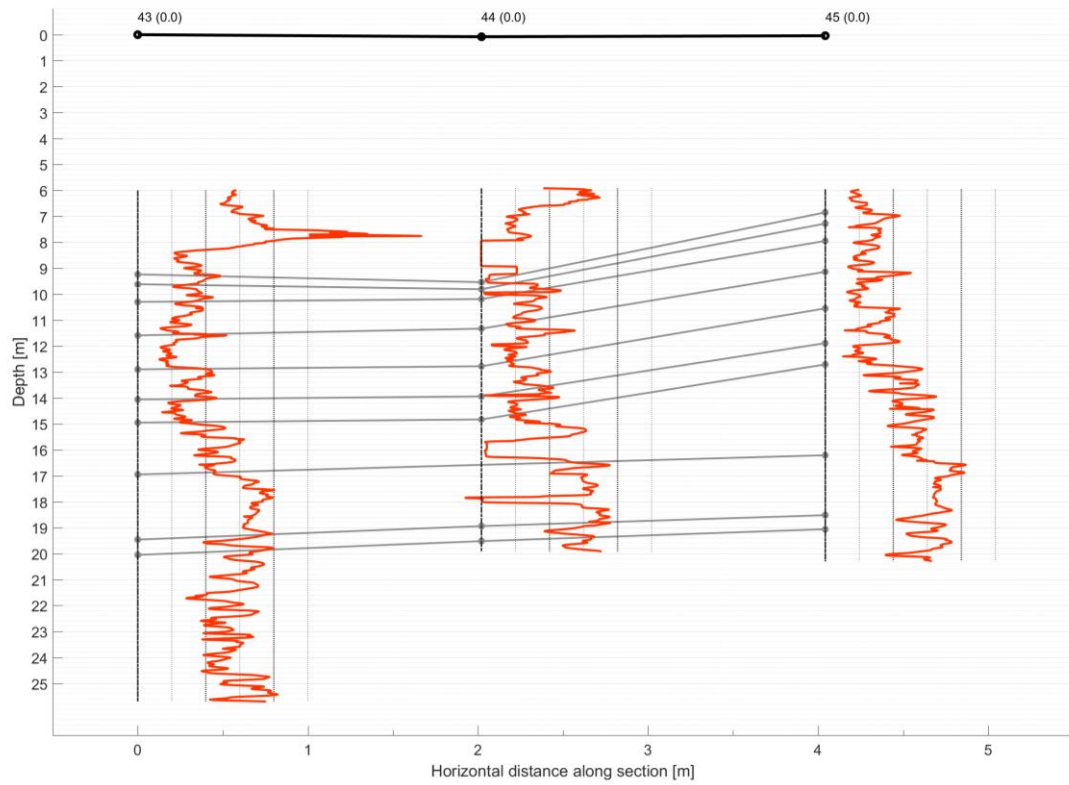
A2. Section plot: Section 2



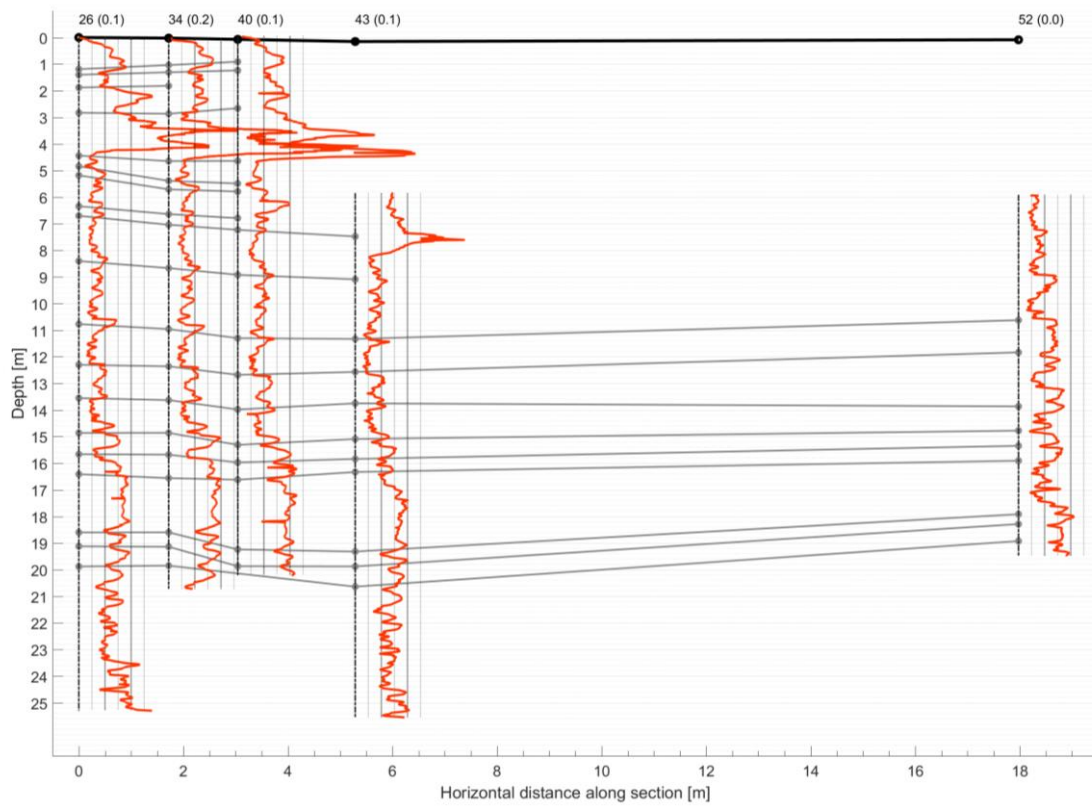
A3. Section plot: Section 3



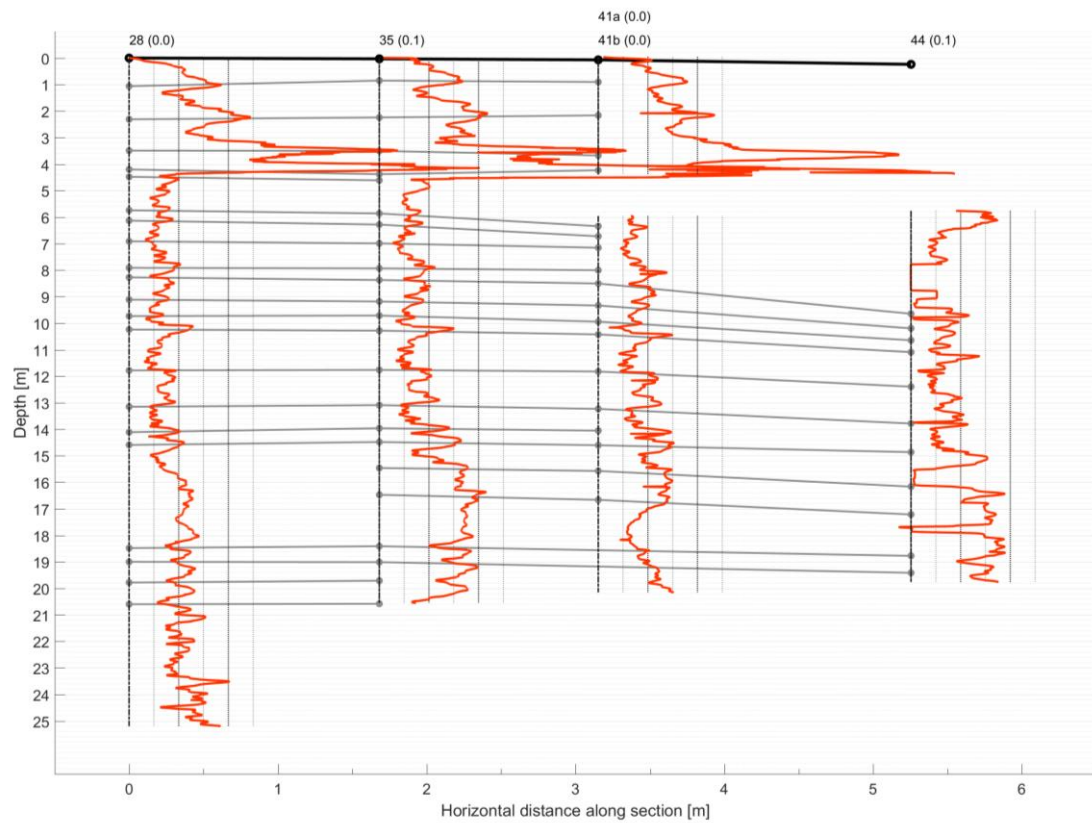
A4. Section plot: Section 4



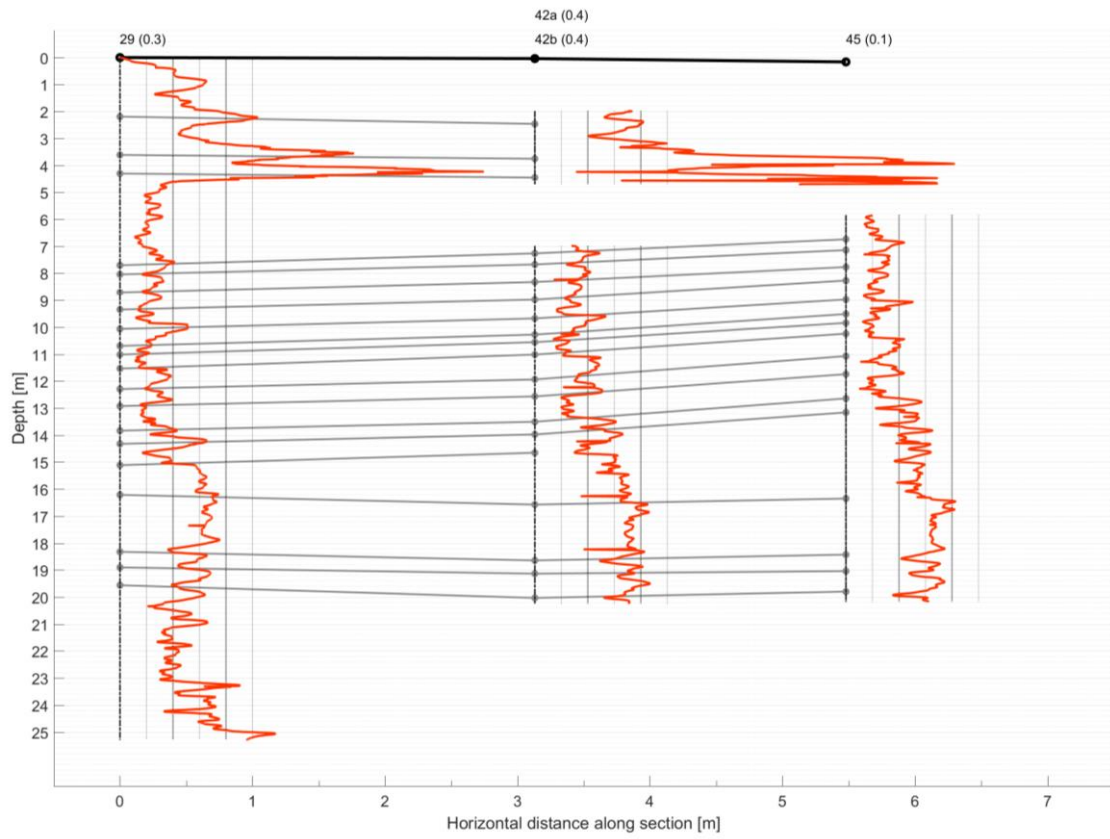
A5. Section plot: Section 5



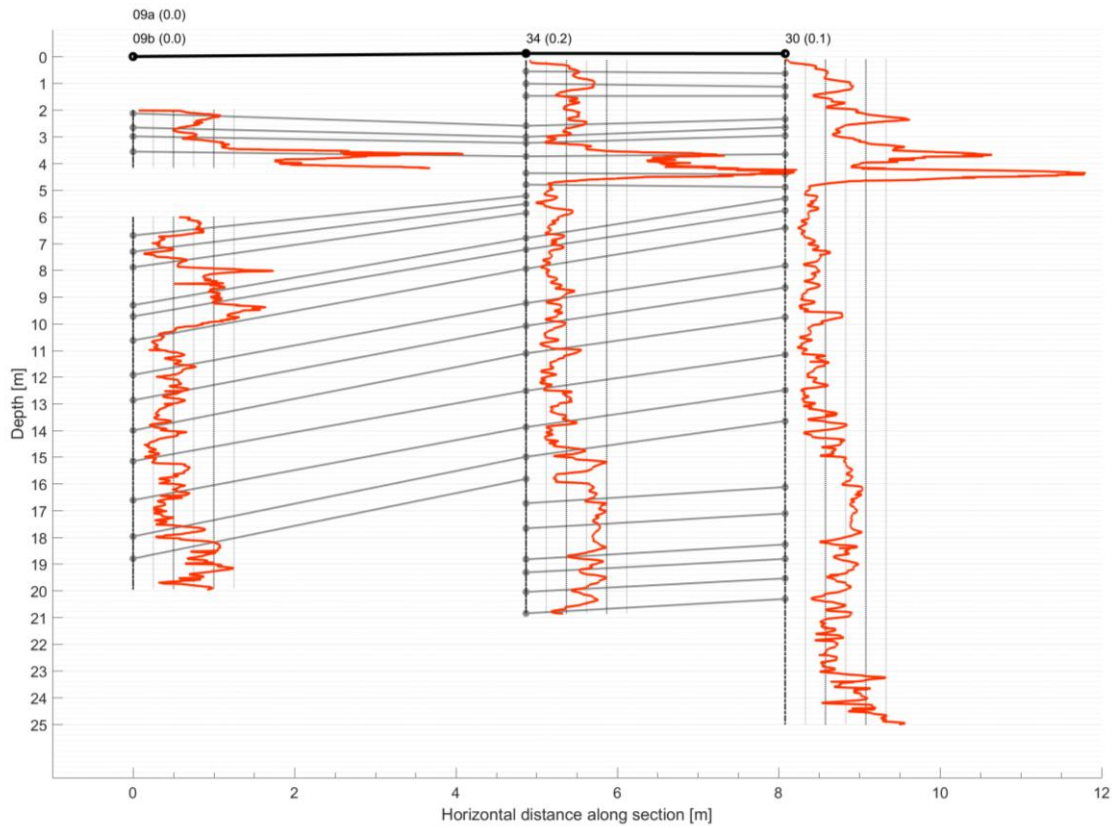
A6. Section plot: Section 6



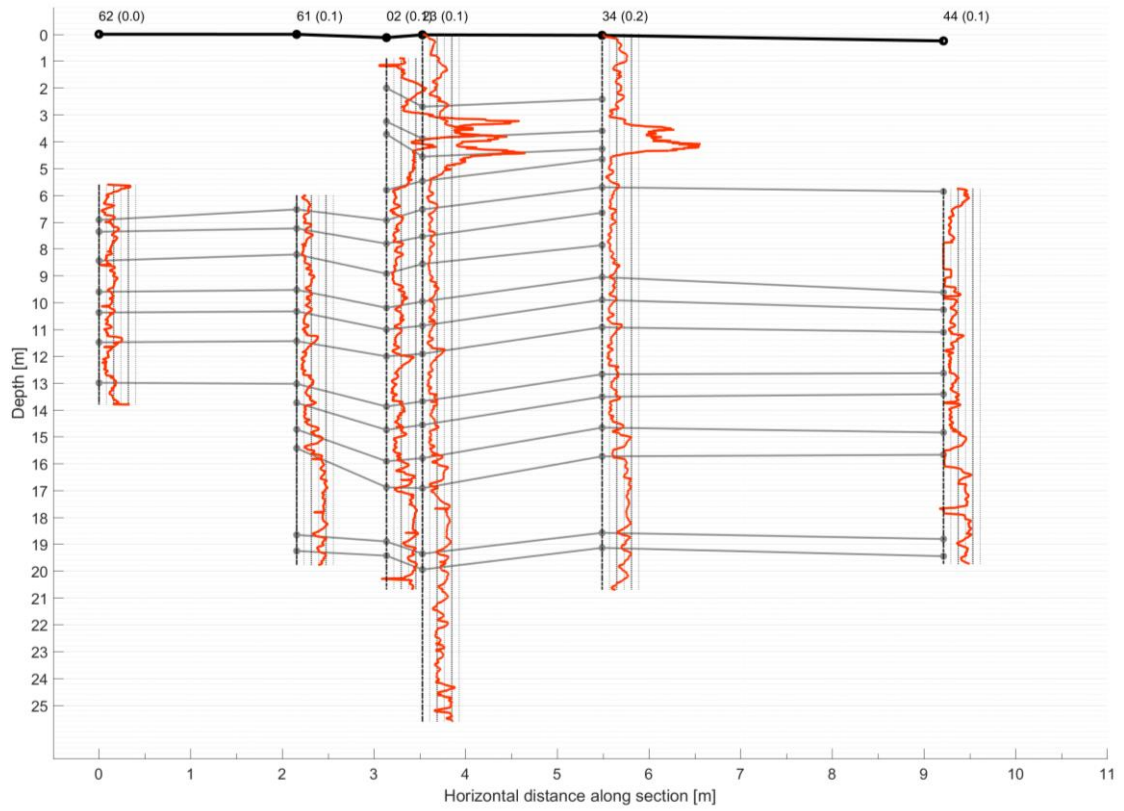
A7. Section plot: Section 7



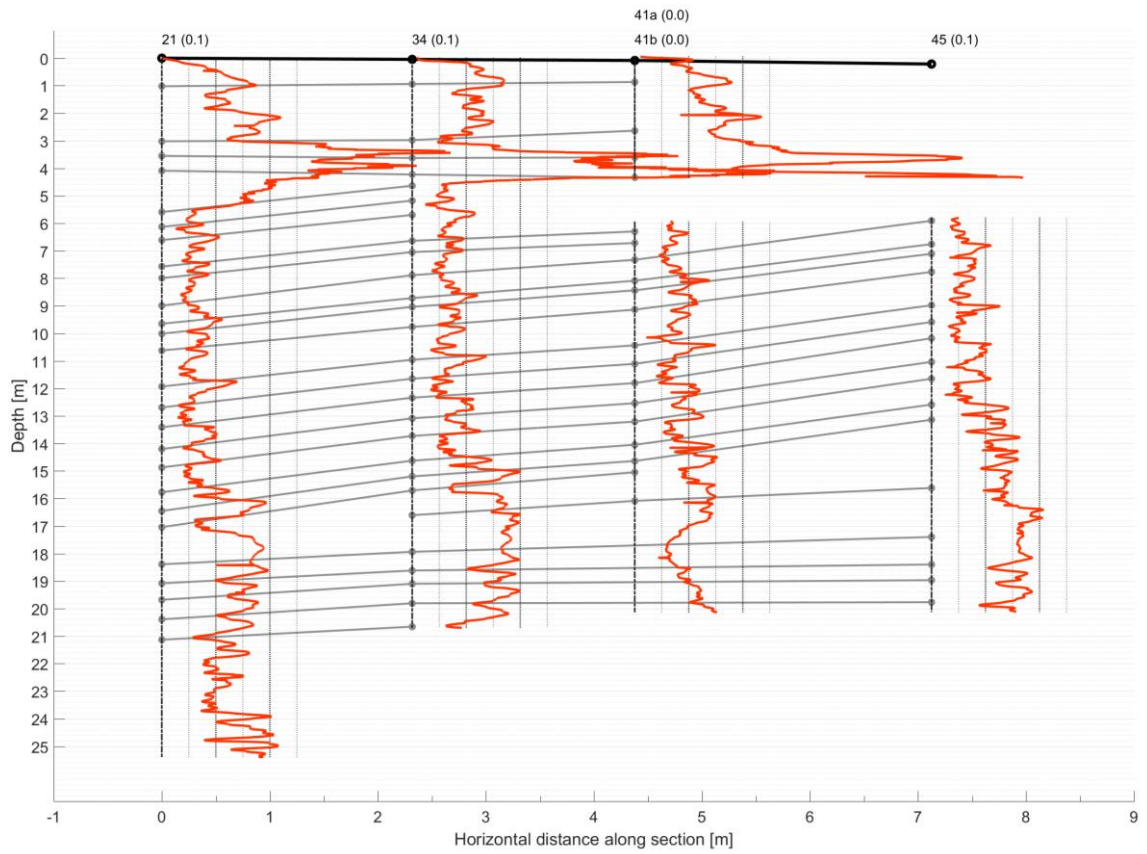
A8. Section plot: Section 8



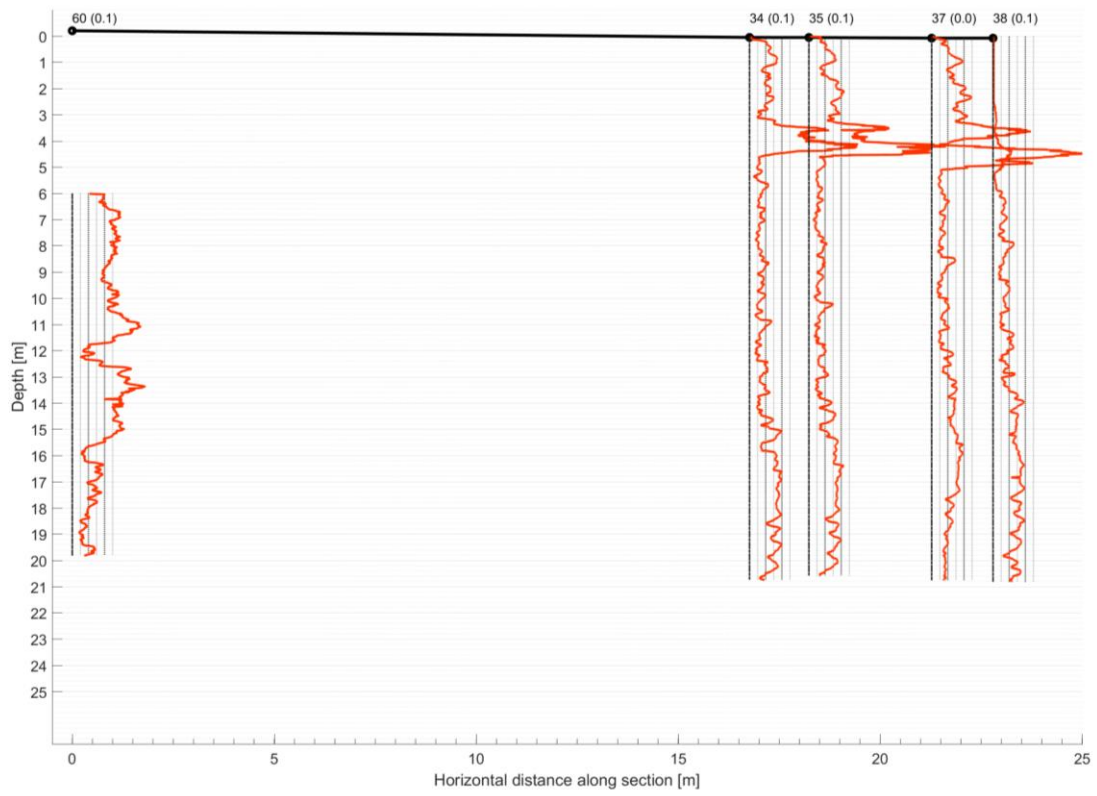
A9. Section plot: Section 9



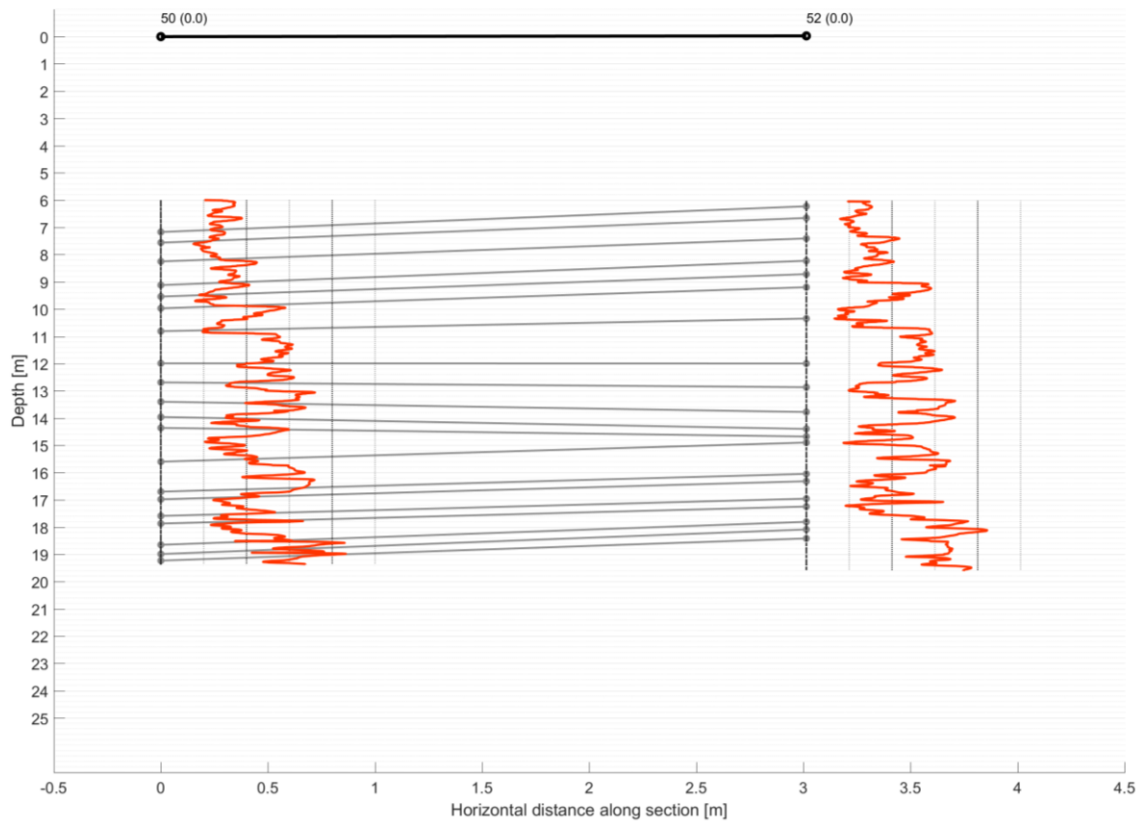
A10. Section plot: Section 10



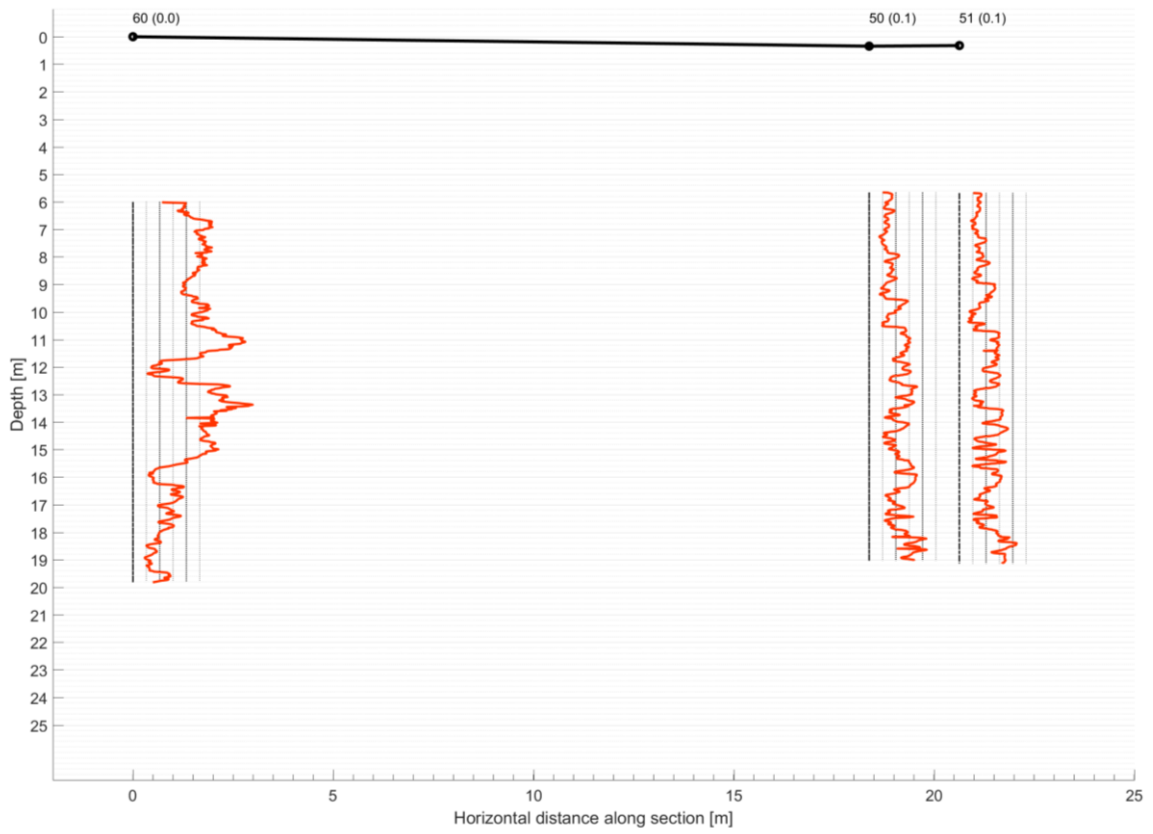
A11. Section plot: Section 11 (without SRLs)



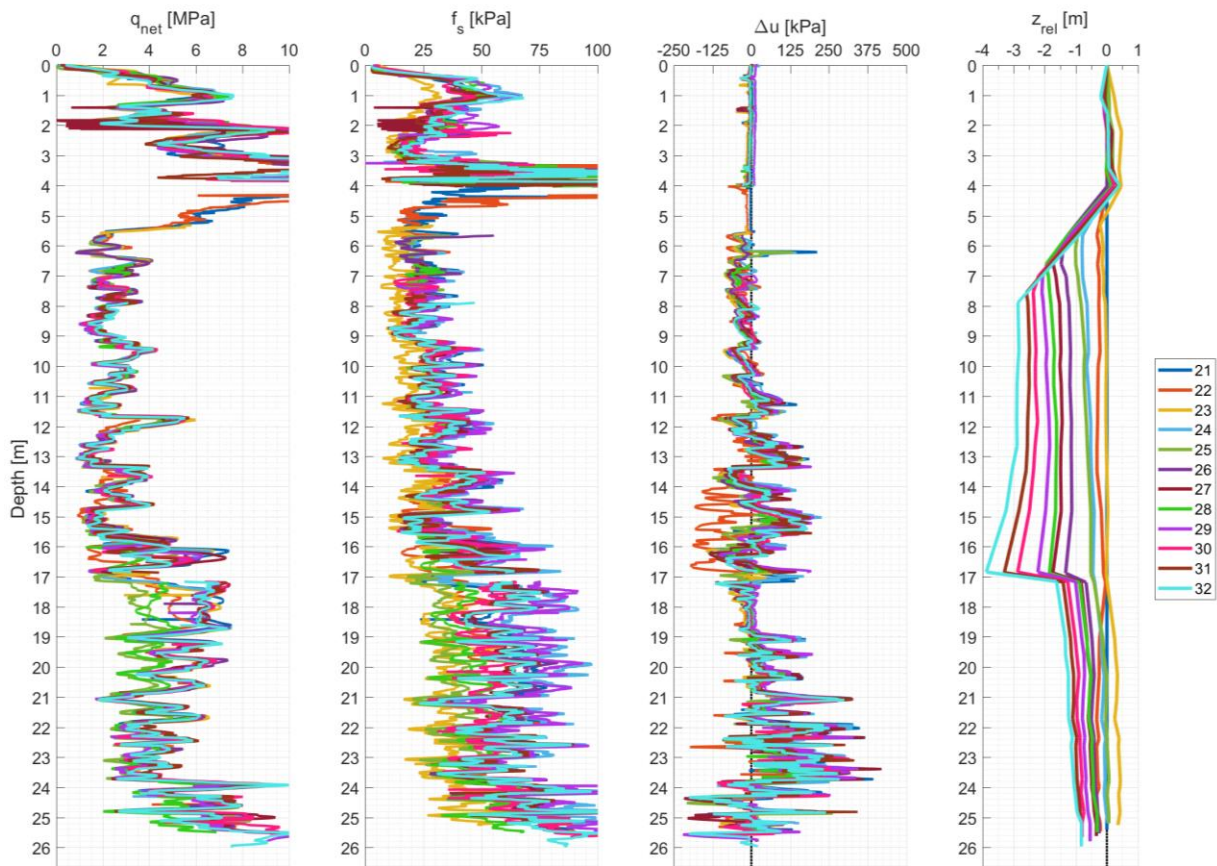
A12. Section plot: Section 12



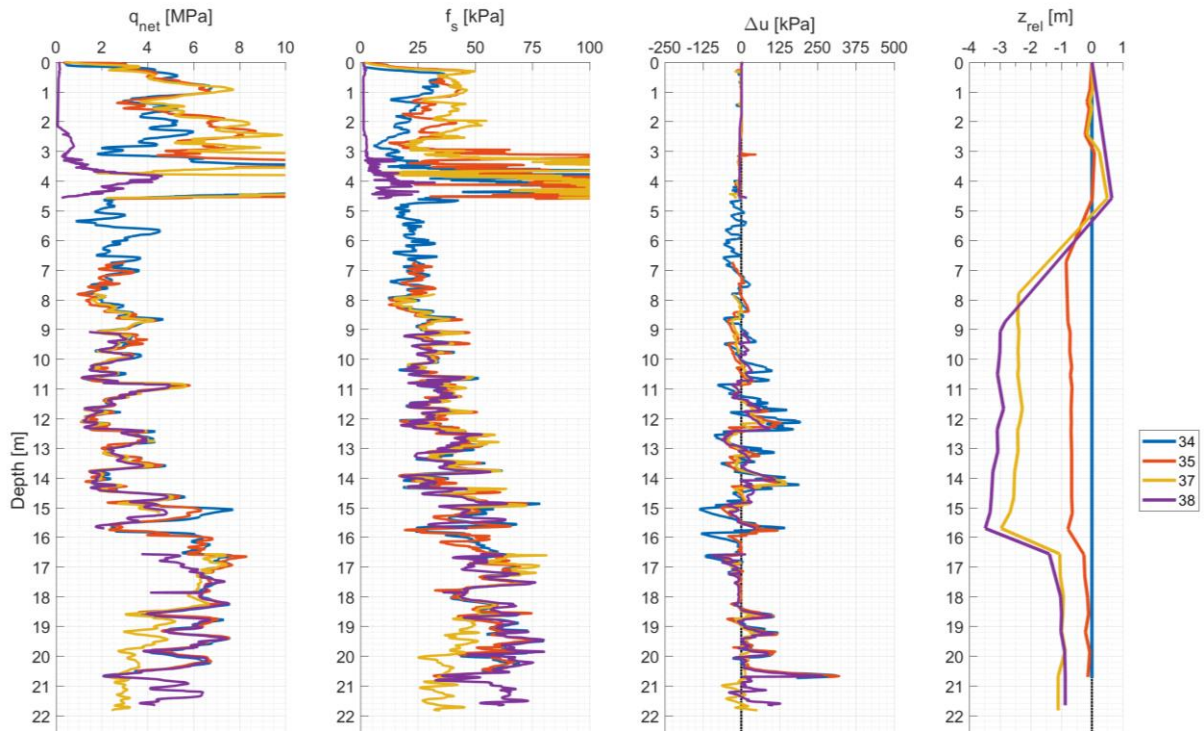
A13. Section plot: Section 13 (without SRLs)



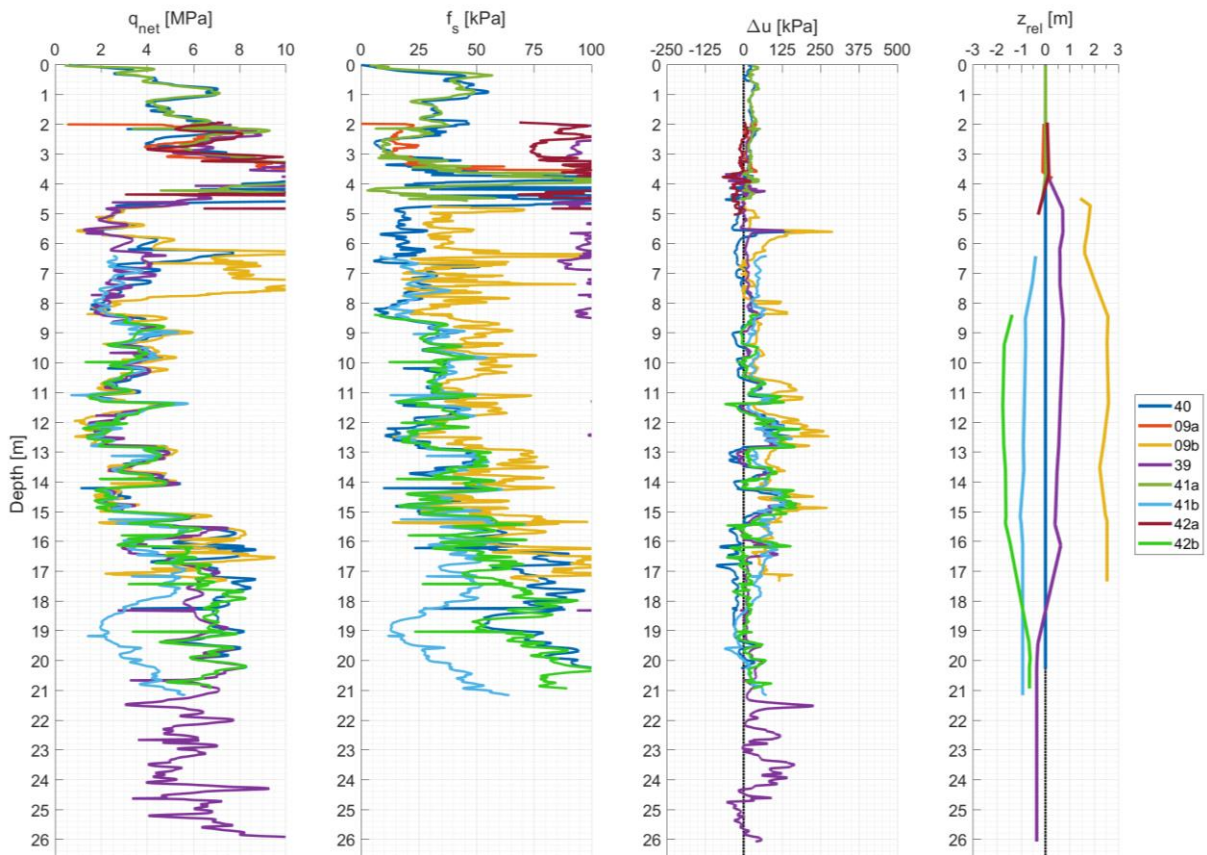
A14. Depth adjusted measurements for section 1



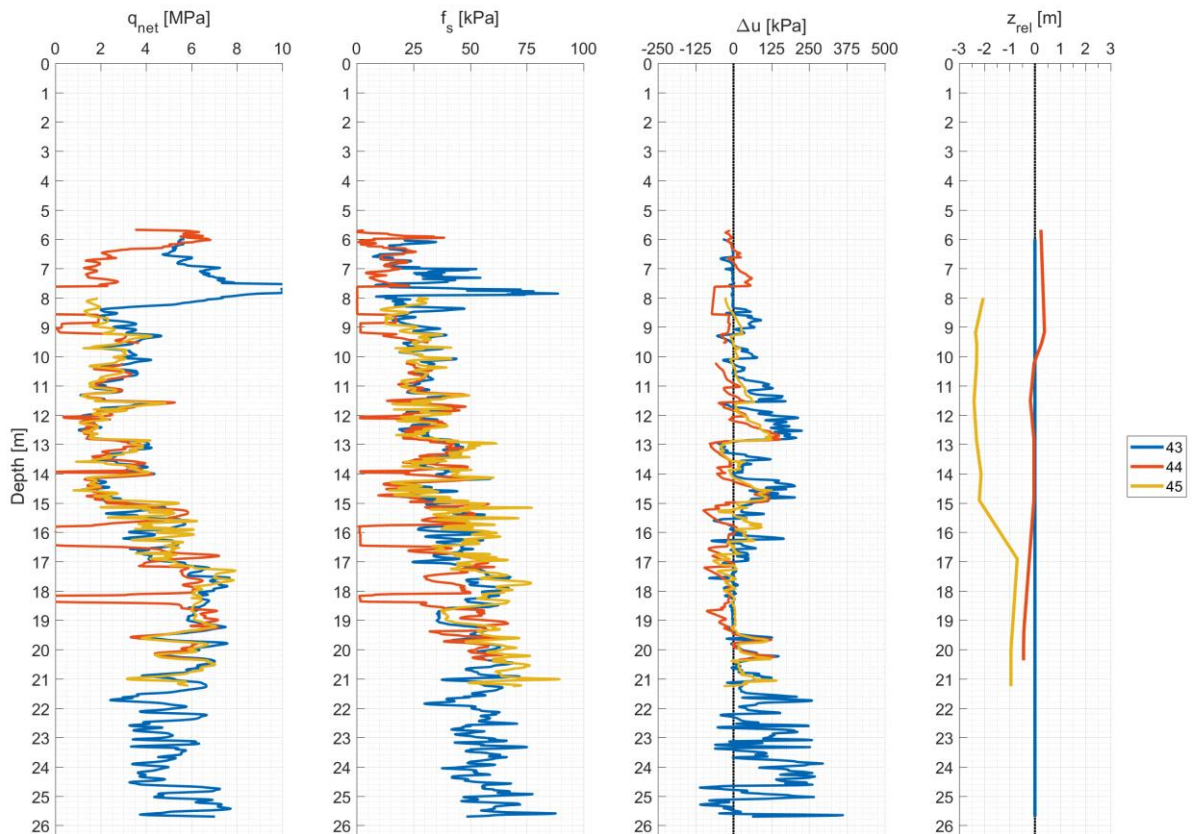
A15. Depth adjusted measurements for section 2



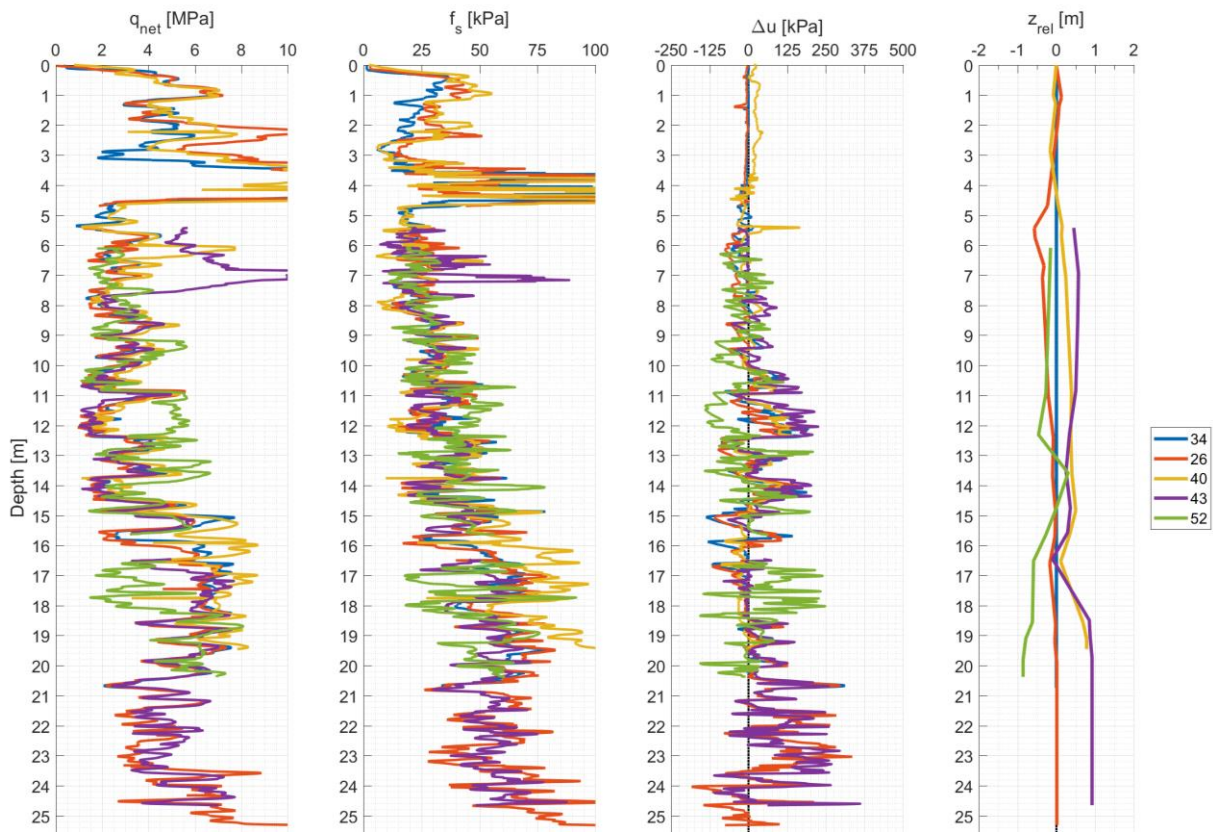
A16. Depth adjusted measurements for section 3



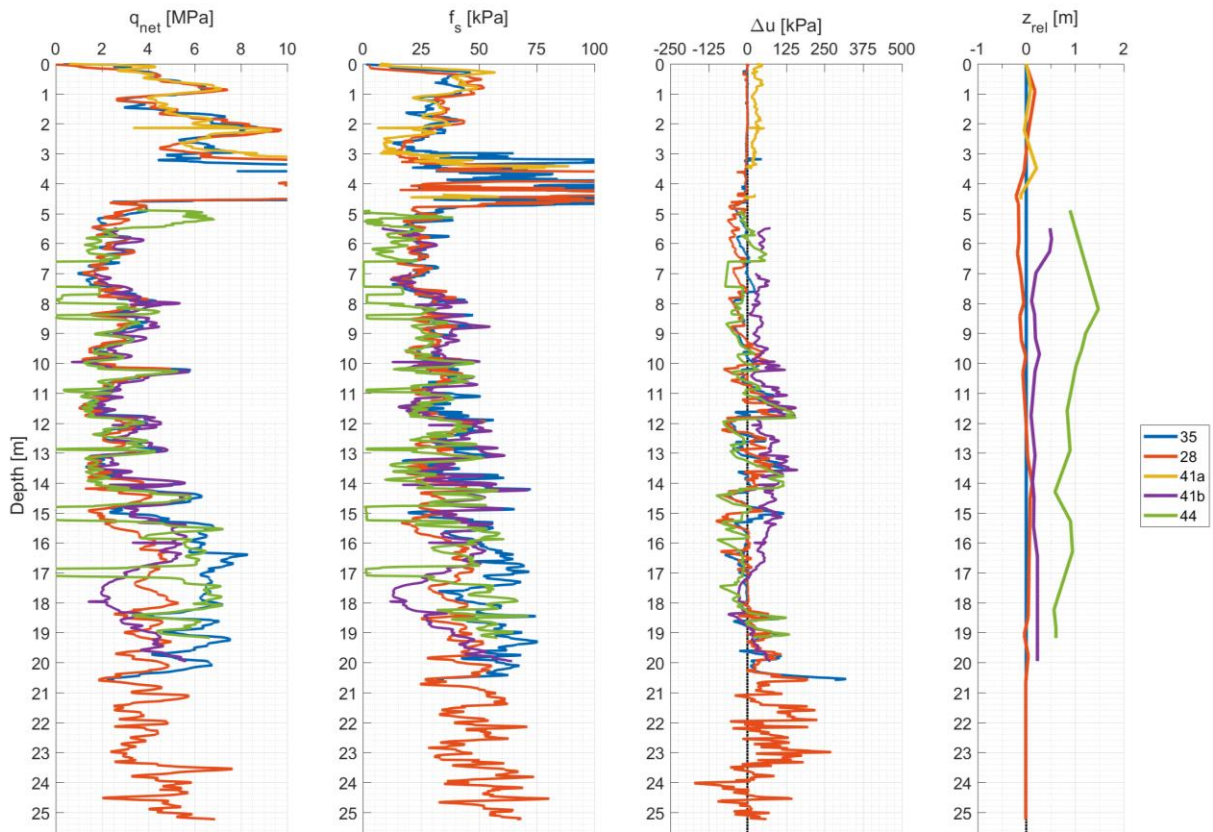
A17. Depth adjusted measurements for section 4



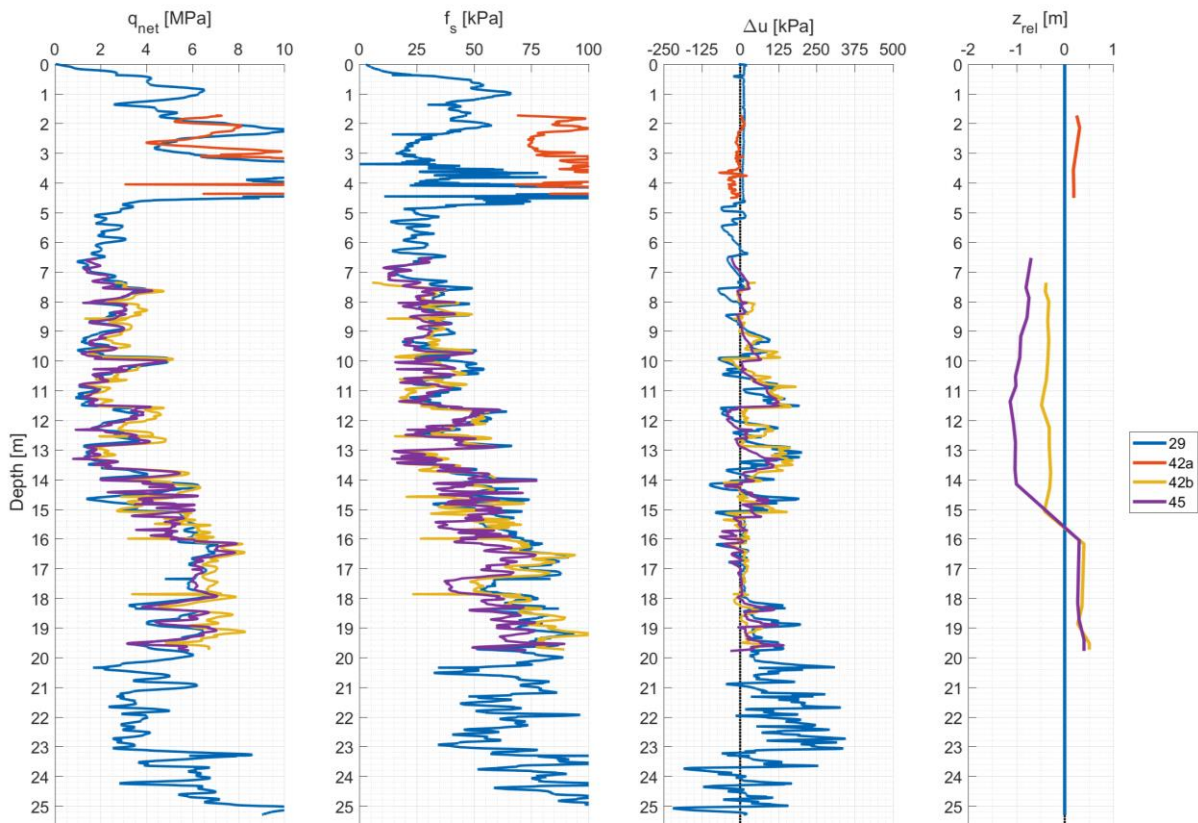
A18. Depth adjusted measurements for section 5



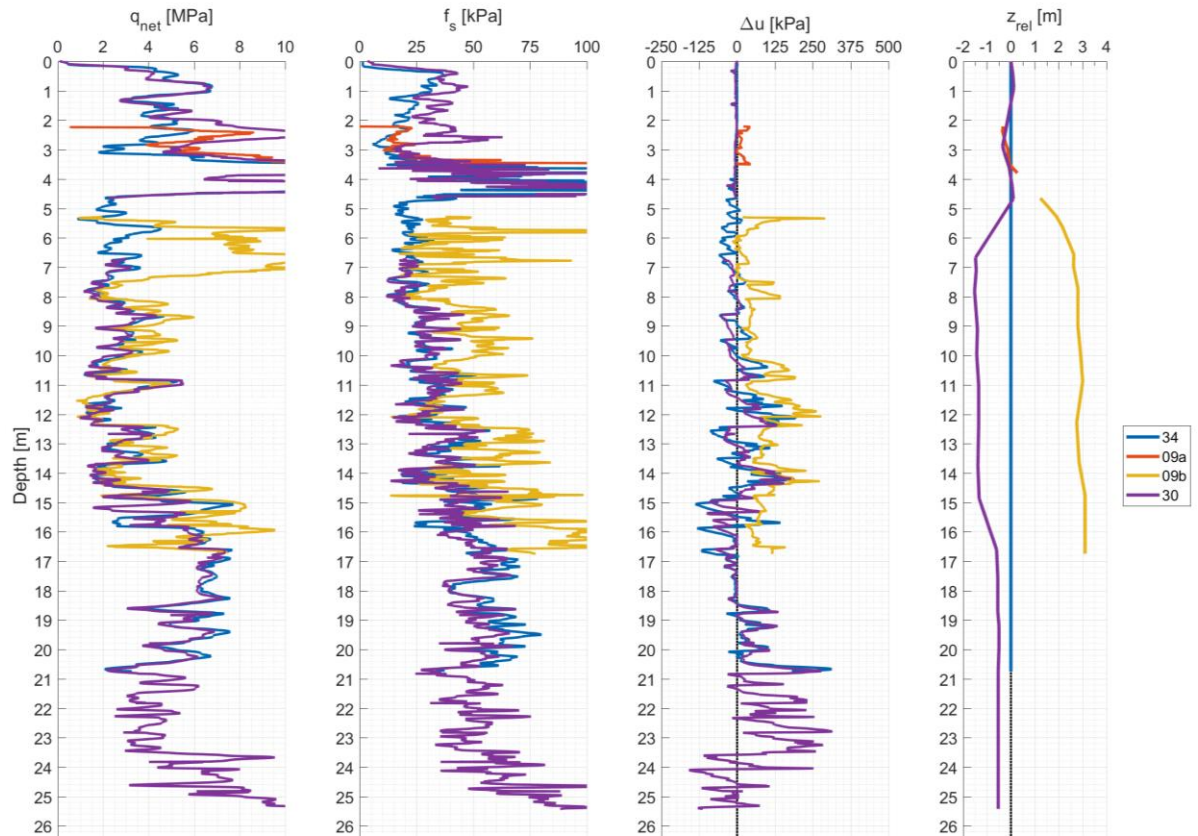
A19. Depth adjusted measurements for section 6



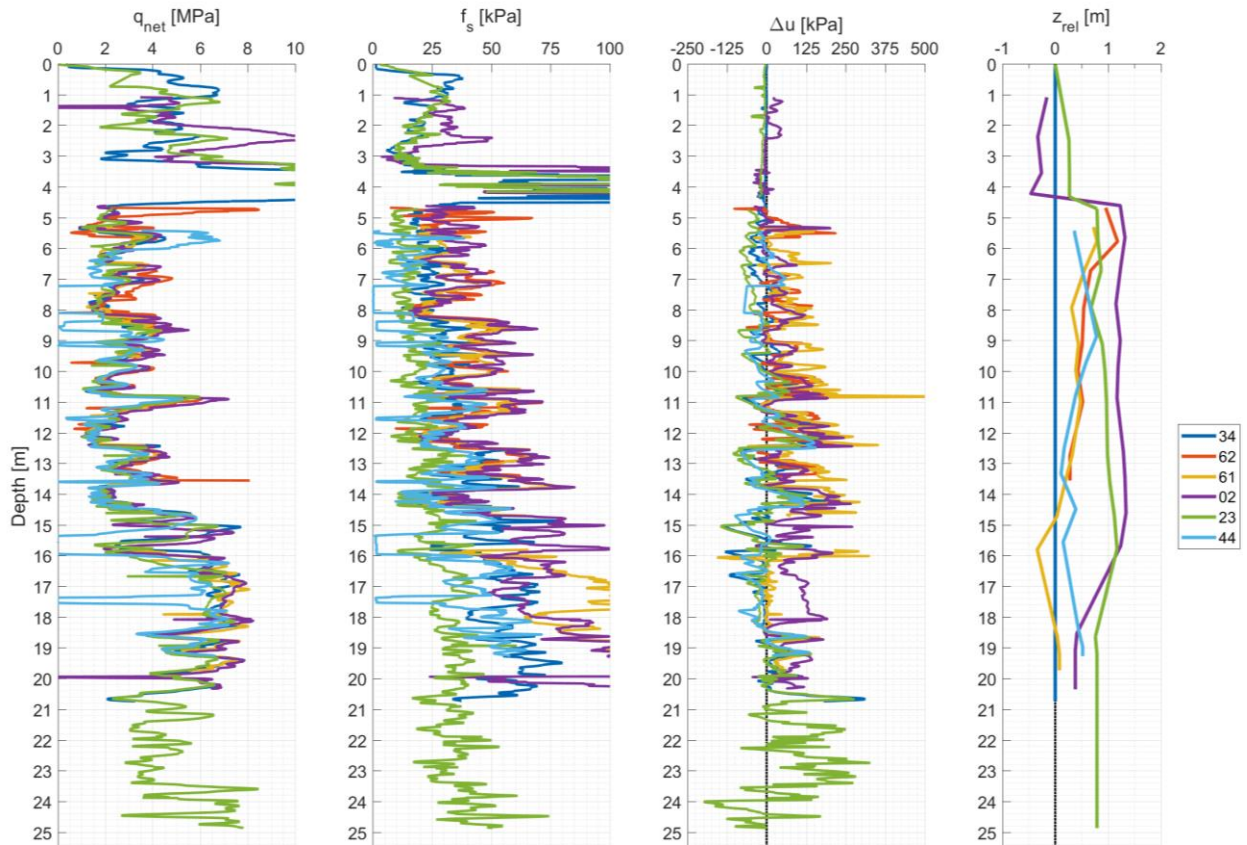
A20. Depth adjusted measurements for section 7



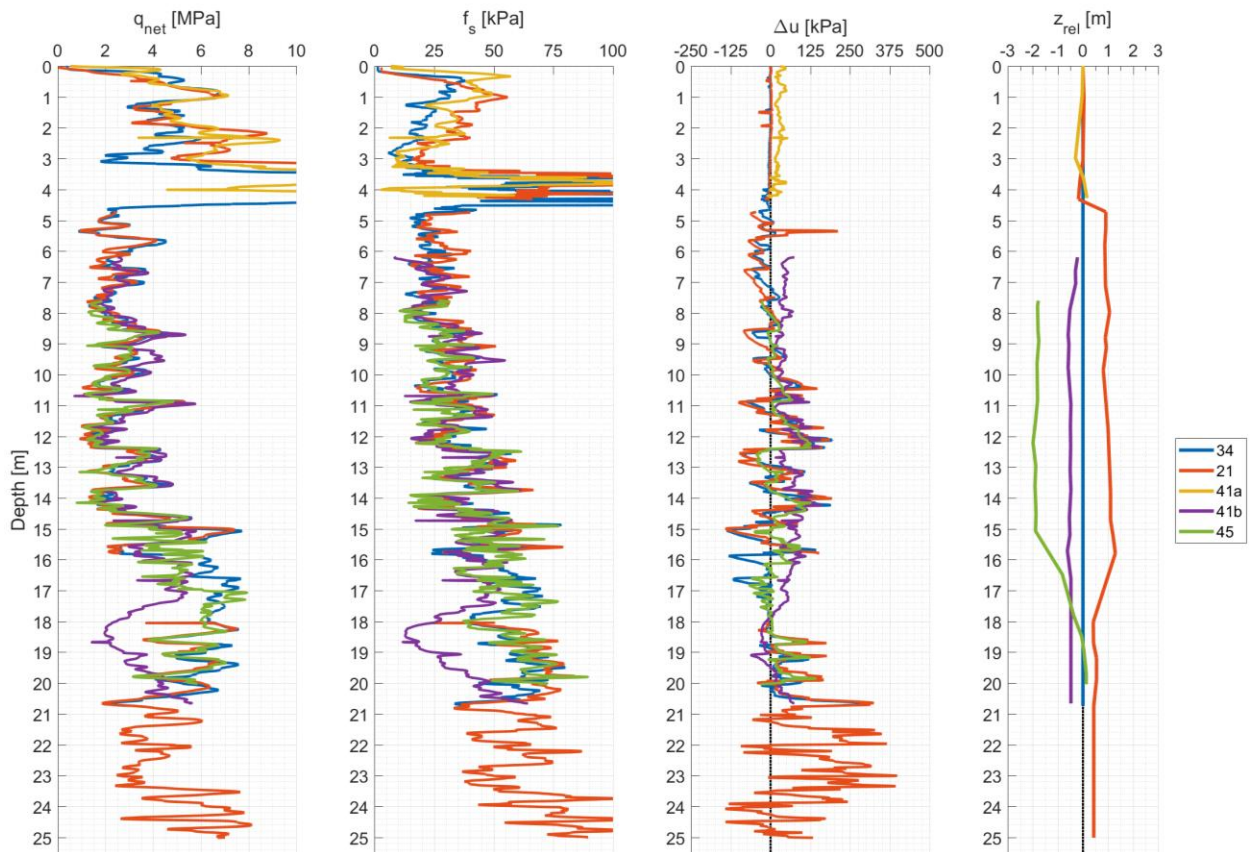
A21. Depth adjusted measurements for section 8



A22. Depth adjusted measurements for section 9



A23. Depth adjusted measurements for section 10



A24. Depth adjusted measurements for section 12

